INFORMATION TO USERS

This manuscript has been reproduced from the microfilm master. UMI films the text directly from the original or copy submitted. Thus, some thesis and dissertation copies are in typewriter face, while others may be from any type of computer printer.

The quality of this reproduction is dependent upon the quality of the copy submitted. Broken or indistinct print, colored or poor quality illustrations and photographs, print bleedthrough, substandard margins, and improper alignment can adversely affect reproduction.

In the unlikely event that the author did not send UMI a complete manuscript and there are missing pages, these will be noted. Also, if unauthorized copyright material had to be removed, a note will indicate the deletion.

Oversize materials (e.g., maps, drawings, charts) are reproduced by sectioning the original, beginning at the upper left-hand corner and continuing from left to right in equal sections with small overlaps.

Photographs included in the original manuscript have been reproduced xerographically in this copy. Higher quality 6" x 9" black and white photographic prints are available for any photographs or illustrations appearing in this copy for an additional charge. Contact UMI directly to order.

Bell & Howell Information and Learning
300 North Zeeb Road, Ann Arbor, MI 48106-1346 USA
800-521-0600

UMI®

Université d'Ottawa · University of Ottawa

ON THE VISCOELASTIC RESPONSE OF LAMINATED COMPOSITES

By

©Jie Feng

A thesis submitted to the University of Ottawa
in partial fulfillment of the requirement for the degree of Master of Applied Science
in Mechanical Engineering

Ottawa-Carleton Institute for Mechanical and Aerospace Engineering

Department of Mechanical Engineering
University of Ottawa
Ottawa, Canada
June, 1999

National Library of Canada
Bibliothèque nationale du Canada

Acquisitions and Bibliographic Services
Acquisitions et services bibliographiques

395 Wellington Street
Ottawa ON K1A 0N4
Canada

395, rue Wellington
Ottawa ON K1A 0N4
Canada

Your file Votre référence

Our file Notre référence

The author has granted a non-exclusive licence allowing the National Library of Canada to reproduce, loan, distribute or sell copies of this thesis in microform, paper or electronic formats.

L'auteur a accordé une licence non exclusive permettant à la Bibliothèque nationale du Canada de reproduire, prêter, distribuer ou vendre des copies de cette thèse sous la forme de microfiche/film, de reproduction sur papier ou sur format électronique.

The author retains ownership of the copyright in this thesis. Neither the thesis nor substantial extracts from it may be printed or otherwise reproduced without the author's permission.

L'auteur conserve la propriété du droit d'auteur qui protège cette thèse. Ni la thèse ni des extraits substantiels de celle-ci ne doivent être imprimés ou autrement reproduits sans son autorisation.

0-612-45219-0

Canada

ACKNOWLEDGEMENTS

I wish to express my sincere gratitude to my research supervisor Prof. Y.M. Haddad of the Department of Mechanical Engineering of the University of Ottawa for his valuable instructions, inspirations, constant encouragement, and generous help during the course of this study. The successful completion of this thesis depended solely on his guidance ideal. I would like also to thank the staff of the Department of Mechanical Engineering of the University of Ottawa for their continued assistance, and to thank the fellow graduate students of the same department for the useful discussions.

This thesis was financially supported by a research grant from Natural Sciences and Engineering Research Council of Canada (NSERC) to my research director Professor Haddad. This support is sincerely acknowledged by the Candidate.

I am grateful to my wife Yan and my parents Yuan-Yi and Kun-Hao for their understanding, support and patience.

ABSTRACT

This thesis addresses the problem of analytical determination of the response behaviour of fibre reinforced composite materials, under both quasi-static and dynamic loadings.

In the first part of the thesis (Chapters 2 and 3), the effects of microstructural parameters, such as fibre aspect ratio, fibre off-axis angle and fibre volume fraction, on the damping and stiffness of a fibre-composite system are examined. Quasi-static models are, then, developed by using a "Forced Balance Approach" to define mechanical response properties of discontinuous fibre reinforced composite materials. Subsequently, simultaneous optimization of damping, stiffness and weight is carried out by using the so-called "Inverted Utility Function Method". The obtained results show that discontinuous fibre-reinforced composites have superior design flexibility and higher damping properties as compared with those pertaining to continuous fibre-reinforced composites of the same material.

In the second part of the thesis (Chapters 4 and 5), the determination of the impact response of laminated composite plates is dealt with. In this context, the "First Shear Deformation Theory (FSDT)" is employed to deal with the so called "Transient Wave Propagation Phenomenon". In this, the "Correspondence Principle" is, then, utilized to extend the obtained elastic solutions to corresponding viscoelastic problems. Here, the closed form displacement solutions are obtained

first in the frequency-domain, then, the "Fast Fourier Transformation (FFT)" is applied to invert numerically the dealt-with solutions from frequency-domain to time-domain. The obtained results emphasize the importance of including viscoelastic effects in the analysis, for the prediction of the mechanical response of laminated composites under impact loading.

TABLE OF CONTENTS

ACKNOWLEDGEMENTS *ii*

ABSTRACT *iii*

TABLE OF CONTENTS *v*

NOMENCLATURE *viii*

LIST OF TABLES *x*

LIST OF FIGURES *xi*

CHAPTER 1 VISCOELASTIC RESPONSE BEHAVIOUR OF ENGINNERING MATERIALS

1.1 Introduction *1*

1.1.1 Creep Response *3*

1.1.2 Stress Relaxation *3*

1.2 Subject of the present research *4*

1.2.1 Theoretical Modelling of Damping and Complex Modulus *5*

1.2.2 Theoretical Modelling of Dynamic Response of Composites under Impact Loading *7*

1.3 Outline of the Present Research *11*

CHAPTER 2 A REVIEW ON MODELLING OF THE VISCOELASTIC RESPONSE OF LAMINATED COMPOSITE MATERIALS

2.1 Introduction *13*

2.2 The Micromechanical Modelling Approach *14*

2.3 The Elastic-Viscoelastic Correspondence Principle *17*

CHAPTER 3 OPTIMIZATION OF THE MECHANICAL BEHAVIOUR OF DISCONTINUOUS FIBRE REINFORCED COMPOSITES WITH THE INCLUSION OF THE MICROSTRUCTURE

3.1 Introduction *19*

3.2 Theoretical Analysis: Force-Balance Approach *22*

3.3 Numerical Results and Discussions *31*

3.4 Optimization *33*

3.4.1 Inverted Utility Function Method *34*

3.4.2 Multivariable Non-Linear Optimization *35*

3.4.3 Implementation of Non-Linear Programming *37*

3.4.4 Numerical Results and Discussions *39*

3.5 Conclusions *41*

CHAPTER 4 WAVE PROPAGATION - A BRIEF REVIEW

4.1 Introduction *61*

4.2 Wave Propagation in Homogeneous Materials *62*

4.2.1 Wave Propagation in Isotropic, Elastic Solids *62*

4.2.2 Wave Propagation in Isotropic, Viscoelastic Solids *65*

4.3 Wave Propagation in Heterogeneous Materials *67*

CHAPTER 5 WAVE PROPAGATION IN VISCOELASTIC COMPOSITE LAMINATE PLATE UNDER AN IMPACT LOAD

5.1 Introduction *72*

5.2 Equations of Motion *75*

5.3 Stress Wave Propagation under Dynamic Loading *80*

5.4 Transient Wave Propagation Under Impact Loading *86*

5.5 Fast Fourier Transformation (FFT) and Programming *89*

5.6 Numerical Results and Discussions *91*

5.7 Conclusions *95*

REFERENCES *109*

APPENDIX A Derivation of Equation (3.2.20) *116*

APPENDIX B Derivation of Viscoelastic "Constants" *119*

APPENDIX C Flowchart of Simplex Optimization Method *123*

APPENDIX D Non-Symmetric Simplex (Nelder & Mead[43]) Non-linear Optimization. *Fortran Program Code* *124*

APPENDIX E FFT Computer Program Flowchart *133*

APPENDIX F Transient Wave Propagation under Impact Loading. *C Program Code* *134*

NOMENCLATURE

a_i	Material constants.
a, b	Length and width of a composite laminate plate, respectively.
c_{ij}	Components of stiffness matrix, $i, j = 1, 2, 3 \ldots . N$.
d	Fibre diameter.
h	Thickness of a composite laminate plate.
l	Fibre length.
$q(.)$	Pressure distribution function.
x	Distance along a fibre from one of its ends.
w_1, w_2, w_3	Weight factor of damping, stiffness and weight, respectively.
A_{ij}, B_{ij}, D_{ij}	Material constants.
ACCUR	Desired accuracy of the optimization.
A, Y, B	"Reflection", "Expansion" and "Contraction" coefficients, respectively, for the "Simplex Method".
E_L	Longitudinal modulus of composite.
E_T	Transverse modulus of composite.
E_x	Modulus of composite along the x-direction.
E_m	Tensile modulus of matrix.
E_f	Tensile modulus of fibre.
G_m	Shear modulus of matrix.

G_{LT}	In-plane shear modulus of composite.
M_x, M_y, M_{xy}	Moment resultants.
$N_x, N_y, N_{xy}, Q_x, Q_y$	Stress resultants.
PLE	Probe length (used to construct the initial "Simplex").
R	One-half of centreline-to-centreline fibre spacing.
U	Utility function.
U, V, W	Displacement components in x, y and z directions.
V_f	Fibre volume fraction.
$W,\ W_f,\ W_m$	Specific weight of composite, fibre and matrix, respectively.
Y^T	Initial starting point for the "Simplex Method".
$\varepsilon_x, \varepsilon_y, \varepsilon_z, \gamma_{xy}, \gamma_{xz}, \gamma_{yz}$	Engineering strain components.
η_x, η_f, η_m	Extensional loss factor (along the x-direction) of composite, fibre and matrix, respectively.
η_{Gm}	Shear loss factor of matrix.
θ	Angle between a fibre-axis and the x-direction.
$\sigma_x, \sigma_y, \sigma_z, \tau_{xy}, \tau_{xz}, \tau_{yz}$	Engineering stress components.

LIST OF TABLES

Table 3.1 Static properties of Scotchply 1002 Matrix Epoxy and E-glass Fibres at room temperature, after Gibson, et al.[25] *43*

Table 3.2 Optimization results for various starting points *44*

LIST OF FIGURES

Figure 1.1 Specific damping capacity in a mechanical system. *12*

Figure 3.1 Representative Volume Element[8].
(a) Aligned Case. (b) Off-Axis Case *45*

Figure 3.2 Non-dimensional Ratios η_x/η_m and E_x'/E_m' *vs* Fibre Volume Fraction V_f and Fibre Aspect Ratio l/d. Off-Axis Angle θ of the dealt with composite materials, with material properties of each component as shown in Table 3.1, is set to be 0°. *46*

Figure 3.3 Non-dimensional Ratios η_x/η_m and E_x'/E_m' *vs* Fibre Volume Fraction V_f and Fibre Aspect Ratio l/d. Off-Axis Angle θ of the dealt with composite materials, with material properties of each component as shown in Table 3.1, is set to be 20°. *47*

Figure 3.4 Non-dimensional Ratios η_x/η_m and E_x'/E_m' *vs* Fibre Volume Fraction V_f and Fibre Aspect Ratio l/d. Off-Axis Angle θ of the dealt with composite materials, with material properties of each component as shown in Table 3.1, is set to be 40°. *48*

Figure 3.5 Non-dimensional Ratios η_x/η_m and E_x'/E_m' *vs* Fibre Volume Fraction V_f and Fibre Aspect Ratio l/d. Off-Axis Angle θ of the dealt with composite materials, with material properties of each component as shown in Table 3.1, is set to be 60°. *49*

Figure 3.6 Non-dimensional Ratios η_x/η_m and E_x'/E_m' *vs* Fibre Volume Fraction V_f and Fibre Aspect Ratio l/d. Off-Axis Angle θ of the dealt with composite materials, with material properties of each component as shown in Table 3.1, is set to be 80°. *50*

Figure 3.7 Non-dimensional Ratios η_x/η_m and E_x'/E_m' *vs* Fibre Volume Fraction V_f and Fibre Aspect Ratio l/d. Off-Axis Angle θ of the dealt with composite materials, with material properties of each component as shown in Table 3.1, is set to be 90°. *51*

Figure 3.8 Non-dimensional Ratios η_x/η_m and E_x'/E_m' *vs* Fibre Volume Fraction V_f and Off-Axis Angle θ. Fibre Aspect Ratio l/d of the dealt with composite materials, with material properties of each component as shown in Table 3.1, is set to be 5. *52*

Figure 3.9 Non-dimensional Ratios η_x/η_m and E_x'/E_m' *vs* Fibre Volume Fraction V_f and Off-Axis Angle θ. Fibre Aspect Ratio l/d of the dealt with composite materials, with material properties of each component as shown in Table 3.1, is set to be 20. *53*

Figure 3.10 Non-dimensional Ratios η_x/η_m and E_x'/E_m' *vs* Fibre Volume Fraction V_f and Off-Axis Angle θ. Fibre Aspect Ratio l/d of the dealt with composite materials, with material properties of each component as shown in Table 3.1, is set to be 40. *54*

Figure 3.11 Non-dimensional Ratios η_x/η_m and E_x'/E_m' *vs* Fibre Volume Fraction V_f and Off Axis Angle θ. Fibre Aspect Ratio l/d of the dealt with composite materials, with material properties of each component as shown in Table 3.1, is set to be 60. *55*

Figure 3.12 Non-dimensional Ratios η_x/η_m and E_x'/E_m' *vs* Fibre Volume Fraction V_f and Off-Axis Angle θ. Fibre Aspect Ratio l/d of the dealt with composite materials, with material properties of each component as shown in Table 3.1, is set to be 80. *56*

Figure 3.13 Non-dimensional Ratios η_x/η_m and E_x'/E_m' *vs* Fibre Volume Fraction V_f and Off-Axis Angle θ. Fibre Aspect Ratio l/d of the dealt with composite materials, with material properties of each component as shown in Table 3.1, is set to be 100. *57*

Figure 3.14 Non-dimensional Ratios η_x/η_m and E_x'/E_m' *vs* Fibre Aspect Ratio l/d and Off-Axis Angle θ. Fibre Volume Fraction V_f of the dealt with composite materials, with material properties of each component as shown in Table 3.1, is set to be 50%. *58*

Figure 3.15 Non-dimensional Ratios η_x/η_m and E_x'/E_m' *vs* Fibre Aspect Ratio l/d and Off-Axis Angle θ. Fibre Volume Fraction V_f of the dealt with composite materials, with material properties of each component as shown in Table 3.1, is set to be 60%. *59*

Figure 3.16 Non-dimensional Ratios η_x/η_m and E_x'/E_m' *vs* Fibre Aspect Ratio l/d and Off-Axis Angle θ. Fibre Volume Fraction V_f of the dealt with composite materials, with material properties of each component as shown in Table 3.1, is set to be 70%. *60*

Figure 5.1 A symmetric composite laminated plate. *98*

Figure 5.2 Impact pressure distribution. *99*

Figure 5.3 Illustration of Fourier Transformation. The top two figures show the wave propagation solutions in frequency-domainwhich can be transformed by using FFTalgorithm (Fast Fourier Transformation) into time-domain as shown in the bottom figure. *100*

Figure 5.4 Impact response of composite laminates with matrices of different damping factors, i.e. 0.05 (solid line) and 0.15 (dashed line). Other material properties are set as: the real modulus of matrix is $E_{mr} = 1158(1 + 100f)^{0.1}$, with f as frequency, the real modulus of glass fibre (continuous) is 72.4Gpa, fibre volume fraction is 60%, and damping factor of fibre is 0.0014. *101*

Figure 5.5 Impact response of composite laminates with elastic and viscoelastic fibres, i.e. fibre damping factor is 0.0014 (solid line) and 0.00 (dashdot line). Other material properties are set as: the real modulus of glass fibre (continuous) is 72.4Gpa, fibre volume fraction is 60%, the real modulus of matrix is $E_{mr} = 1158(1 + 100f)^{0.1}$, with f as frequency, and damping factor of matrix is 0.05. *102*

Figure 5.6 Impact response of composite laminates with various fibre volume fractions, i.e. 50% (solid line), 60% (dashdot line) and 70% (dashed line). Other material properties are set as: the real modulus of glass fibre (continuous) is 72.4Gpa, fibre damping factor is 0.0014, the real modulus of matrix is $E_{mr} = 1158(1 + 100f)^{0.1}$, with f as frequency, and damping factor of matrix is 0.15. *103*

Figure 5.7 Impact response of composite laminates with various fibre volume fractions, i.e. 50% (solid line), 60% (dashdot line) and 70% (dashed line). Other material properties are set as: the real modulus of glass fibre (continuous) is 72.4Gpa, fibre damping factor is 0.0014, the real modulus of matrix is $E_{mr} = 1158(1 + 100f)^{0.1}$, with f as frequency, and damping factor of matrix is 0.05. *104*

Figure 5.8 Impact response of composite laminates with various fibre aspect ratios, i.e. continuous (solid line) and 100 (dashdot line). Other material properties are set as: the real modulus of glass fibre is 72.4Gpa, fibre damping factor is 0.0014, fibre volume fraction is 60%, the real modulus of matrix is $E_{mr} = 1158(1 + 100f)^{0.1}$, with f as frequency, and damping factor of matrix is 0.15. *105*

Figure 5.9 Impact response of composite laminates with various fibre aspect ratios, i.e. continuous (solid line) and 100 (dashdot line). Other material properties are set as: the real modulus of glass fibre is 72.4Gpa, fibre damping factor is 0.0014, fibre volume fraction is 60%, the real modulus of matrix is $E_{mr} = 1158(1 + 100f)^{0.1}$, with f as frequency, and damping factor of matrix is 0.05. *106*

Figure 5.10 Impact response of composite laminates with various fibre aspect ratios, i.e. 5 (solid line), 30 (dashdot line), and 100 (dashed line). Other material properties are set as: the real modulus of glass fibre is 72.4Gpa, fibre damping factor is 0.0014, fibre volume fraction is 60%, the real modulus of matrix is $E_{mr} = 1158(1 + 100f)^{0.1}$, with f as frequency, and damping factor of matrix is 0.15. *107*

Figure 5.11 Impact response of composite laminates with various fibre aspect ratios, i.e. 5 (solid line), 30 (dashed line), and 100 (dashdot line). Other material properties are set as: the real modulus of glass fibre is 72.4Gpa, fibre damping factor is 0.0014, fibre volume fraction is 60%, the real modulus of matrix is $E_{mr} = 1158(1 + 100f)^{0.1}$, with f as frequency, and damping factor of matrix is 0.05. *108*

CHAPTER 1

VISCOELASTIC RESPONSE BEHAVIOUR OF ENGINEERING MATERIALS

1.1 Introduction

With the recent advances in modern industrial materials, such as high polymers and polymeric base composite materials, and their extensive applications in aerospace and other industries, the subject of the study of the mechanical response of such class of material is attracting more and more attention from material scientists and engineers, and it has become one of the most active research fields in materials science.

In classical materials science, the theory of elasticity plays an extremely important role, because conventional engineering materials such as metals can be considered as elastic, provided that the occurring deformations are small. Linear elasticity is a concept which is based on the observation that, in a perfectly elastic body, the stress which is induced by loading is to be directly proportional to the occurring strain and is independent of the strain rate. Thus, the load-deformation curve of a perfectly elastic solid will follow the same path for both loading and unloading, and the material will regain its original dimensions instantaneously upon the removal of the load. The mathematical description of such response behaviour is given by the well-known Hooke's law. The constant proportionality coefficient between the stress and the corresponding strain is the Young's

modulus of the materials. For an ideal elastic material, all the energy is stored and recovered in each loading cycle.

On the other hand, the mechanical response of a viscous fluid can be dealt with within the realm of the classical theory of viscosity. Thus, in a Newtonian fluid, the rate of strain is assumed to be directly proportional to the imposed stress. The mathematical description of such material property is given by Newton's law of linear viscosity. The Newtonian viscous fluid has no capacity of storing mechanical energy.

In the real world, materials may not often exhibit linear elastic or perfect viscous behaviour alone. The classical theories of linear elasticity and viscosity deal with two idealized concepts which are used to describe two types of totally different physical phenomena. A real material, however, may possess properties characteristic of both elastic and viscous media. This phenomenon is termed "viscoelasticity". A viscoelastic material is, thus, characterized by a certain level of rigidity of an elastic solid body, but, at same time, it flows and dissipates energy by frictional losses as a viscous fluid (e.g., Haddad[1] 1995). From a phenomenological point of view, two fundamental concepts in the theory of viscoelasticity can be defined, i.e. creep response under constant stress and stress-relaxation response under constant strain.

1.1.1 Creep Response

When a viscoelastic material is subjected to a constant stress, it neither behaves like a Hookean elastic material which responds instantaneously with a corresponding state of constant deformation, nor does it respond by a corresponding steady flow process as a Newtonian viscous fluid. A viscoelastic material may experience an instantaneous deformation, but does not hold it constantly, instead, it continues to flow with time. This distinct property is termed "creep". The ratio of the occurring time-dependent strain to the magnitude of the constant stress input is a measure of the time-dependent creep response of the viscoelastic material and is referred to as the "creep compliance function".

1.1.2 Stress Relaxation

When a viscoelastic material is subjected to a constant strain, the occurring stress in the material decays gradually with the passage of time. The ratio of the occurring time-dependent stress to the magnitude of the constant strain input is a measure of the time-dependent stress-relaxation response of the viscoelastic material and is termed as the "stress- relaxation modulus".

In addition to the above two fundamental phenomena, damping is considered to be an important characteristic of the materials in many applications, including, for instance, ground-based and air-borne vehicles, space structures, and many others.

Damping can be considered as the transformation of vibrational energy into some other form of irrecoverable energy. In response to a transient or dynamic loading, and in particular impact loading, structures can experience excessive vibrations that create high noise levels, stress fatigue failure, premature wear, operator discomfort, and unsafe operating conditions. An improved understanding of various theoretical and experimental aspects of vibration in composites, and of the involved damping mechanisms in these materials, is essential for the ultimate purpose of avoiding or eliminating such potential problems.

Consider the stress-strain curve, Figure 1.1, corresponding to a particular load cycle applied repeatedly to a viscoelastic material. The process of "friction" causes a loss of energy per cycle which is equal to the area, ΔW, within the hysteresis loop. The modulus is defined by the average slope of the stress-strain loop. For most materials, the loop almost degenerates into a straight line, which provides a unique definition of modulus. The energy dissipation under steady-state vibration is usually defined in terms of the specific damping capacity ϕ, which is taking as the ratio $\Delta W/W$, where W is the maximum strain energy per unit volume.

1.2 Subject of the Present Research

The theoretical modeling of damping and dynamic (complex) modulus as two most widely used vibration characteristics, and the study of dynamic response under impact

loading in composites attract more and more attention from research scientists and engineers, and have become one of the most active research fields in engineering mechanics. The construction of precise models for describing these properties for composite materials, and for predicting material response under various loading conditions, has become a very important task in understanding in depth the viscoelastic nature of composite materials and their potential failure modes. This subject is selected to be the topic of the present research.

1.2.1 Theoretical Modeling of Damping and Complex Modulus

In order to analyze and predict vibration in composites, several models have been developed in the literature. These models may be classified into the following two categories.

1. **Conventional Macromechanical Models**

Conventional macromechanical method uses classical lamination theory to predict damping and modulus properties in composites[2]. The classical lamination theory requires the determination of eighteen material parameters (constants) in the elastic constitutive equations of laminated composites. In view of the correspondence principle, these elastic constants may then be correspondingly replaced by their viscoelastic counterparts. Following this approach, one could eventually obtain models for the determination of the damping and complex modulus of the dealt with composite system.

Another version of modeling which is dealt with within the realm of macromechanics utilizes the strain energy approach[3, 4]. In this approach, both the strain energy and the energy dissipated in any element of each layer are separated into three components, corresponding to longitudinal tension/compression, transverse tension/compression, and longitudinal shear loading. These components have to be measured experimentally. The total energy dissipation ΔW is obtained by integrating the sum of the three energy dissipation components over the whole plate section. The maximum strain energy W stored by the plate can also be calculated by the plate theory. The specific damping capacity of the laminate is then given by $\phi = \Delta W / W$. The solution to the equations in this method is usually only feasible using a computerized numerical technique.

2. Micromechanical Models

For unidirectional continuous fibre reinforced composites, the loss factor (damping) is traditionally derived from a simple rule-of-mixture equation in conjunction with the elastic/viscoelastic correspondence principle[5].

On the other hand, for aligned discontinuous fiber composites, a theoretical analysis of internal damping and dynamic stiffness is developed based on micromechanics models in order, for instance, to determine the complex moduli[6-9]. In this approach, the expression for the elastic stiffness of the discontinuous fibre reinforced composite is often derived first. Then, the elastic/viscoelastic correspondence principle is used to obtain the expression for the complex modulus and damping.

The most distinct advantage of the micromechanical modeling method over conventional macromechanical modeling method is that the micromechanical modeling method allows the inclusion, in the analysis, of basic microstructural parameters such as fibre aspect ratio, fibre volume fraction, fibre orientation, ... etc. This allows the determination of the effects of such parameters on both the damping and dynamic modulus of the composite. Therefore, micromechanical modeling is recently attracting more and more attention from researchers. The reader is referred to Chapter 2 for a brief review on the micromechanical modeling method (see, also, Jang[2]).

One objective of this thesis is to adopt the micromechanical modeling method in order to obtain expressions for the damping and complex modulus of the composite, in terms of fibre aspect ratio, fibre volume fraction, and fibre orientation. In this context, the aim is to develop a new approach to optimize the design of the considered composite material in order to achieve optimum damping and optimum mechanical stiffness simultaneously.

1.2.2 Theoretical Modeling of Dynamic Response of Composites under Impact Loading.

Impact response of fiber-reinforced polymer composites is a complex phenomenon. Such response behaviour is not a unique function of the response characteristic of the constituent fibre and matrix and, hence, the response characteristics can not be predicted by a simple law like the rule-of-mixture principle. This subject, i.e., the impact response of composites, has become a critical subject of materials research. However, our grasp of the impact response in composites is still quite limited, possibly because this complex

phenomenon involves many different microstructural interactions and their involved kinematical and kinetical parameters. Studies of impact dynamics aim at providing in-depth understanding of the nature of impact response of composites, thus, we may then possibly predict post-impact residual properties and consequently improve the damage resistance of composites.

To achieve the above objective, numerous analytical models have been developed by research workers in the field to simulate the impact response of composite laminates. These models may be selectively classified into the following three main categories.

1. **Simplified Analysis**

Simple models allow us to understand the main features of impact and are useful in handling experimental data. Simplification is achieved by assuming the form of the contact pressure distribution. There are three main simplified approaches followed in the literature. These may be described as follow:

(a) <u>The spring-dashpot-mass approach</u>

Spring-dashpot-mass models are often used to analyze impacts when the structure behaves quasi-statically. This approach represents the structure as an assemblage of springs and masses so that a discrete mechanical system with few degrees of freedom is analyzed instead of a continuum[10-12].

(b) The energy-balance approach

The spring-dashpot-mass models are used to determine the entire history of the contact force and the displacements. However, when only the maximum contact force and the contact duration are needed, these data can be obtained more efficiently by the energy-balance approach[12]. In the latter approach, one considers the conservation of energy without the need of computing the entire time history. When the contact force reaches its maximum, the kinetic energy of the projectile is zero, and its total kinetic energy has been used to deform the target and produce local indentation. Both the energy stored during the deformation of the target and the energy absorbed by the indentation process can be expressed in terms of the maximum impact force which can, then, be related to the initial velocity of the projectile.

(c) The wave propagation approach

When the dynamics of the structure must be accounted for, beam, plate or shell theories are often used. Hence, the complexity of the models increases, and, in general, exact solutions can not be found. Approximations can be sought, however, using Fourier transform and/or Laplace transform methods. "Mindlin's Plate theory" and "First Order Shear Deformation Plate theory", for instance, have been used by various researchers[13-17] to obtain wave propagation solutions.

The review on the wave propagation approach can be found in Chapter 4. The reader is also referred, among others, to Abrate[18, 19].

2. The Indentation Approach

The analysis procedure for the indentation approach consists of three steps[20]:

(i) Determination of impactor-induced surface pressure and its distribution;

(ii) Determination of internal stresses in the composite target caused by the surface pressure;

(iii) Determination of failure modes in the target caused by the internal stresses.

The stresses due to contact between the impactor and the target can produce damage in the composite locally. The contact phenomenon is rather complex, whereas the contact force and the pressure distribution over the contact zone are not known *a priori* and must be determined as part of the solution. In the case of flexible targets, the overall deflection of the structure as well as the local stresses near the contact region must be considered.

Another objective of the present research is to simulate the dynamic response of viscoelastic laminated composites under impact loading, e.g., when the viscoelastic nature of polymer composites must be accounted for. Here, the complexity of the models increases due to the time-dependency of the problem and, hence, the presence of integro-differential constitutive relations (see Haddad[1]). In this context, models can be established in frequency-domain by using Fourier transform and/or Laplace transform. Consequently, the solution is obtained by inverting the original transform using, e.g., an inversion of Fast Fourier Transform (IFFT) algorithm (see, also, Haddad[21]).

1.3 Outline of the Present Research

The present research can be divided into two parts, and has been carried out according to the following steps:

A) Modeling and optimization of damping and stiffness properties of viscoelastic discontinuous fibre reinforced composites under quasi-static loading.

B) Simulation of dynamic response of a viscoelastic laminated composite plate.

In this context, new approaches to modeling and simulation of the response behaviour of the referred to composite system, under various loading conditions, have been established.

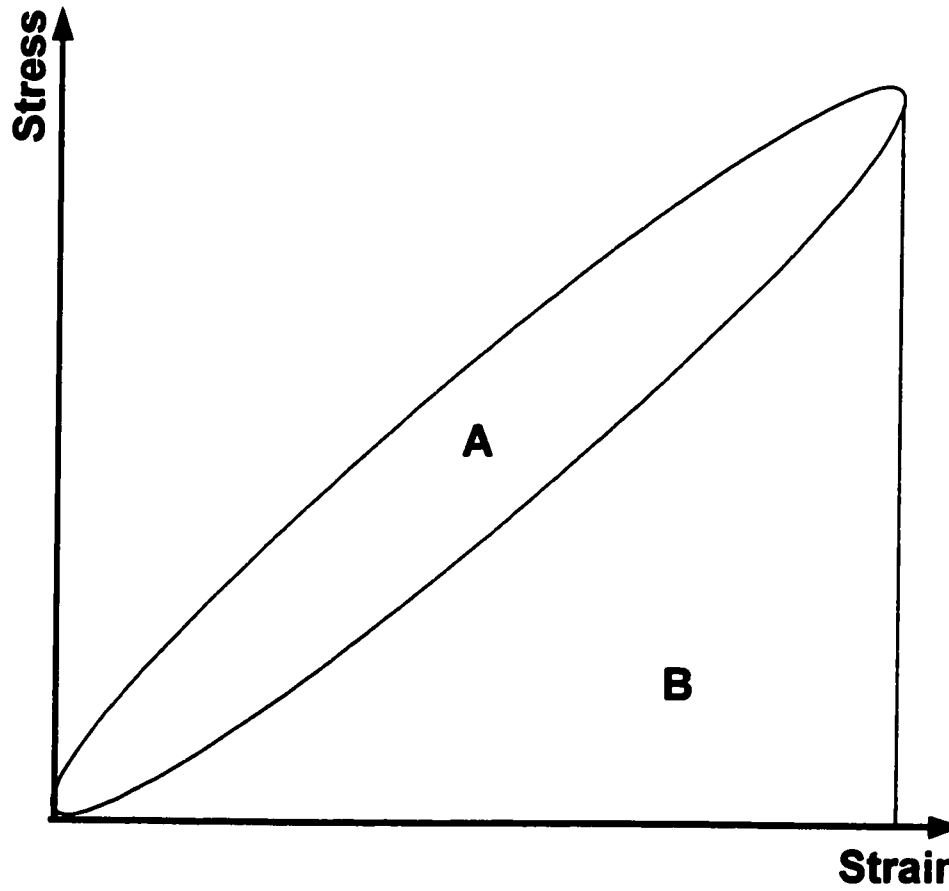

$A = \Delta W =$ energy dissipated
$W = A + B =$ energy input
$\Delta W / W =$ specific damping capacity

Figure 1.1 Specific damping capacity in a mechanical system

CHAPTER 2

A REVIEW ON MODELING OF THE VISCOELASTIC RESPONSE OF LAMINATED COMPOSITE MATERIALS

2.1 Introduction

Laminated composite materials, with their high specific modulus, high specific strength, and capability of being tailored for a specific application, offer definite advantages when compared to their metallic counterparts. These materials are used extensively in aerospace, automotive and other applications.

However, the behavior of laminated composite materials under various loading conditions is a concern, as they may experience more complex deformation mechanisms than their metallic counterparts under ordinary service loading conditions. Our grasp of their response under various loading conditions is still limited, possibly because the deformation process occurring in such materials involves many different microstructural interactions and pertaining dynamic parameters, as we mentioned earlier. Modeling such response may provide in-depth understanding of the mechanisms involved and consequently would improve the damage resistance of such material.

2.2 Micromechanical Modeling Approach

The methods of modeling damping and stiffness properties can be classified into two categories, namely, the macromechanical and micromechanical approaches. The micromechanical approach, as being widely used in damping and stiffness modeling methods, will be utilized in the present thesis. The review of this topic is carried out in this section.

Yim[22], for instance, assumed that the composite is loaded along the fiber direction and that all the energy dissipation occurs in the matrix. Yim[22] derived an expression for the loss factor of a unidirectional continuous fibre composite from a simple rule-of-mixture equation in conjunction with the elastic-viscoelastic correspondence principle. The arrived at expression is written as

$$\eta_c = (1 - V_f)\eta_m E_m / E_c \tag{2.2.1}$$

where η_c and η_m are the loss factor of the composite and the matrix under direct loads, respectively, E_m is elastic modulus of matrix and E_c is the elastic modulus of the composite in the fibre direction.

This approach underestimates considerably the true value of the damping property of the considered composite. This discrepancy is likely due to the following contributing factors[5]:

- For composites with the same fibre volume fraction, the smaller the fibre diameter, the larger the surface area per unit volume. A consistent increase in η_c with reduction in fibre diameter was observed[22] in the case of glass fibre-polyester system. This implies that fibre contribution cannot be neglected.
- The effect of fibre misalignment was not considered in the derived-at Equation (2.2.1).
- Structural defects, such as voids and interfacial debonding cracks, can lead to interfacial rubbing and hence additional energy loss.

Sun, et al.[6-9], developed a theoretical analysis of internal damping and dynamic stiffness for aligned discontinuous fibre reinforced composites based on the "Force-Balance Approach", which will be explained in detail in Chapter 3, for the complex moduli. In this approach, the expression for the elastic stiffness of the discontinuous composite was derived first. Then, the elastic/viscoelastic correspondence principle was used to obtain the expression for the complex modulus and damping. This method can predict an optimum fiber aspect ratio for maximum damping.

When the anisotropic nature of the fibre-composite system is taken into account, the micromechanical models can be modified to give expressions for the complex transverse modulus and the complex in-plane shear modulus of the desired composite.

Other researchers[23, 24] used a similar approach to obtain the complex moduli and damping of composites subjected to off-axis loading.

Alternative micromechanical models for the prediction of damping properties of continuous fibre reinforced laminas from constituent material properties and volume fractions have been proposed[25, 26]. Gibson, et al.,[27] also conducted research to analyze the vibration response of randomly oriented short fiber-reinforced laminae. A micromechanical strain energy/finite element technique[28, 29] for modeling damping in discontinuous aligned fibre composites has been developed. This technique has the capability of predicting the effects of interaction between fibres, as well as fibre/matrix interface on composite damping. The numerical data and experimental measurements show that the above mentioned interaction does affect the damping of discontinuous fiber composites, and that the damping can be improved by increasing the fibre end gap size or by decreasing the fiber-aspect ratio.

2.3 The Elastic/Viscoelastic Correspondence Principle

For a fairly large number of viscoelastic problems, and composite materials in particular, the difficulty in determining the expression for the complex modulus arises due to the viscoelastic nature along with the heterogeneity and anisotropic properties of the dealt with composite system.

There exists an analogy method which relates mathematically the solution of a linear, viscoelastic problem to an analogous problem of a linear elastic body of the same geometry and under the same initial and boundary conditions. This is carried out by transforming the governing equations of the viscoelastic problem to be mathematically equivalent to those governing a corresponding elastic problem. In this, both Laplace and Fourier transforms are often used. Accordingly, one would be able to employ the tools of the theory of elasticity to solve problems in linear viscoelasticity[1]. This analogy method is referred to as the "correspondence principle".

Researchers, e.g. [30, 31], utilize the elastic/viscoelastic correspondence analogy to derive transformed viscoelastic solutions for isotropic media by using existing elastic analysis procedures. Relatively few researchers have attempted to apply the correspondence principle to anisotropic materials.

Hashin[32] examined and developed the correspondence principle for the purpose of application on viscoelastic composites. His research concluded that the effective complex

moduli $B^{*}_{ijkl}(i\omega)$ of a viscoelastic heterogeneous specimen are found by replacement of phase elastic moduli by phase complex moduli $B^{(r)}_{mnop}(i\omega)$ within the expressions ${}^{e}C^{*}_{ijkl}$ for the effective elastic moduli of an associated heterogeneous elastic specimen, with identical phase geometry. Symbolically, this was expressed as[32]

$$B^{*}_{ijkl}(i\omega) = {}^{e}C^{*}_{ijkl}[B^{(r)}_{mnop}(i\omega)] \tag{2.3.1}$$

Then, the effective complex moduli B^{*}_{ijkl} can be further separated into real and imaginary parts as(Hashin [32])

$$B^{*}_{ijkl}(i\omega) = B^{*R}_{ijkl}(\omega) + iB^{*I}_{ijkl}(\omega) \tag{2.3.2}$$

In the following Chapter, quasi-static models are developed by using a "Micromechanical Approach" ("Forced Balance Approach") to define mechanical response properties of discontinues fibre reinforced composite materials. The effects of micromechanical parameters, such as fibre aspect ratio, fibre off-axis angle and fibre volume fraction, on the damping and stiffness of a fibre-composite system are, then, examined. Subsequently, simultaneous optimization of damping, stiffness and weight is carried out by using the so-called "Inverted Utility Function Method".

CHAPTER 3

OPTIMIZATION OF THE MECHANICAL BEHAVIOUR OF DISCONTINUOUS FIBRE REINFORCED COMPOSITES WITH THE INCLUSION OF THE MICROSTRUCTURE

3.1 Introduction

It is well-known that light-weight fibre reinforced polymer composite materials have higher specific strength and specific stiffness when compared with conventional materials. Much effort has been devoted to the improvement and optimization of these properties in various composite structures. Good vibration damping properties are also particularly important for composite structures when they are used under dynamic loading, such as in aerospace structures, rotor blades, circuit boards, high-speed printer components, etc. As mentioned in the following, due in part to the extensive accumulated experience with conventional structural metals having poor internal damping characteristics, the potential for significant improvement and optimization of damping in advanced fibre reinforced composites has not been yet fully realized. At the same time, the full use of discontinuous fibre reinforcement has not yet been realized in advanced composite materials research, because of the direct realization of higher strength and stiffness currently available in continuous fibre composites.

In the conventional damping theory, the damping factor is considered to vary comparatively little

with frequency[33] for most polymers, at temperatures near their glass-transition temperature. Thus, most researchers, by following this theory, considered the damping factor as constant. However, in the case of fibre reinforced composites, discontinuous fibre composite in particular, the damping factor is not only frequency-dependant, but it also varies considerably with the microstructure, e.g., fibre aspect ratio, fibre volume fraction and fibre off-axis angle[6-9].

The damping properties of continuous fibre composites have been studied by a number of investigators[34, 35]. There are relatively few reports on such work in the case of discontinuous fibre composites. However, studies reported by McLean and Read[36] and Gibson, et al.[6-9,37] indicate that vibration damping properties of fibre reinforced composite materials of polymeric matrix may be significantly improved and possibly optimized by using, as a reinforcement, discontinuous fibres rather than continuous fibres. More specifically, these studies[6-9,36,37] examine the effects of fibre aspect ratio, fibre spacing, fibre orientation and the viscoelastic properties of matrix and fibre materials on the damping and stiffness of discontinuous fibre reinforced polymer matrix composite materials.

One possible explanation for the above mentioned advantages for the case of discontinuous fibre composites is the presence of shear stress concentrations at the fibre ends in the discontinuous fibre composites, and the resulting additional shear stress transfer mechanism from the fibre end to the viscoelastic matrix. It is often argued that shear deformation may be responsible for most of the vibrational energy dissipation in viscoelastic materials such as polymers.

An analysis by Bert[35] of the damping of discontinuous constrained viscoelastic layers appears to offer an analogous solution for the case of discontinuous, aligned fibre reinforcement. This analogy is based on the similarity of the interfacial shear stress distribution along discontinuous constraining layers and that along discontinuous reinforcing fibres. The approximate stress distribution along a discontinuous fibre embedded in a matrix was first reported by Cox[38]. Meanwhile Bert[35] also showed, both analytically and experimentally, that there is an optimum constraining layer aspect ratio which would correspond to a maximum damping in the constrained viscoelastic layer. Thus, the existence of such an optimum aspect ratio in the case of the short fibre composites may seem apparent.

The research work of Gibson et al.[6-9,37] indicates that by varying the fibre aspect ratio and fibre orientation, the maximum damping and stiffness properties could be achieved separately. This observation implies that the optimum fibre aspect ratio and orientation for damping are not necessarily the optimum for stiffness. Consequently, it is important to study the influence of the various governing microstructural parameters on both damping and stiffness. The optimization of the trade-offs between damping and stiffness is the main intention of this chapter.

It is obvious that the most ideal situation for designing a discontinuous fibre reinforced polymer composite structure is to optimize damping and stiffness with respect to the composite microstructure controlling parameters. In this chapter, the general procedure of the "Force-Balance Approach", which was proposed by Sun et al.[8], is used to derive the analytical models for optimizing the damping and stiffness of discontinuous fibre reinforced composite materials.

In this context, a multi-objective optimization method is adopted to optimize these two properties at the same time. A particular application is being dealt with here, i.e., a discontinuous E-glass/epoxy composite system.

3.2 Theoretical Analysis: Force-Balance Approach

There appear to be two primary sources of enhanced damping in polymeric matrix materials: (i) the viscoelastic nature of the bulk matrix and, by consequence, that of the interface, and (ii) the friction mechanism at the interface as caused by the relative motion between the matrix and the fibre. Both of these effects may prove to be significant in the case of discontinuous fibre composites whereas high shear stresses are developed at the fibre-matrix interface. When a short fibre composite is subjected to a cyclic strain, the matrix at the fibre interface near the ends of the fibre undergoes a high cyclic shear strain, thus producing significant viscoelastic energy loss. It should be noted that most of the energy dissipation in polymers is due to shear strains, and very little energy dissipation is caused by dilatational strains (see, e.g., Gibson et. al.[7,8]). Thus, only in pure hydrostatic loading would there be no energy dissipation.

The shear stress concentration may also induce partial debonding at the fibre/matrix interface that would result in slip between the fibre and the matrix and in accompanying frictional losses. Such a fibre/matrix debonding would, however, affect adversely the strength and stiffness of the

composite. It is desirable, therefore, to have a strong interfacial bond so that slip at the interface may be avoided. Thus, the most viable mechanism of enhanced dissipation appears to be the shear deformation in the matrix caused by shear stress concentration near the fibre ends. Based on the stress transfer mechanism between the fibre and the matrix, it is obvious that there are several microstructural parameters (e.g. fibre aspect ratio, fibre volume fraction, fibre/matrix modulus ratio, etc.) that would influence the shear stress distribution at the interface and also the stress transfer mechanism between the fibre and the matrix. The matrix surrounding a short fibre in a composite experiences, in general, a three dimensional state of stress even though the composite may only be subjected to a uniaxial state of stress. The situation becomes further complicated when the interaction with neighbouring fibres is also taken into account. We therefore chose to use the "Force-Balance Approach"[7] to predict the damping and stiffness for this class of materials. The "Force-Balance Approach" is often regarded as a combination of an elastic "Mechanics-of-Materials" analysis, which could reasonably predict the stress transfer at the interface, in conjunction with the "Elastic-Viscoelastic Correspondence Principle"(see, e.g.,Hashin[32]).

The basic assumptions concerning the model for the "Force Balance Approach" are:

(a) A round fibre, surrounded by a cylindrical matrix, is acted upon by an extensional load, Figure 3.1.

(b) Both the fibre and matrix are isotropic.

(c) The matrix is linearly viscoelastic in response.

(d) The fibre has some contribution to energy dissipation and it is assumed to behave in a

linearly viscoelastic manner, therefore the loss factor of fibre may be nonzero.

(e) There is a perfect bond between the fibre and the matrix, and the interface is assumed to have the same viscoelastic properties as that of the bulk matrix.

(f) There is no load transfer between the fibre and the matrix through the ends of the fibre.

(g) The transfer of load from the matrix to the fibre depends upon the difference between the actual displacement at a point on the interface and the displacement that would exist if the fibre was absent[39].

In the force-balance approach, the expression for the elastic stiffness of the discontinuous-fibre composite is derived from the average fibre stress based upon Cox's fibre stress distribution[38]. Then, the elastic-viscoelastic correspondence principle is used to obtain the expression for the complex modulus for the dealt with linear viscoelastic composite. This involves replacement of the elastic moduli of the fibre, matrix and composite in all expressions with the corresponding viscoelastic complex moduli under sinusoidal vibration. The complex equation for the composite modulus then becomes two equations for storage and loss moduli (see, e.g., Haddad[1]).

For a typical representative volume element, as shown in Figure 3.1, the expression of the modulus, E_x, of the composite along the loading direction axis was given by (see, e.g., Agarwal, et al.[40]),

$$\frac{1}{E_x} = \frac{\cos^4\theta}{E_L} + \frac{\sin^4\theta}{E_T} + \left(\frac{1}{G_{LT}} - \frac{2\nu_{LT}}{E_L}\right)\sin^2\theta\cos^2\theta \tag{3.2.1}$$

This equation is originally derived for continuous fibre reinforced composites, and can also be applied here to the case of short fibre reinforced composites. In this equation, E_L, E_T, G_{LT} and ν_{LT} are longitudinal modulus, transverse modulus, in-plane shear modulus and major Poisson's ratio, respectively and can be expressed in term of E_f, E_m, G_f, G_m, *etc*, and fibre volume fraction, V_f, for continuous fibre reinforced composite, either by using the rule-of-mixtures, or the Halpin-Tsai equation (see, also, Agarwal, et al.[40]). For short aligned fibre composites, however, one cannot use the rule-of- mixtures or Halpin-Tsai equation to represent E_L [38]. For short aligned fibre composites, the longitudinal modulus also depends on the fibre aspect ratio, l/d. Based upon Cox's shear-lag model[38], E_L is given for the short fibre composite by

$$E_L = E_f\left(1 - \frac{\tanh(\beta l/2)}{(\beta l/2)}\right)V_f + E_m(1 - V_f) \tag{3.2.2}$$

where,

$$(\beta l)^2 = 8\frac{G_m}{E_f}\frac{(l/d)^2}{\ln(2R/d)} \tag{3.2.3}$$

The ratio R/d is related to the fibre volume fraction V_f, for the particular packing array under consideration. For example,

$$\left(\frac{R}{d}\right)^2 = \frac{\pi}{16V_f} \text{ for a square array} \tag{3.2.4}$$

$$\left(\frac{R}{d}\right)^2 = \frac{\pi}{8(3V_f)^{1/2}} \text{ for a hexagonal array} \tag{3.2.5}$$

Based upon the work of Gibson, et al.[7], packing geometry has an insignificant effect on the magnitude of damping. Therefore, one can use a square packing array in the subsequent analysis. Substitution of Equation (3.2.4) into Equation (3.2.3) gives,

$$(\beta l)^2 = 8\frac{G_m}{E_f}\frac{(l/d)^2}{\ln\left(\frac{\pi}{4V_f}\right)^{1/2}} \tag{3.2.6}$$

Equation (3.2.6) above shows that the parameter ($\beta\ l$) is essentially a function of fibre matrix stiffness ratio, E_f/G_m, fibre aspect ratio, l/d, and fibre volume fraction V_f.

The transverse modulus, E_T and the transverse in-plane shear modulus G_{LT}, of the short fibre composite are almost independent of fibre aspect ratio, l/d. Therefore, one can use the same formula as in the case of continuous fibre composites. In this research the Halpin-Tsai equations (see, e.g., Agarwal, et al.[40]) are used as,

$$E_T = E_m(1+2\eta_1 V_f)/(1-\eta_1 V_f) \tag{3.2.7}$$

$$G_{LT} = G_m(1+\eta_2 V_f)/(1-\eta_2 V_f) \tag{3.2.8}$$

where the coefficients η_1 and η_2 of above two equations can be expressed, respectively, as

$$\eta_1 = [(E_f / E_m) - 1] / [(E_f / E_m) + 2] \tag{3.2.9}$$

$$\eta_2 = [(G_f / G_m) - 1] / [(G_f / G_m) + 1] \tag{3.2.10}$$

The major Poisson's ratio, ν_{LT}, of the short fibre composite which is also insensitive to fibre length, may be expressed in a 'rule-of-mixture' form as,

$$\nu_{LT} = V_f \nu_f + \nu_m (1 - V_f) \tag{3.2.11}$$

According to the previous assumptions, both fibre and matrix are considered, in the present analysis, to be linear viscoelastic materials. This permits us to use the elastic-viscoelastic correspondence principle in order to redefine the basic material properties as,

$$E_x = E_x^* = E_x' + iE_x''$$

$$E_f = E_f^* = E_f' + i E_f''$$

$$E_m = E_m^* = E_m' + i E_m''$$

$$G_m = G_m^* = G_m' + iG_m'' \tag{3.2.12}$$

Here, primed quantities designate the storage moduli and the double primed quantities designate the loss moduli. The damping (or loss) factor is defined as the ratio between the loss modulus to

the storage modulus as

$$\eta_c = E_x''/E_x'$$

$$\eta_f = E_f''/E_f'$$

$$\eta_m = E_m''/E_m'$$

$$\eta_{Gm} = G_m''/G_m' \tag{3.2.13}$$

After using Equation (3.2.12), Equations (3.2.2), (3.2.6) to (3.2.10) may be written respectively as

$$E_L^* = (E_f' + iE_f'')\left(1 - \frac{\tanh(\frac{\beta^* l}{2})}{(\frac{\beta^* l}{2})}\right) + (E_m' + iE_m'')(1 - V_f) \tag{3.2.14}$$

$$E_T^* = (E_m' + iE_m'')\frac{1 + 2\eta_1^* V_f}{1 - \eta_1^* V_f} \tag{3.2.15}$$

$$G_{LT}^* = (G_m' + iG_m'')\frac{1 + \eta_2^* V_f}{1 - \eta_2^* V_f} \tag{3.2.16}$$

where

$$(\beta^* l)^2 = 8\frac{(G_m' + iG_m'')(l/d)^2}{(E_f' + iE_m'')\ln(\frac{\pi}{4V_f})^{1/2}} \tag{3.2.17}$$

$$\eta_1^* = \frac{[(E_f'+iE_f'')/(E_m'+iE_m'')]-1}{[(E_f'+iE_f'')/(E_m'+iE_m'')]+2} \tag{3.2.18}$$

$$\eta_2^* = \frac{[(G_f'+iG_f'')/(G_m'+iG_m'')]-1}{[(G_f'+iG_f'')/(G_m'+iG_m'')]+1} \tag{3.2.19}$$

Substituting E_L^*, E_T^* and G_{LT}^* from Equations (3.2.14) to (3.2.16) for E_L, E_T and G_{LT}, respectively, and E_x^* for E_x into Equation (3.2.1), one obtains

$$\frac{1}{E_x'+iE_x''} = \frac{\cos^4\theta}{E_L^*} + \frac{\sin^4\theta}{E_T^*} + \left(\frac{1}{G_{LT}^*} - \frac{2\nu_{LT}}{E_L^*}\right)\sin^2\theta\cos^2\theta \tag{3.2.20}$$

This equation can be used to determine E_x' and E_x'' for the composite by separating its real and imaginary parts.

By careful examination of Equation (3.2.14), one finds that E_L^* is an exponential function of ($\beta^* l$) which depends upon the complex stiffness ratio G_m^*/E_f^*.

Since the loss moduli are generally small, one may neglect the higher order terms of loss factors such as η_f^2 and $\eta_{Gm}\,\eta_f$. Following this approach, and by careful manipulation, one can obtain the following expression from Equation (3.2.17),

$$\frac{\beta^{*} l}{2} = \frac{\beta l}{2}\left[1+\frac{1}{2} i\left(\eta_{Gm} - \eta_{f}\right)\right] \tag{3.2.21}$$

Then, one may use a Taylor's series approximation and similarly neglect any resulting higher order terms in the loss factors to obtain

$$\tanh\frac{\beta^{*} l}{2} = \tanh\frac{\beta l}{2} + \frac{i}{2}\frac{\beta l}{2}\frac{(\eta_{Gm} - \eta_{f})}{\cosh^{2}\frac{\beta l}{2}} \tag{3.2.22}$$

Finally, by combining Equations (3.2.14) to (3.2.16), and Equations (3.2.18) to (3.2.22), one determines analytical representations of E_x', E_x'' and η_x as dealt with in Appendix A.

The analytical expressions reached out in Appendix A are represented here symbolically as,

$$E_x' = \psi_1(E_m', E_f', G_m', (l/d), \theta, V_f, \eta_f, \eta_m, \eta_{Gm}, \nu_m, \nu_f) \tag{3.2.23}$$

$$E_x'' = \psi_2(E_m', E_f', G_m', (l/d), \theta, V_f, \eta_f, \eta_m, \eta_{Gm}, \nu_m, \nu_f) \tag{3.2.24}$$

$$\eta_x = \psi_3(E_m', E_f', G_m', (l/d), \theta, V_f, \eta_f, \eta_m, \eta_{Gm}, \nu_m, \nu_f) \tag{3.2.25}$$

3.3 Numerical Results and Discussions

In the Equation (3.2.25), η_x is defined as the ratio of E_x''/E_x' and does not have the same changing pattern as E_x'. Therefore, two dependent variables, the non-dimensional ratios E_x'/E_m' and η_x/η_m, are used in the following numerical presentations. In general, from the expressions for η_x and E_x', e.g., Equations (3.2.23) and (3.2.25), we have eleven variables, namely $E_f, E_m, \theta, V_f, G_m, \eta_f, \eta_m, \eta_{Gm}, \nu_f, \nu_m$ and l/d. A cross-plot and an optimization that would include all possible variations of these eleven variables are almost impossible and unnecessary. Therefore, in the following optimization analysis, we choose, as a particular example, epoxy as matrix material and E-glass as fibre material in the dealt with layers. The corresponding material properties of these two selected materials are presented in Table 3.1 (after Gibson et al.[25]). Consequently, we narrow down the optimization variables to three, namely, θ, V_f and l/d.

For most composite materials used in aerospace and automotive industries, the fibre volume fraction varies within the range of 50% to 70%. Meanwhile, the observation made by Cox[38] shows that, for short fibre reinforced composite materials, the reduction of the effective longitudinal modulus due to the load transfer from fibre to fibre is considered significant only for fibre aspect ratios, l/d, less than 100. Therefore, one could set that the fibre volume fraction to range from 50% to 70% and the fibre aspect ratio to range from 1 to 100.

Figures 3.2 to 3.7 are established by setting, respectively, the fibre off-axis angle θ as 0°, 20°, 40°, 60°, 80° and 90°, and plotting the non-dimensional ratios η_x/η_m and E_x'/E_m' against the fibre volume fraction V_f and the fibre aspect ratio l/d. It is obvious that with the increase of fibre off-axis angle θ, the values of the non-dimensional ratio η_x/η_m are increasing and those for E_x'/E_m' are decreasing. When fibre off-axis angle reaches a value between 40° to 60°, both η_x/η_m and E_x'/E_m' curves change their directions, which demonstrate that around a fibre off-axis angle θ within the range from 40° to 60°, both the ratios η_x/η_m and E_x'/E_m' reach their extreme values (maximum and minimum, respectively) almost simultaneously.

Figures 3.8 to 3.13, which are plotted by setting the fibre aspect ratio l/d at 5, 20, 40, 60, 80 and 100, respectively, present the non-dimensional ratios η_x / η_m and E_x' / E_m' against the fibre volume fraction V_f and the fibre off-axis angle θ. One can note that the value η_x / η_m decreases monotonously as the fibre aspect ratio l/d increases and for value of $l/d > 15$, the rate of decrease in value slows down until the fibre aspect ratio l/d reaches 20 and the value of η_x / η_m maintains a constant value afterwards. The non-dimensional ratio E_x' / E_m' also increases sharply until the fibre aspect ratio l/d reaches a value of about 20. Within the fibre aspect ratio ranging from 20 to 60, the non-dimensional ratio E_x' / E_m' increases slowly with the increase of the fibre aspect ratio l/d and seems to have a constant value from $l/d = 60$ upwards.

By setting the fibre volume fraction V_f at 50%, 60% and 70%, the non-dimensional ratios η_x / η_m and E_x' / E_m' against the fibre aspect ratio l/d and the fibre off-axis angle θ can be plotted as shown in Figures 3.14 to 3.16. Analyzing carefully these figures, one could identify that with the increase of the fibre volume fraction V_f, both the non-dimensional ratios η_x / η_m and E_x' / E_m' change almost linearly, with the values of η_x / η_m are monotonously decreasing and those for E_x' / E_m' are monotonously increasing.

It is apparent from the above mentioned results that among the three considered independent variables, the fibre off-axis angle θ has the most significant influence on the damping and stiffness of fibre reinforced composites (see, also Sun et al.[8]). All the numerical results obtained from Equations (3.2.23) and (3.2.25) appear to have good agreement with the observation made by Sun, Gibson and Chaturvedi, etc.[7-9]

3.4 Optimization

From the above numerical results and discussion, one could note that in order to increase the damping properties of a discontinuous fibre reinforced composite, it is necessary to sacrifice the stiffness for these materials. The analysis of trade-offs between damping and stiffness will gain more and more attention from research and design engineers in both automobile and aerospace industries because of high-volume use of discontinuous fibre reinforced composite materials in

these areas which require not only high stiffness and strength but also excellent damping properties in most applications. Therefore, the optimization of these two properties at the same time, in order to design high performance discontinuous fibre reinforced composite structure, becomes more important to the development of structural materials and structural dynamics technology.

One of the most important advantages of fibre reinforced composite materials over their metallic counterparts is its light weight which appears to be attractive to aerospace and automobile industries. Apparently, it is necessary to include this property in our optimization. Therefore, there are now three objective functions in this optimization problem, i.e., the maximization of both damping and stiffness and at the same time, minimization of weight simultaneously. The inverted utility function method [41] appears to be suitable to deal with this multiobjective optimization problem.

3.4.1 Inverted Utility Function Method

In this method, the utility function $U_i(f_i)$ is defined for each objective function depending on its importance compared to the other objective function as[41]

$$U_i = -w_i f_i(X) \tag{3.4.1}$$

where $f_i(X)$ is said to be the ith objective function, with the weighting factor as w_i, to be minimized. In the process of optimization, one can invert each utility function and try to minimize or reduce the total undesirability which is obtained as

$$U^{-1} = \sum_{i=1}^{k} U_i^{-1} = \sum_{i=1}^{k} \left(\frac{1}{U_i}\right) = \sum_{i=1}^{k} -\frac{1}{w_i}\frac{1}{f_i(X)} = \sum_{i=1}^{k} -a_i\left(\frac{1}{f_i(X)}\right) \tag{3.4.2}$$

where a_i is defined as

$$a_i = \frac{1}{w_i}; \qquad \sum_{i=1}^{k} a_i = 1$$

The solution of the problem is found by minimizing U_i^{-1} subject to the constraints. The selection of scalar weighting factor a_i depends on the importance of each objective function.

3.4.2 Multivariable Non-Linear Optimization

Therefore, in the present work, the corresponding utility functions of each objective function are set as

$$U_1 = w_1\left(\frac{\eta_x}{\eta_m}\right) \tag{3.4.3}$$

$$U_2 = w_2\left(\frac{E_x'}{E_m'}\right) \tag{3.4.4}$$

$$U_3 = -w_3\left(\frac{\overline{W}}{\overline{W}_m}\right) \tag{3.4.5}$$

where $\overline{W}$ is the weight for designed discontinuous fibre reinforced composite materials, which is defined in term of fibre volume fraction V_f as

$$\overline{W} = \overline{W}_f V_f + \overline{W}_m (1 - V_f) \tag{3.4.6}$$

η_x and E_x' are defined by Equations (3.2.23) and (3.2.25), respectively. $\overline{W}_f$, $\overline{W}_m$, E_m' and η_m are set corresponding to the material properties of considered E-glass/epoxy discontinuous fibre reinforced composite as Table 3.1 shown.

Substitute Equations (3.4.3), (3.4.4) and (3.4.5) into Equation (3.4.2), the total undesirability of this design problem becomes

$$U^{-1} = a_1\left(\frac{\eta_m}{\eta_x}\right) + a_2\left(\frac{E_m'}{E_x'}\right) - a_3\left(\frac{\overline{W}_m}{\overline{W}}\right) \tag{3.4.7}$$

In the present optimization problem, both damping and stiffness are assumed to have almost same importance and are more important than weight. Then, one can arbitrarily set $a_1 = 0.5$, $a_2 = 0.4$, $a_3 = 0.1$. As the reason stated early in this chapter, the constraints for this optimization problem could be set as

$$0.5 \le V_f \le 0.7$$

$$1 \le l/d \le 100$$

$$0^o \le \theta \le 90^o \tag{3.4.8}$$

3.4.3 Implementation of Non-Linear Programming

Apparently, the optimization of this design work becomes

Minimize U^{-1}

Subject to $0^o \le \theta \le 90^o$

$$0.5 \le V_f \le 0.7$$

$$1 \le l/d \le 100 \tag{3.4.9}$$

This is a typical constrained non-linear optimization problem. In order to simplify this problem. One can adopt the mapping technique (variable transformation technique) to deal with the above parametric constraints[41]. By using this technique, the constrained optimization problem could be solved by non-constrained optimization techniques, (see, also, Rao[41]).

For the minimization problem $f(X)$ where $X^T = [x_1, x_2, \ldots, x_j]$ with the parametric constraints as

$$l_i \le x_i \le u_i \tag{3.4.10}$$

where $j = 1, 2, 3, \ldots, n$; $i = 1, 2, 3, \ldots, m$..

We can use the general mapping procedure[41] to model Equation (3.4.10) as

$$x_i = l_i + (u_i - l_i)\sin^2 y_i \tag{3.4.11}$$

By substituting Equation (3.4.11) into the objective function $f(X)$, one can incorporate the constrains, Equation (3.4.10), into the objective function $f(X)$. Therefore, the objective function $f(X)$ changes to $f(X^*, Y)$ with no constrains, where $Y^T = [y_1, y_2, \ldots, y_i]$ and X^* become all the components of variable vector X except x_i. If $m = n$, $f(X^*, Y)$ becomes $f(Y)$.

So, in this chapter, the mapping procedure can be utilized on the above mentioned parametric constraints, Equation (3.4.8), as

$$\begin{aligned} \theta &= 90^o \sin^2 y_1 \\ l/d &= 1 + 99 \sin^2 y_2 \\ V_f &= 0.5 + 0.2 \sin^2 y_3 \end{aligned} \tag{3.4.12}$$

where $Y^T = [\, y_1, y_2, y_3 \,]$ are the mapping variables in the above procedure. Therefore, one can convert this constrained non-linear optimization problem $U^{-1}(\theta,\ l/d,\ V_f)$, e.g., as Equation (3.4.9), to non-constrained non-linear optimization $U^{-1}(y_1,\ y_2,\ y_3)$ and solve this problem by using non-constrained optimization techniques for the sake of ease of calculation.

The "Simplex Method" which was originally given by Spendley, Hext and Himsworth[42] and later developed by Nelder and Mead[43] seems suitable for this non-constrained non-linear optimization with relatively small amount of variables. The movement of the "Simplex" of n+1 points in n-dimensional space towards an optimal point is achieved by using three operations known as "Reflection", "Contraction" and "Expansion" techniques (see, also, Rao[41]).

Following the algorithm of "Simplex Method" which is known as non-symmetric Nelder & Mead Simplex method (see Appendix C for flowchart), we implement a Fortran program called SIMPLX (see Appendix D) to solve this optimization problem.

3.4.4 Numerical Results and Discussions

Before running the Fortran program Appendix D, we have to set few parameters, namely, a starting point, desired accuracy of this problem, and a probe length which is used to construct the initial "Simplex", as well as "Reflection", "Expansion" and "Contraction" coefficients, as shown in the "Simplex" flowchart (see Appendix C). By setting the starting point as $Y^T = [\ 0, 0, 0\ ]$, the accuracy of this problem as $ACCUR = 0.001$, the probe length, which is used to construct the initial "Simplex", as $PLE = 0.1$, the "Reflection" coefficient $A = 1.0$, the "Expansion" coefficient as $Y = 2.0$, the "Contraction" coefficient $B = 0.5$ [41], the final result is given out as: the optimal fibre off-axis angle $\theta = 44.4^o$, the optimal fibre volume fraction $V_f = 60.60\%$ and the fibre aspect ratio $l/d = 1.49$.

These results have good agreement with the observations made by Sun and Gibson[8] that for small off-axis angles θ (say $\theta \leq 45^o$), η_x becomes maximum in whisker or microfibre composites range (i.e. for very small l/d, say $l/d \leq 5$) and the stiffness E_x' for microfibre and whisker composites is also relatively high. Therefore, in order to achieve high stiffness E_x' and high damping η_x, microfibre and whisker composites seem to be the ideal candidates. There is no comment available, in the referred-to reference, on the influence of fibre volume fraction V_f on the damping, stiffness and weight (as defined early, weight is only a function of fibre volume fraction V_f).

If the starting points, Y^T, are set at various points within useful intervals from [0,0,0] to [95,95,95] and with the various increments (0.5 or 5.0), and the same input parameters are used as above case. One could get outputs as shown in Table 3.2. In this case, it is obvious that we get multiple local minima, i.e., 0.5827. For each case of these local minima, the off-axis angle remains almost the same, i.e., approximately 43.75°, and fibre volume fraction and fibre aspect ratio change in opposite ways and could be catalogued into two groups, i.e., $l/d \approx 1.38$, $V_f \approx 62\%$ and $l/d \approx 85.09$, $V_f \approx 54\%$. It is obvious that this interesting observation gives more flexibility to the design of high performance fibre reinforced composites by using fibre with either lower fibre aspect ratio, i.e., $l/d \approx 1.38$ and relatively higher fibre volume fraction, i.e., $V_f \approx 62\%$, or higher fibre aspect ratio, i.e., $l/d \approx 85.09$ and relatively lower fibre volume fraction, i.e., $V_f \approx 54\%$ in the present research. A few studies[9] demonstrated that the high

fibre volume fraction, 62%, for the discontinuous fibre reinforced composites with lower fibre aspect ratio was practically achievable. It could be concluded from the above results that, when at the small fibre off-axis angle $\theta = 43.75^o$ and by approximately setting fibre aspect ratio at $l/d \approx 1.38$ or $l/d \approx 85.09$, the corresponding fibre volume fraction V_f reaches about 62% or 54%. In this case, we could get the maximum damping η_x, relatively high stiffness $E_{x'}$ and relatively low weight $\overline{W}$.

3.5 Conclusions

(1) Analytical predictions which were determined by the "Force-Balance Method" show that damping and stiffness are functions of fibre off-axis angle, fibre volume fraction and fibre aspect ratio. In order to increase the damping, it is necessary to sacrifice the stiffness, and vice versa.

(2) For a given E-glass/epoxy composite material, the results of optimization of damping, stiffness and specific weight show that approximately at fibre off-axis angle $\theta = 43.75^o$, by setting fibre aspect ratio $l/d \approx 1.38$ or $l/d \approx 85.09$, the corresponding fibre volume fraction V_f reaches 62% or 54%, respectively, and one could get the maximum damping, relatively high stiffness and relatively low special weight for this class of materials.

(3) The existence of multiple local minima gives more flexibility in the design of high performance discontinuous fibre reinforced composite materials, that is, in this research, both the microfibre or whisker composites ($l/d \approx 1.45$) and the discontinuous fibre reinforced composites with longer fibre ($l/d \geq 40$) can be selected as to the predefined design specifications.

(4) The "Inverted Utility Function Method" and "Simplex Method"[41], dealt with in Sections 3.4.1 and 3.4.3, respectively, are found to be suitable for dealing with this multiobjective optimization with relatively small amount of variables. The use of the "Variable Transformation Technique"[41], as dealt with in Section 3.4.3, to convert constrained non-linear optimization problem into non-constrained non-linear optimization makes this optimization problem easier to handle.

Table 3.1 Static properties of Scotchply 1002 Matrix Epoxy and E-glass fibres at room temperature, after Gibson, et al. [25]

Material Properties	Epoxy	E-glass
Young's modulus *GPa(10^6 Psi)*	3.79(0.55)	72.4(10.5)
Shear Modulus *GPa(10^6 Psi)*	1.38(0.2)	30.3(4.4)
Damping Factor	0.015	0.0014
Shear Damping Factor	0.018	0.0014
Poisson's Ratio	0.36	0.2
Specific Gravity (g)	1.23	2.54

Table 3.2 Optimization results for various starting points Y^T

Starting Point	Fibre Off-Axis Angle θ	Fibre Aspect Ratio l/d	Fibre Volume Fraction V_f	Local Minima
[0,0,0]	44.4°	1.49	60.6%	0.5833
[0.5,0.5,0.5]	43.9°	83.6	54.2%	0.5827
[1.0,1.0,1.0]	43.9°	66.7	54.6%	0.5828
[2.5,2.5,2.5]	44.1°	1.46	60.8%	0.5832
[5.0,5.0,5.0]	43.9°	97.4	54.3%	0.5827
[7.5,7.5,7.5]	44.3°	38.2	55.2%	0.5830
[10,10,10]	43.7°	49.7	54.3%	0.5829
[15,15,15]	44.0°	1.47	60.8%	0.5832
[20,20,20]	43.7°	100.0	54.1%	0.5827
[25,25,25]	43.0°	1.05	65.0%	0.5837
[30,30,30]	43.7°	99.8	54.2%	0.5827
[35,35,35]	43.5°	97.0	54.0%	0.5827
[40,40,40]	44.2°	1.44	60.6%	0.5832
[45,45,45]	43.8°	99.1	54.0%	0.5827
[50,50,50]	43.7°	57.9	54.8%	0.5828
[55,55,55]	43.7°	72.6	53.8%	0.5828
[60,60,60]	43.3°	97.2	53.6%	0.5827
[65,65,65]	43.4°	95.3	53.8%	0.5827
[70,70,70]	43.7°	96.4	54.2%	0.5827
[75,75,75]	43.4°	99.1	53.9%	0.5827
[80,80,80]	44.8°	88.0	54.2%	0.5827
[85,85,85]	43.8°	75.1	54.1%	0.5827
[90,90,90]	43.5°	84.8	54.1%	0.5827
[95,95,95]	43.2°	89.4	53.7%	0.5827

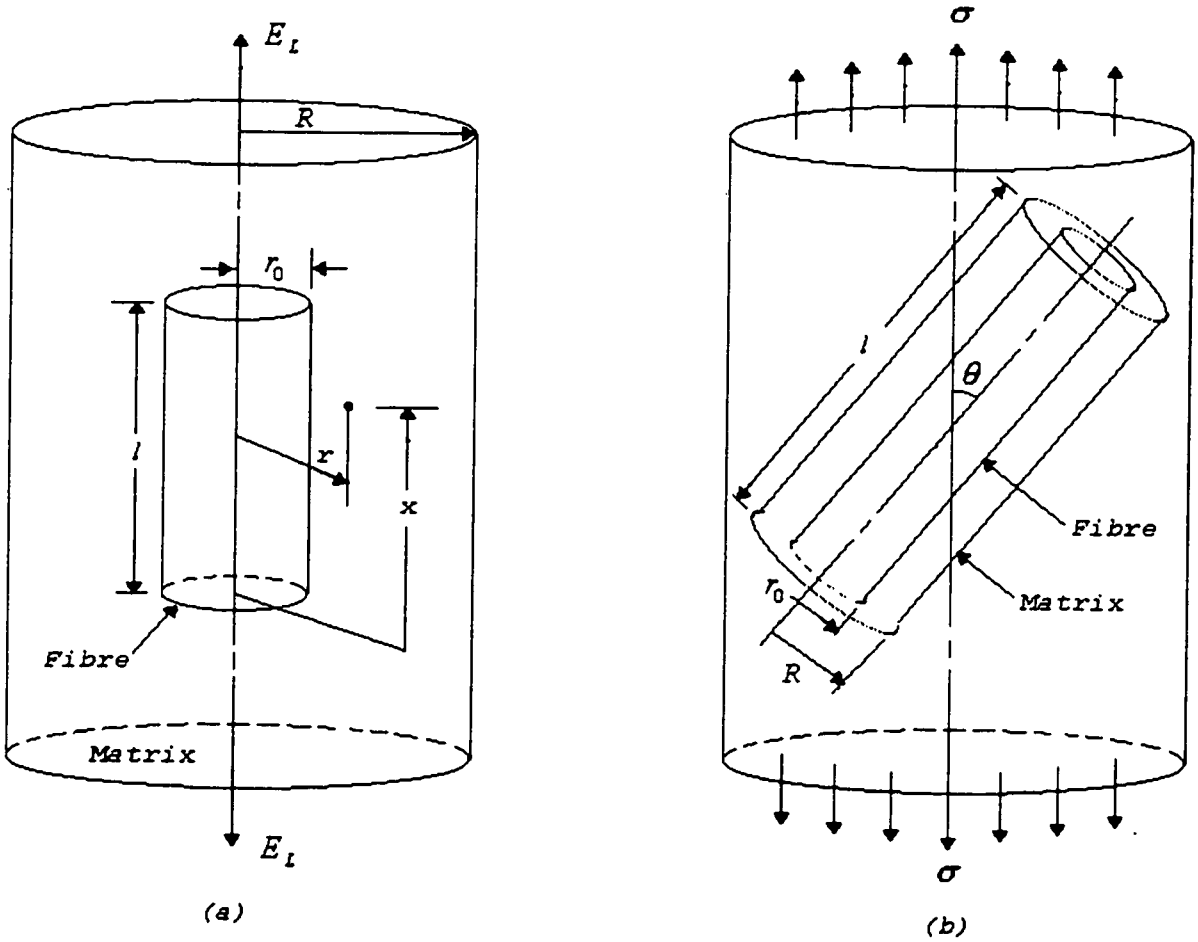

Figure 3.1 Representative Volume Element[8],
(a) Aligned Case, and (b) Off-Axis Case

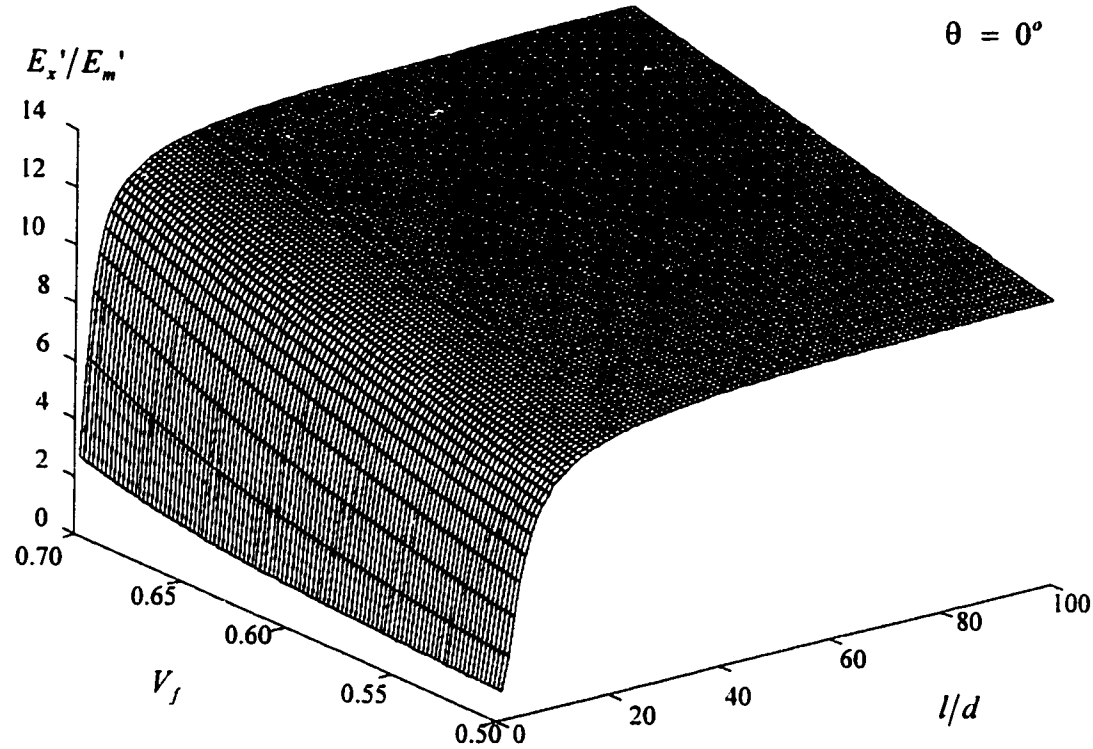

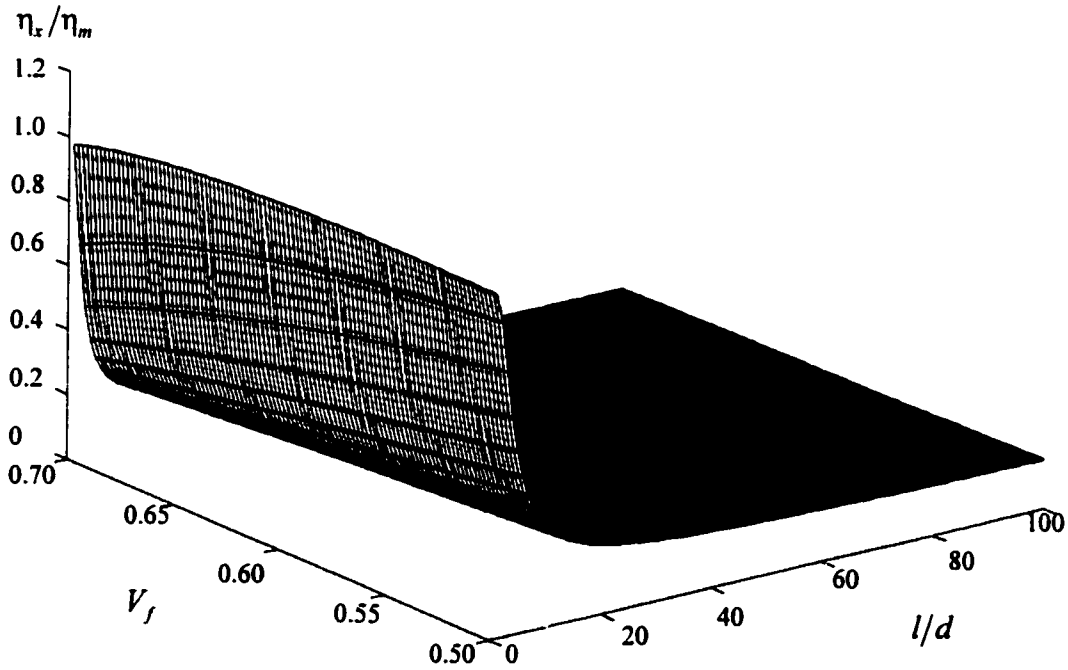

Figure 3.2 Non-dimensional Ratios η_x/η_m and E_x'/E_m' *vs* Fibre Volume Fraction V_f and Fibre Aspect Ratio l/d. Off-Axis Angle θ of the dealt with composite materials, with material properties of each component as shown in Table 3.1, is set to be 0°.

$\theta = 20^o$

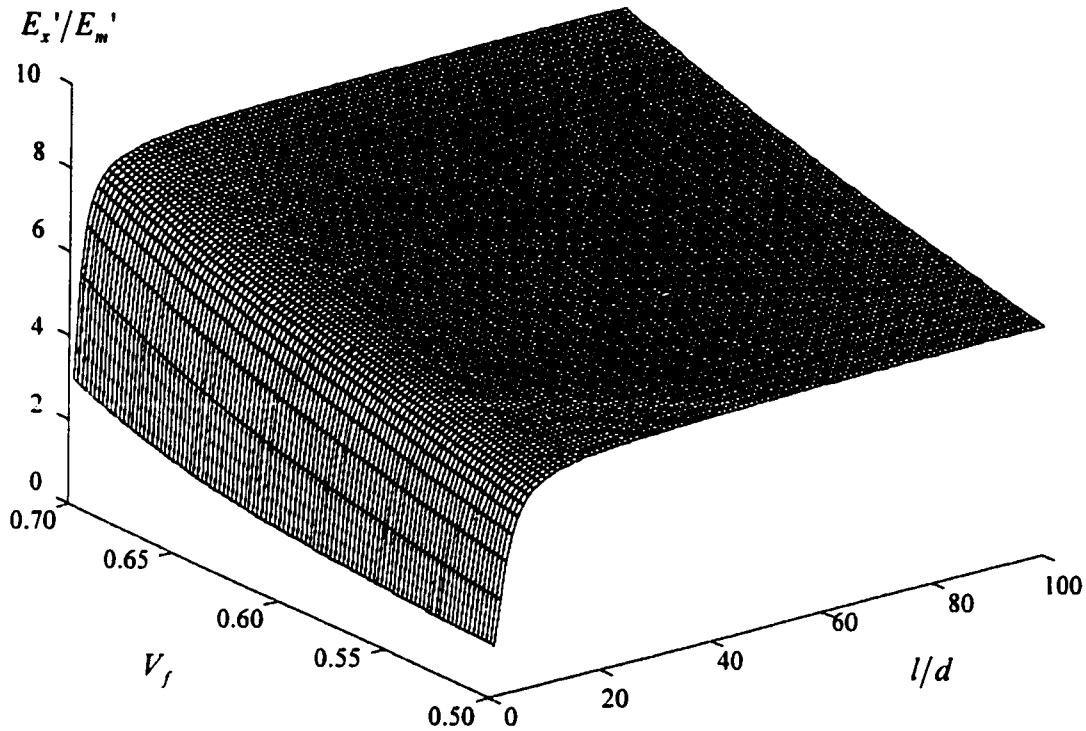

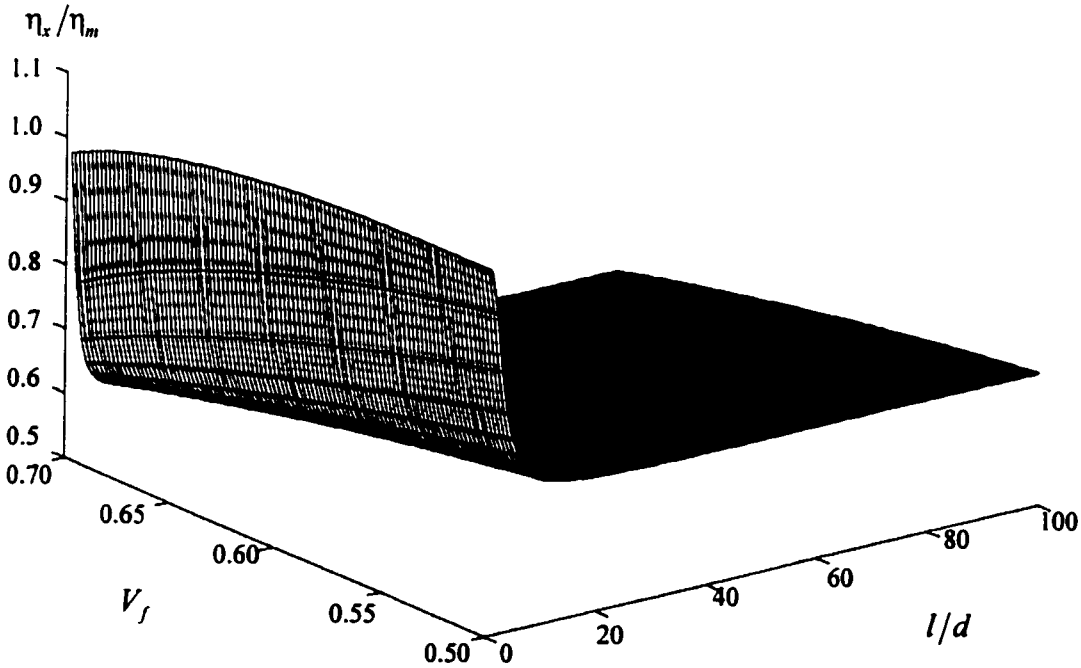

Figure 3.3 Non-dimensional Ratios η_x/η_m and E_x'/E_m' *vs* Fibre Volume Fraction V_f and Fibre Aspect Ratio l/d. Off-Axis Angle θ of the dealt with composite materials, with material properties of each component as shown in Table 3.1, is set to be 20°.

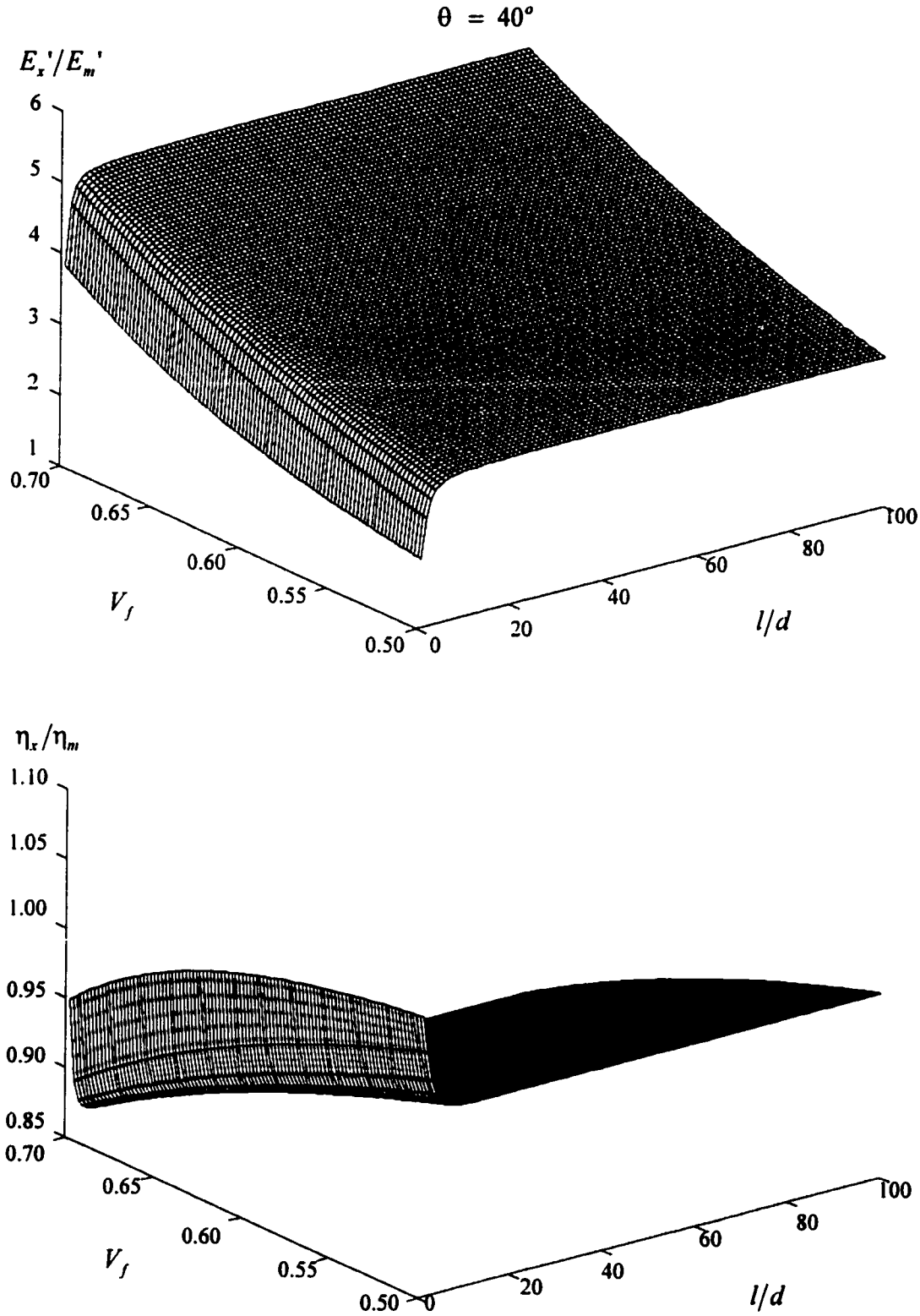

Figure 3.4 Non-dimensional Ratios η_x/η_m and E_x'/E_m' *vs* Fibre Volume Fraction V_f and Fibre Aspect Ratio l/d. Off-Axis Angle θ of the dealt with composite materials, with material properties of each component as shown in Table 3.1, is set to be $40°$.

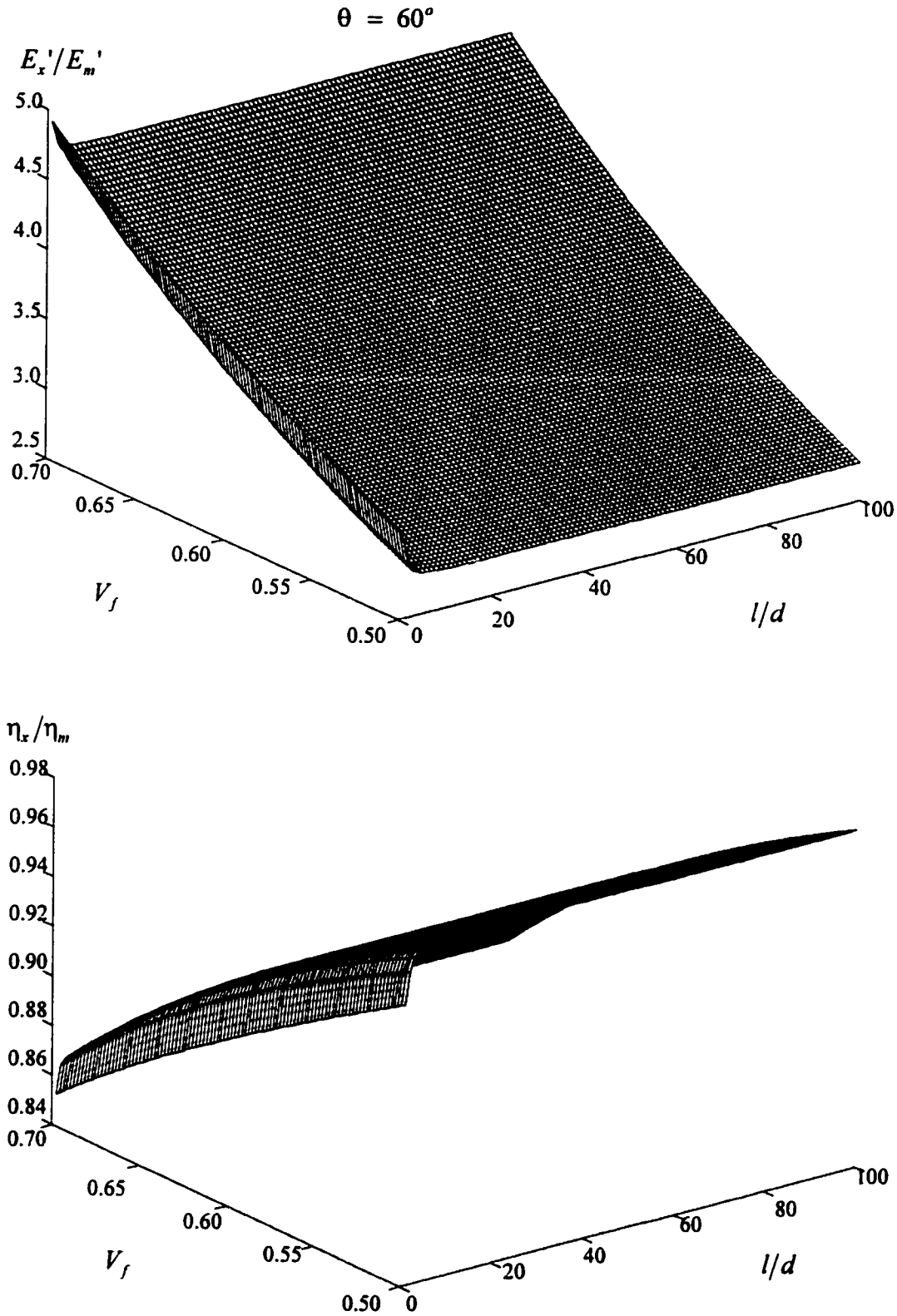

Figure 3.5 Non-dimensional Ratios η_x/η_m and E_x'/E_m' *vs* Fibre Volume Fraction V_f and Fibre Aspect Ratio l/d. Off-Axis Angle θ of the dealt with composite materials, with material properties of each component as shown in Table 3.1, is set to be 60°.

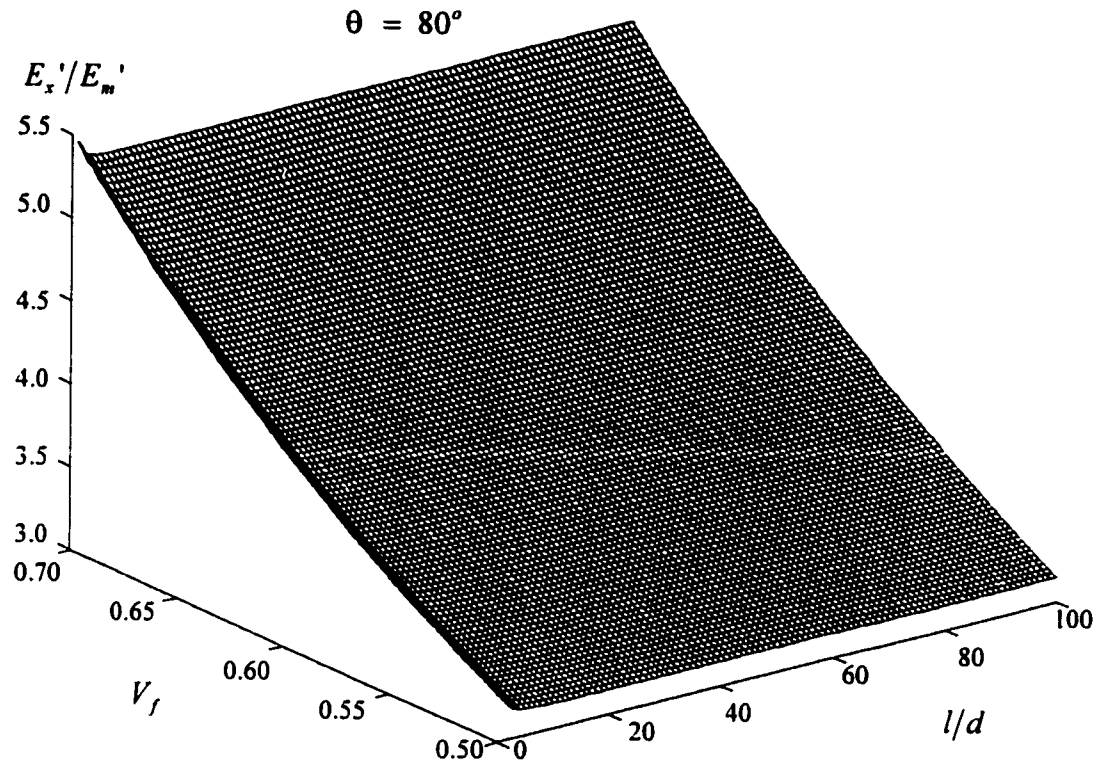

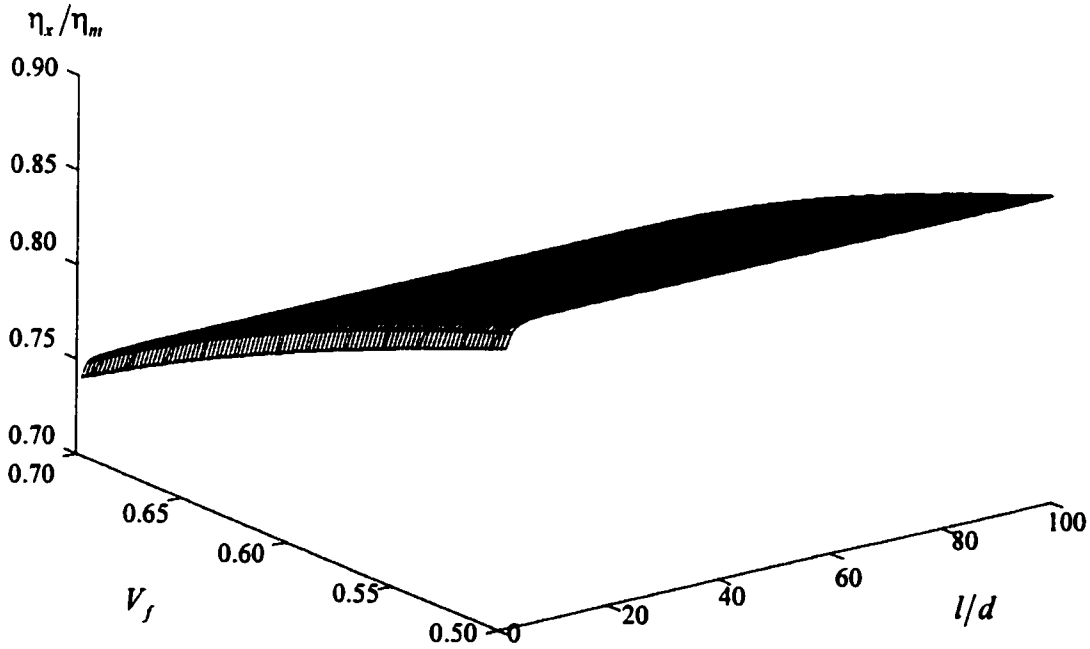

Figure 3.6 Non-dimensional Ratios η_x/η_m and E_x'/E_m' *vs* Fibre Volume Fraction V_f and Fibre Aspect Ratio l/d. Off-Axis Angle θ of the dealt with composite materials, with material properties of each component as shown in Table 3.1, is set to be 80°.

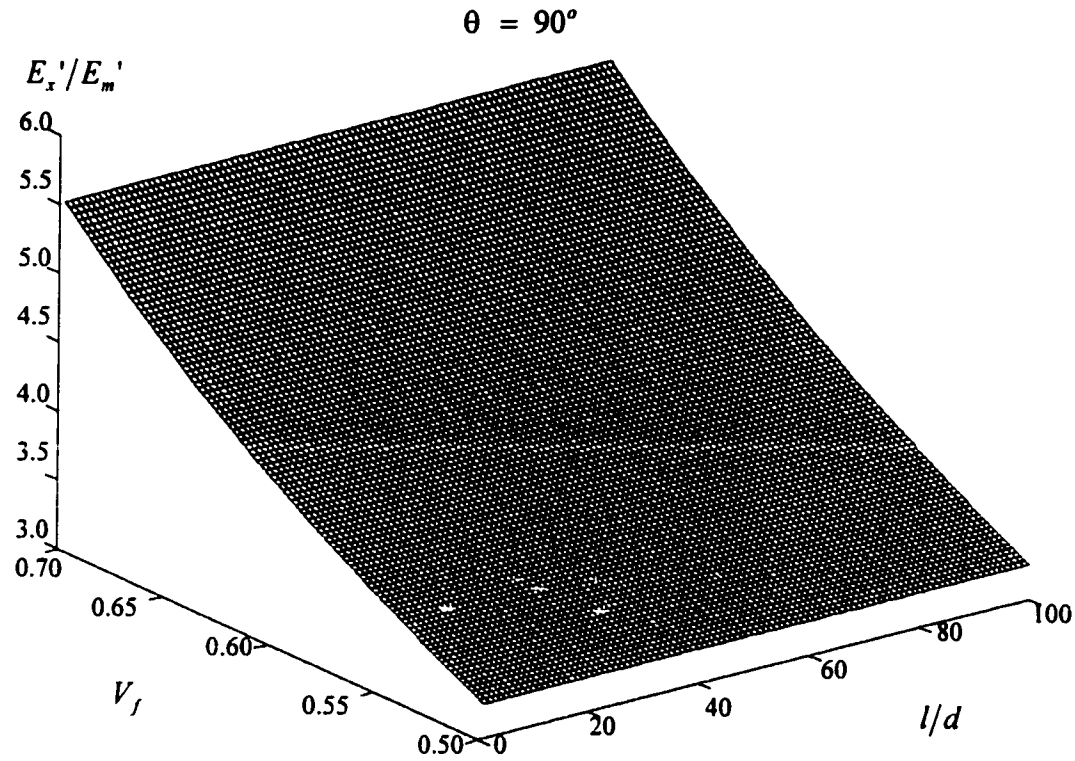

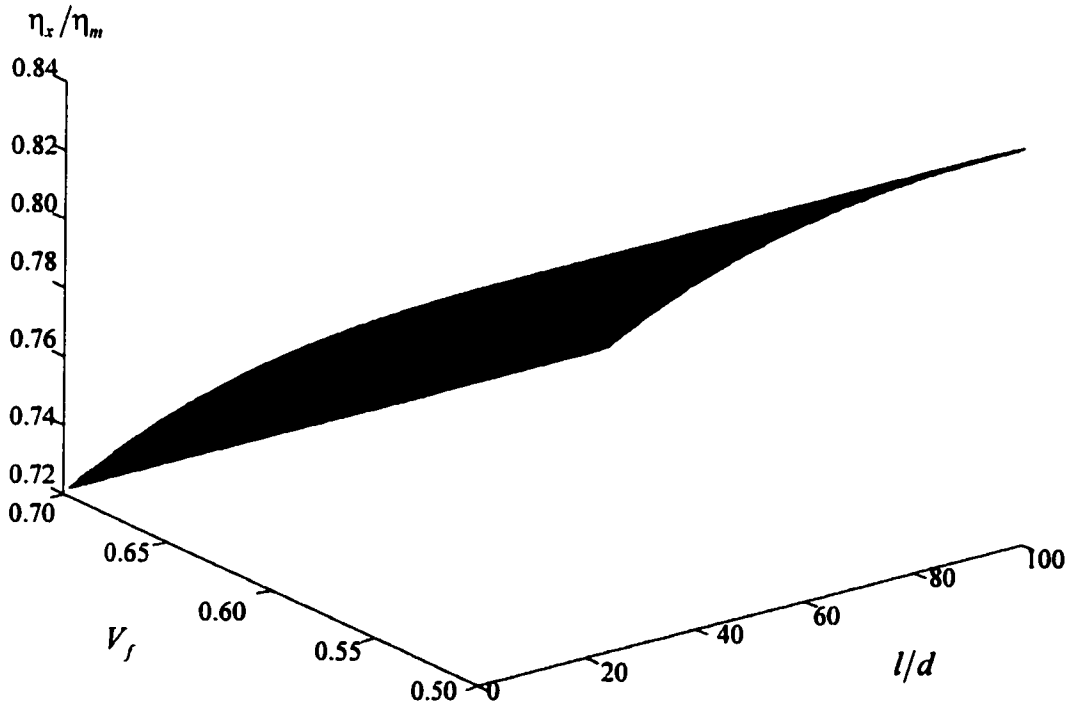

Figure 3.7 Non-dimensional Ratios η_x/η_m and E_x'/E_m' *vs* Fibre Volume Fraction V_f and Fibre Aspect Ratio l/d. Off-Axis Angle θ of the dealt with composite materials, with material properties of each component as shown in Table 3.1, is set to be 90°.

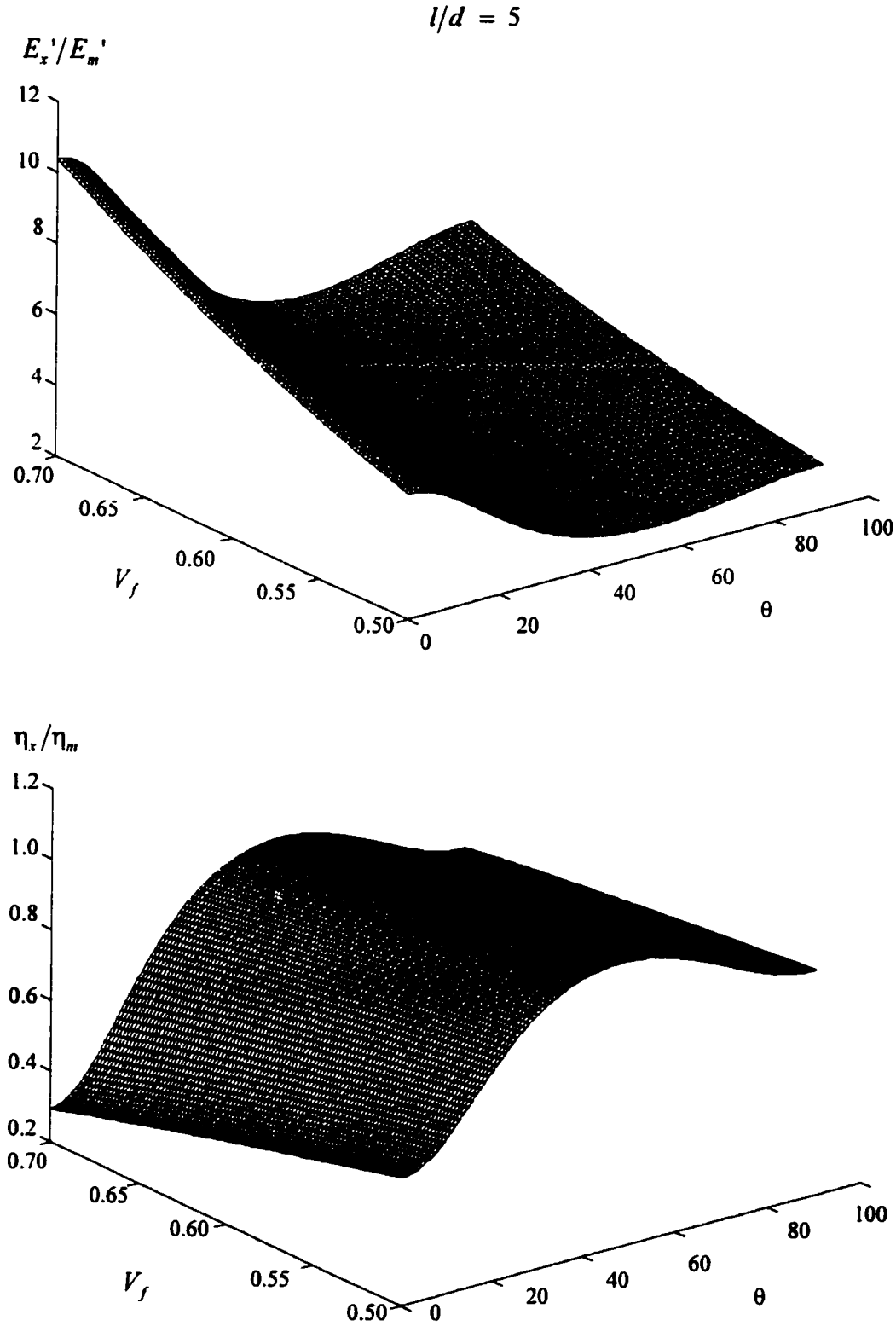

Figure 3.8 Non-dimensional Ratios η_x/η_m and E_x'/E_m' *vs* Fibre Volume Fraction V_f and Off-Axis Angle θ. Fibre Aspect Ratio l/d of the dealt with composite materials, with material properties of each component as shown in Table 3.1, is set to be 5.

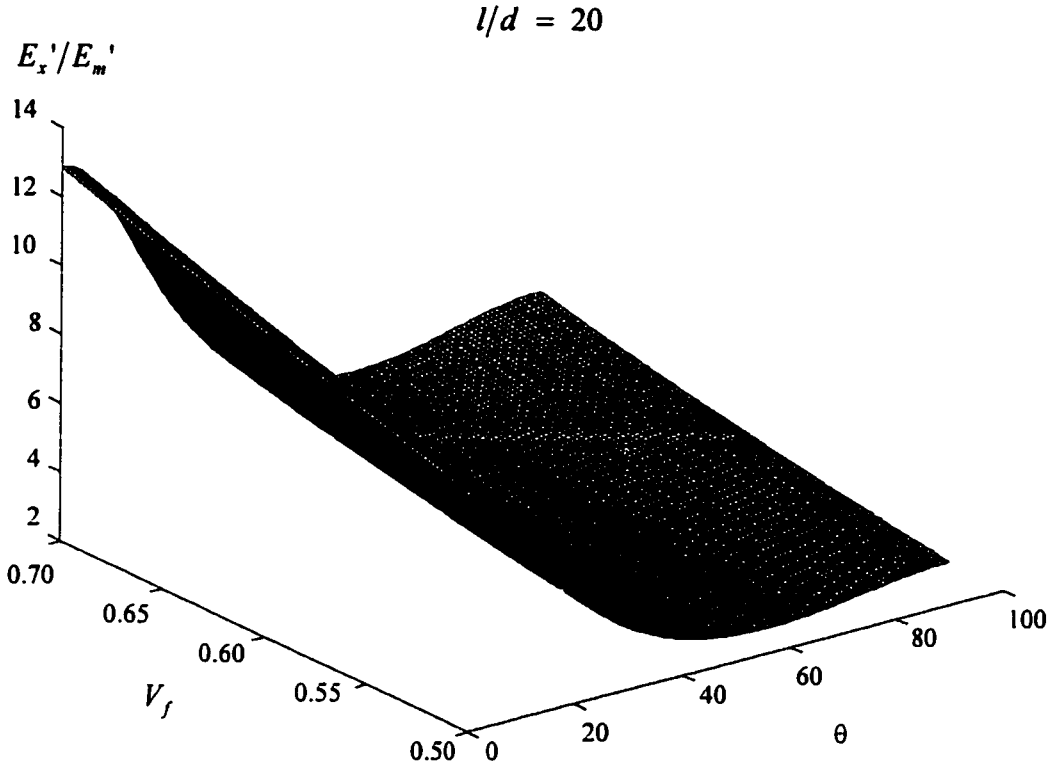

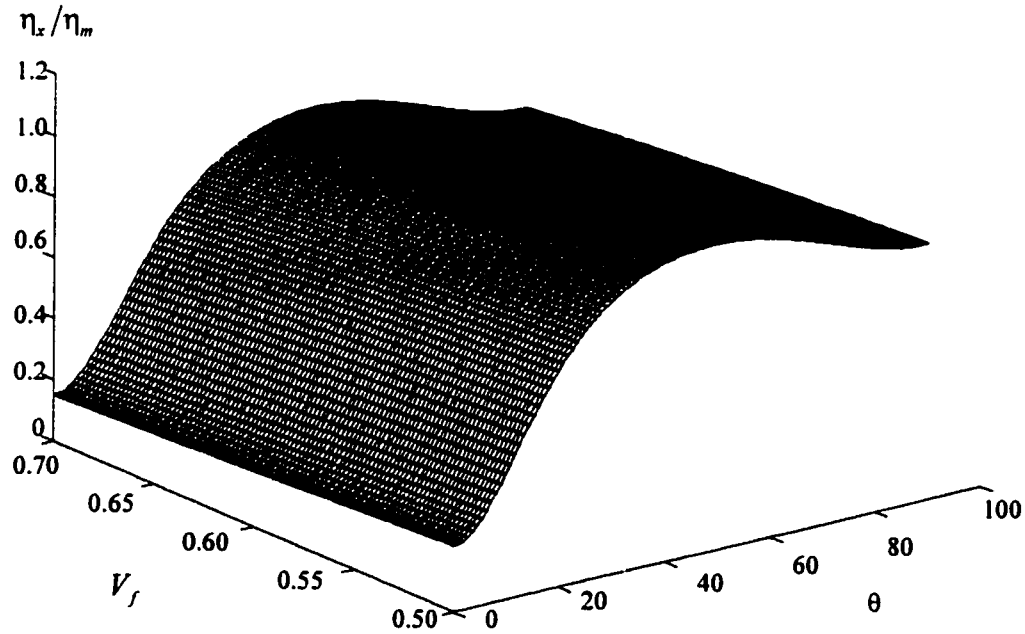

Figure 3.9 Non-dimensional Ratios η_x/η_m and E_x'/E_m' *vs* Fibre Volume Fraction V_f and Off-Axis Angle θ. Fibre Aspect Ratio l/d of the dealt with composite materials, with material properties of each component as shown in Table 3.1, is set to be 20.

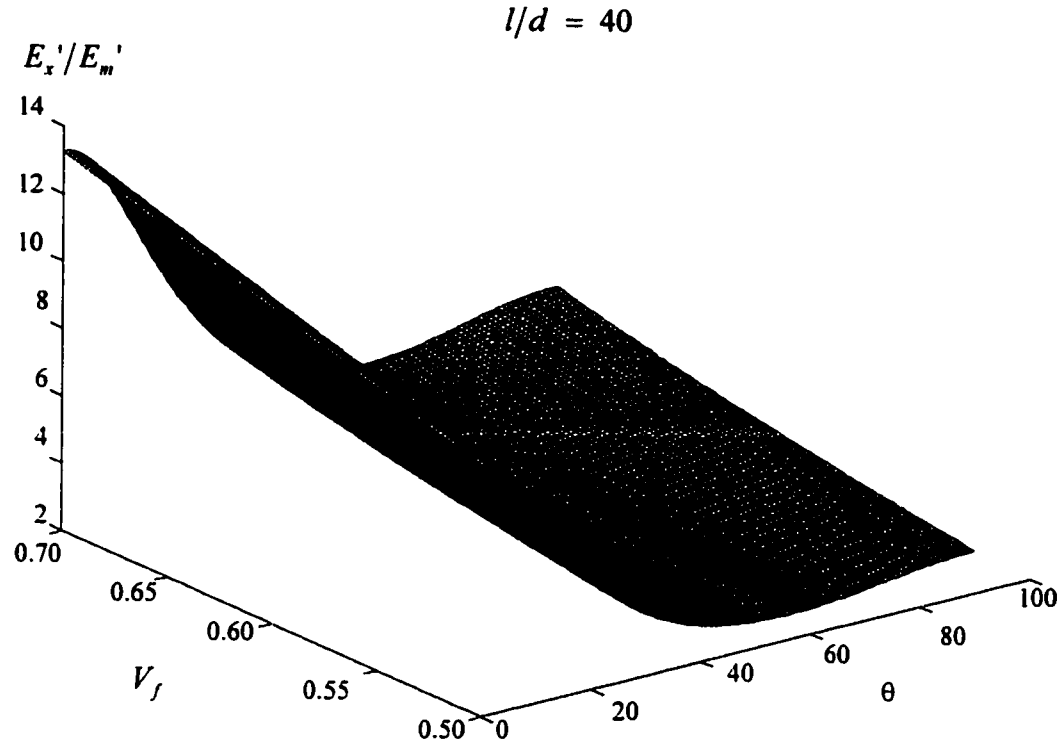

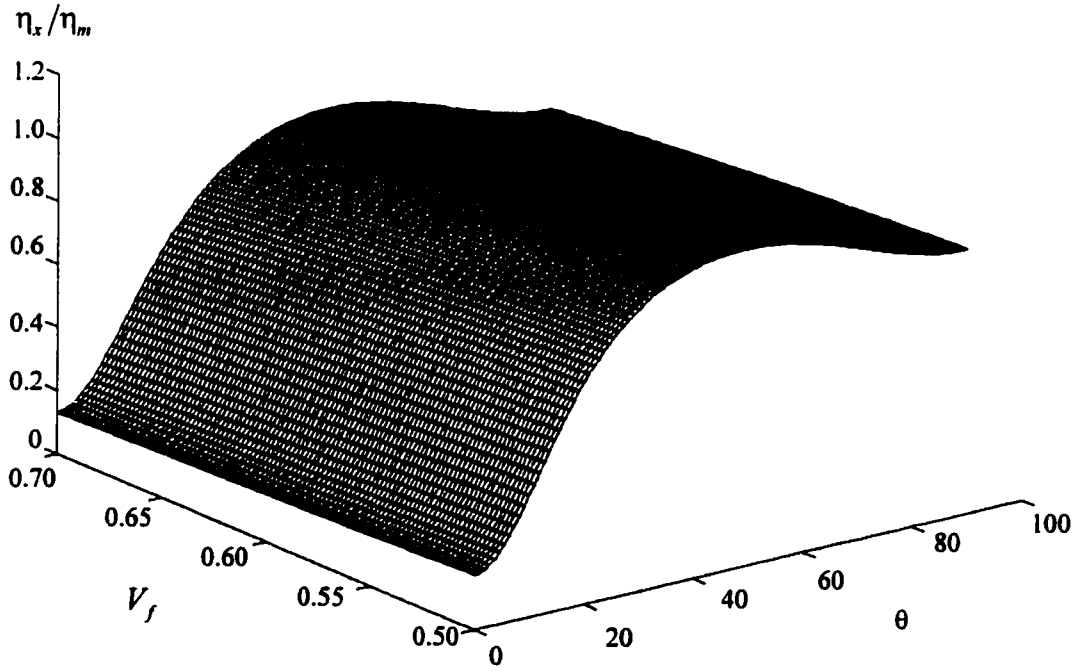

Figure 3.10 Non-dimensional Ratios η_x/η_m and E_x'/E_m' *vs* Fibre Volume Fraction V_f and Off-Axis Angle θ. Fibre Aspect Ratio l/d of the dealt with composite materials, with material properties of each component as shown in Table 3.1, is set to be 40.

$l/d = 60$

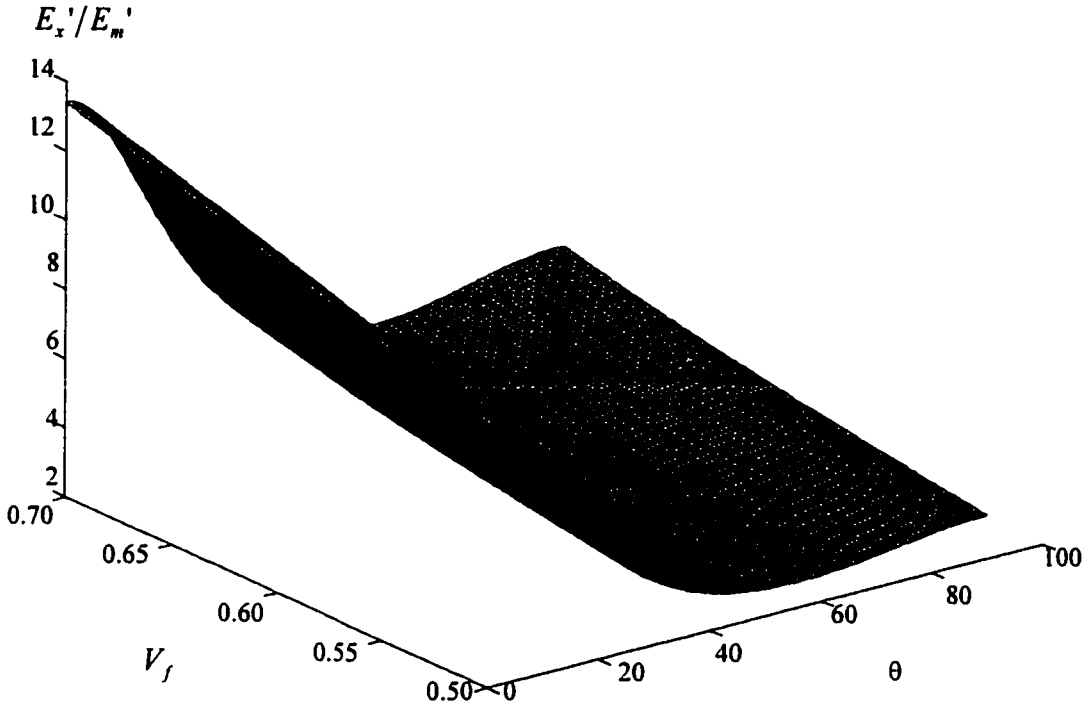

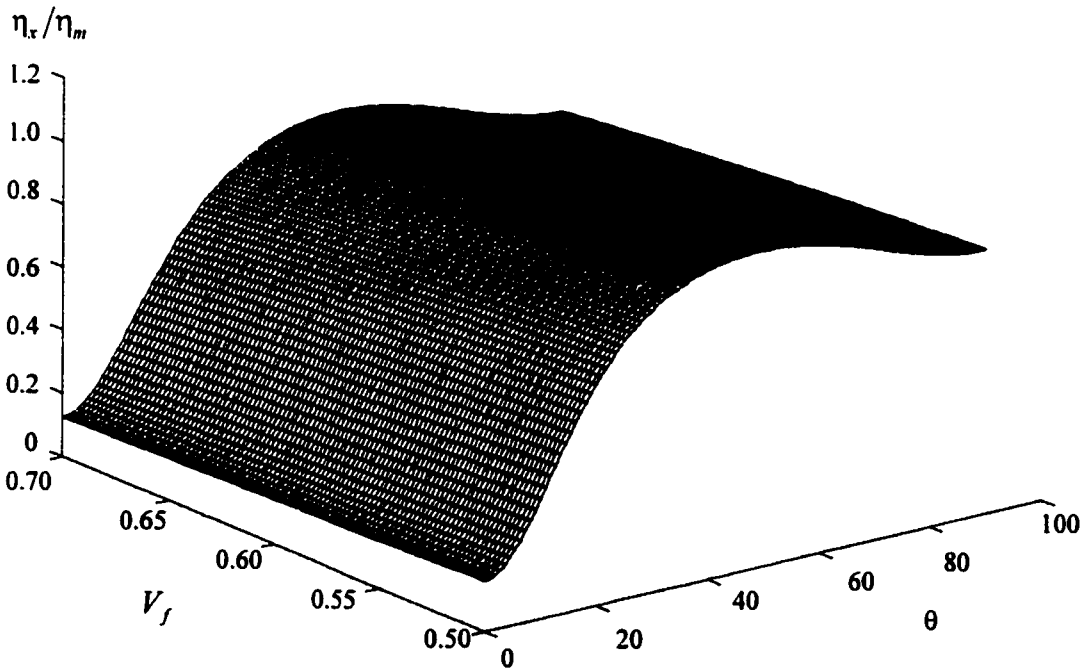

Figure 3.11 Non-dimensional Ratios η_x/η_m and E_x'/E_m' *vs* Fibre Volume Fraction V_f and Off-Axis Angle θ. Fibre Aspect Ratio l/d of the dealt with composite materials, with material properties of each component as shown in Table 3.1, is set to be 60.

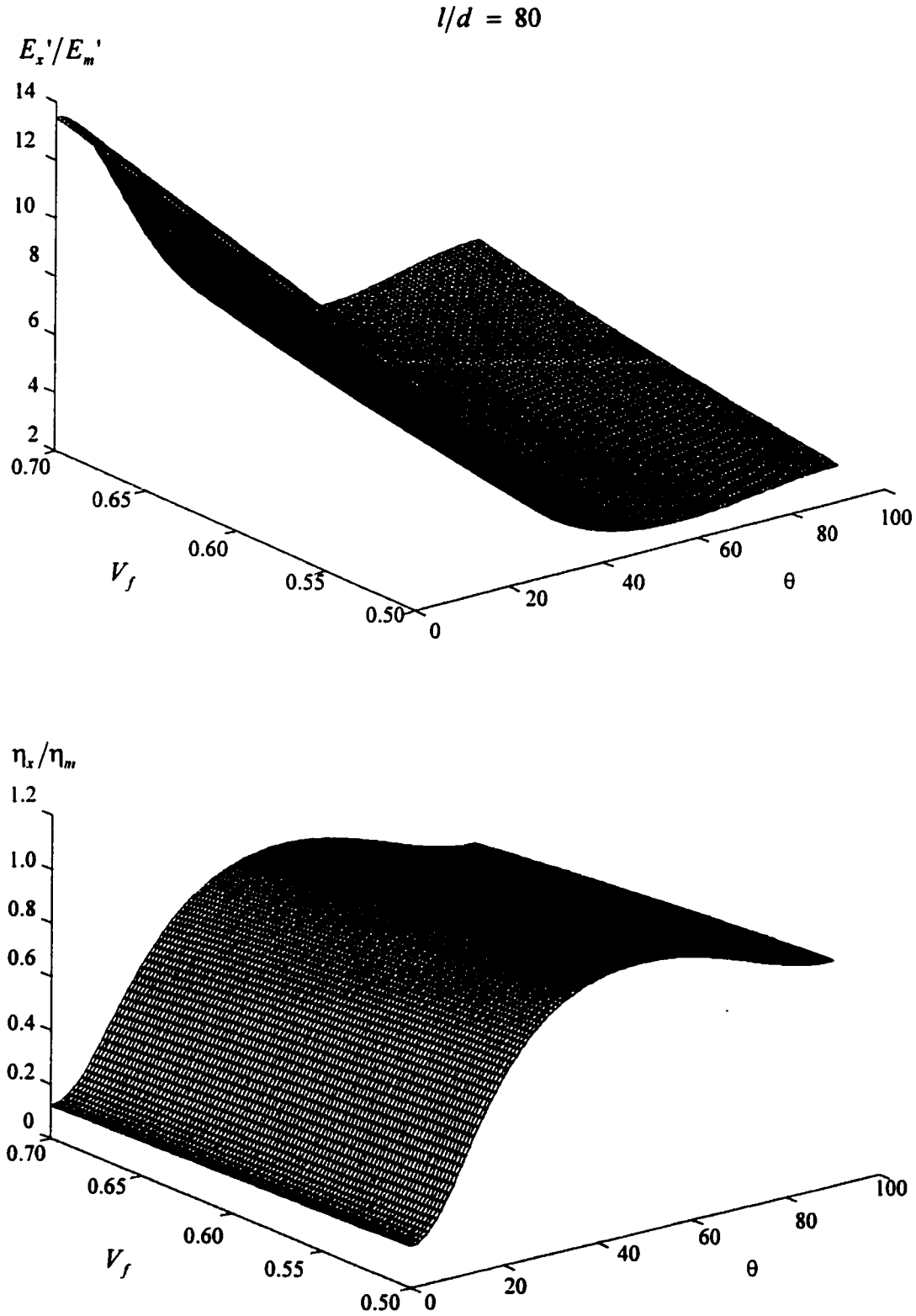

Figure 3.12 Non-dimensional Ratios η_x/η_m and E_x'/E_m' *vs* Fibre Volume Fraction V_f and Off-Axis Angle θ. Fibre Aspect Ratio l/d of the dealt with composite materials, with material properties of each component as shown in Table 3.1, is set to be 80.

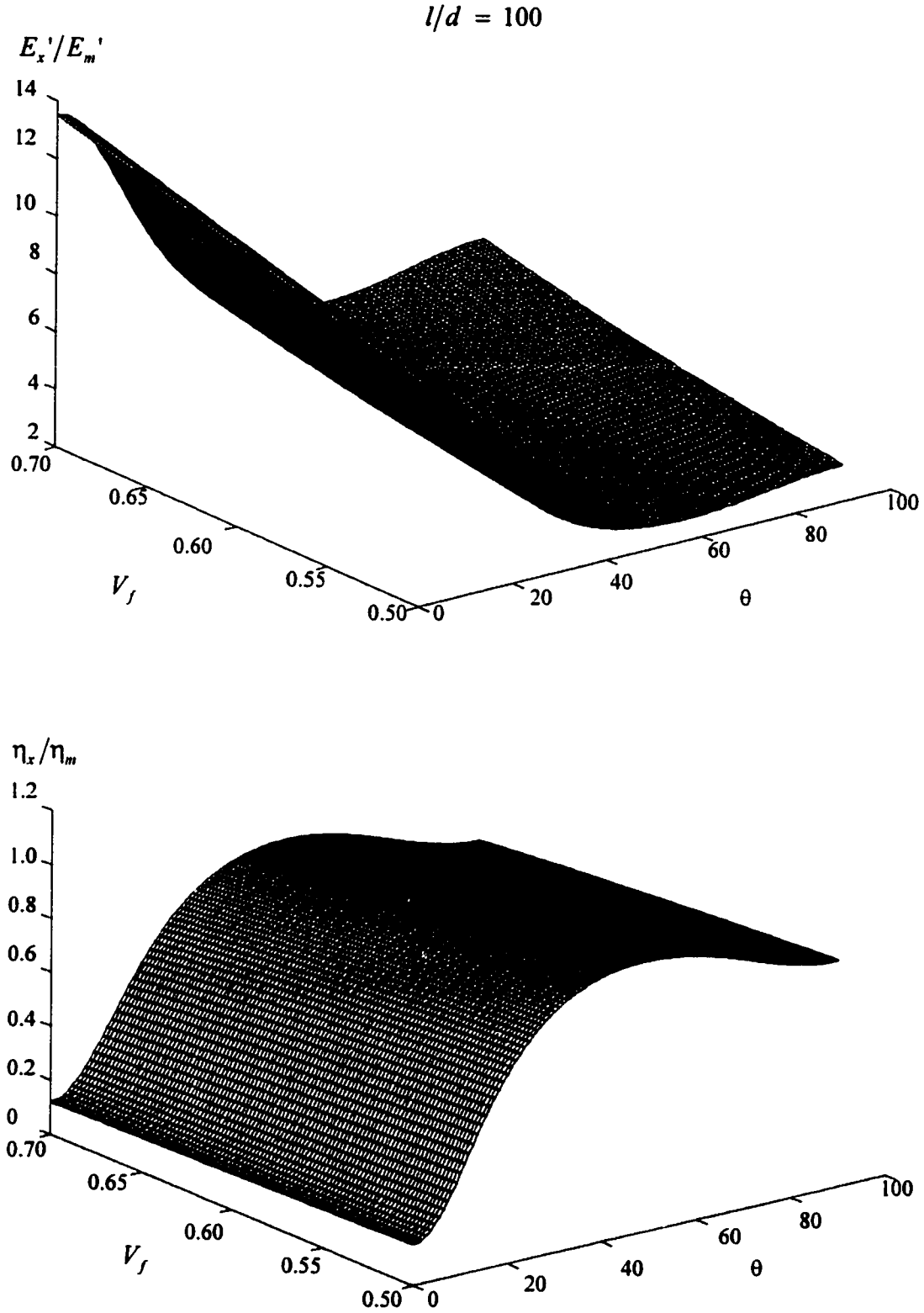

Figure 3.13 Non-dimensional Ratios η_x/η_m and E_x'/E_m' *vs* Fibre Volume Fraction V_f and Off-Axis Angle θ. Fibre Aspect Ratio l/d of the dealt with composite materials, with material properties of each component as shown in Table 3.1, is set to be 100.

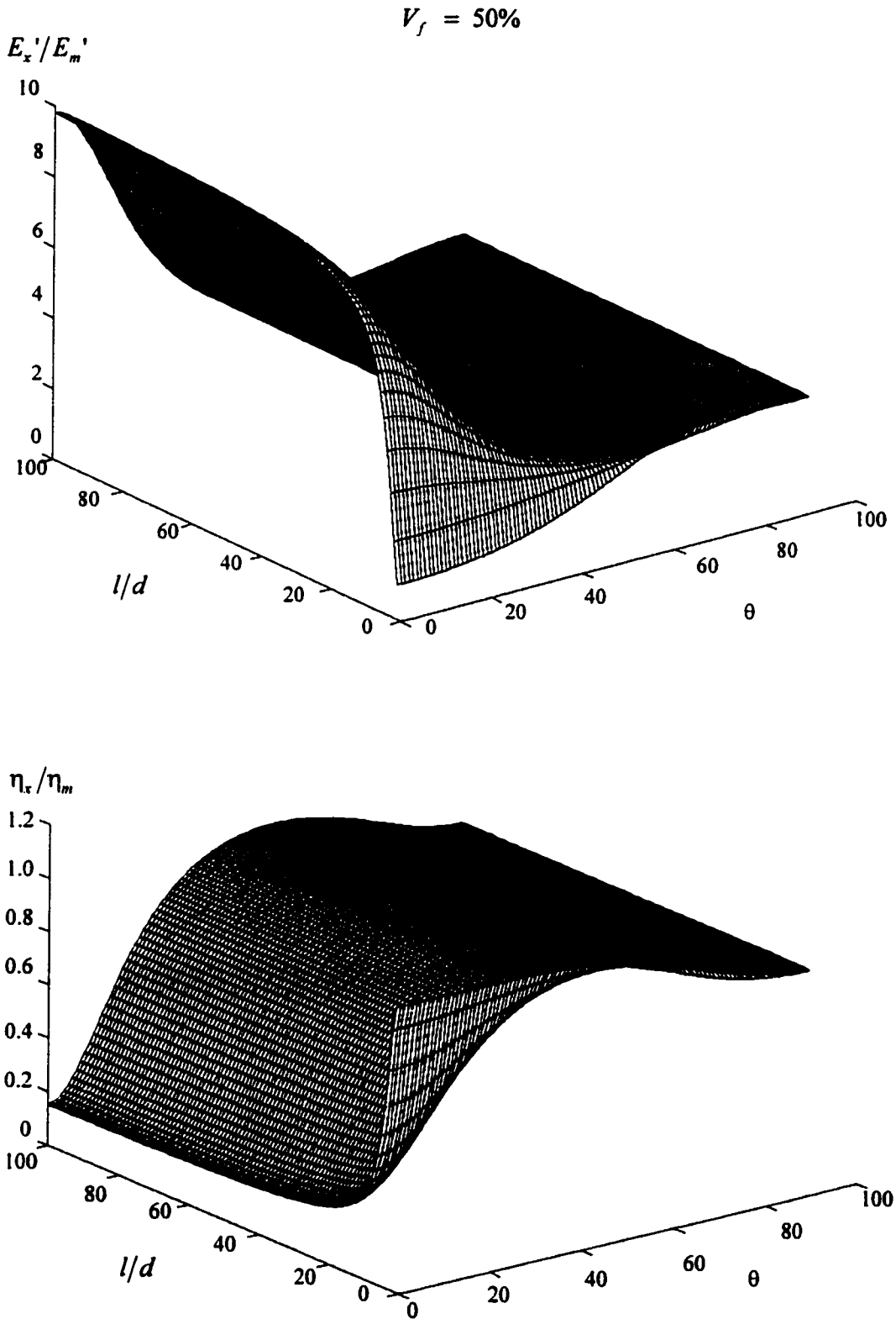

Figure 3.14 Non-dimensional Ratios η_x/η_m and E_x'/E_m' *vs* Fibre Aspect Ratio l/d and Off-Axis Angle θ. Fibre Volume Fraction V_f of the dealt with composite materials, with material properties of each component as shown in Table 3.1, is set to be 50%.

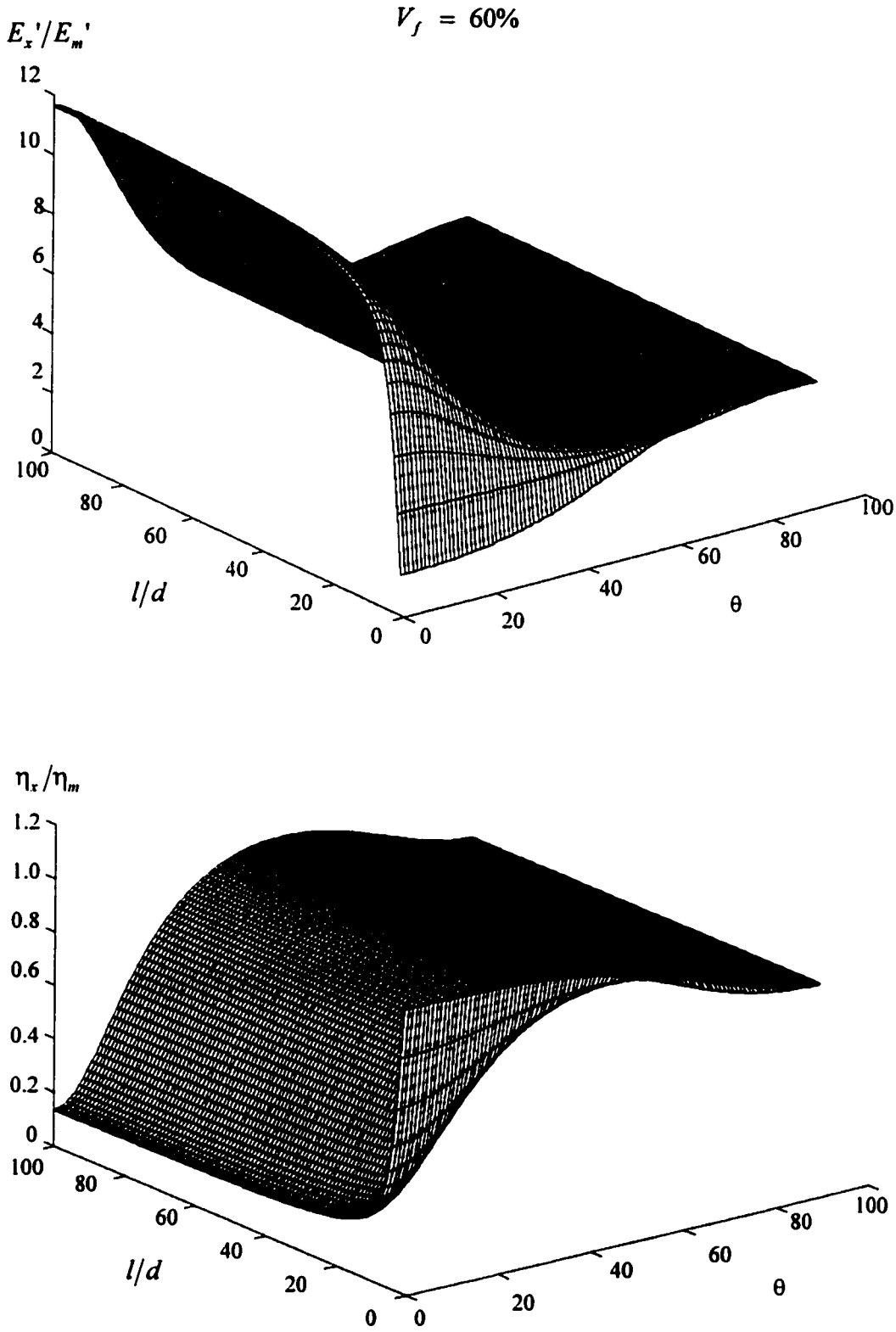

Figure 3.15 Non-dimensional Ratios η_x/η_m and E_x'/E_m' *vs* Fibre Aspect Ratio l/d and Off-Axis Angle θ. Fibre Volume Fraction V_f of the dealt with composite materials, with material properties of each component as shown in Table 3.1, is set to be 60%.

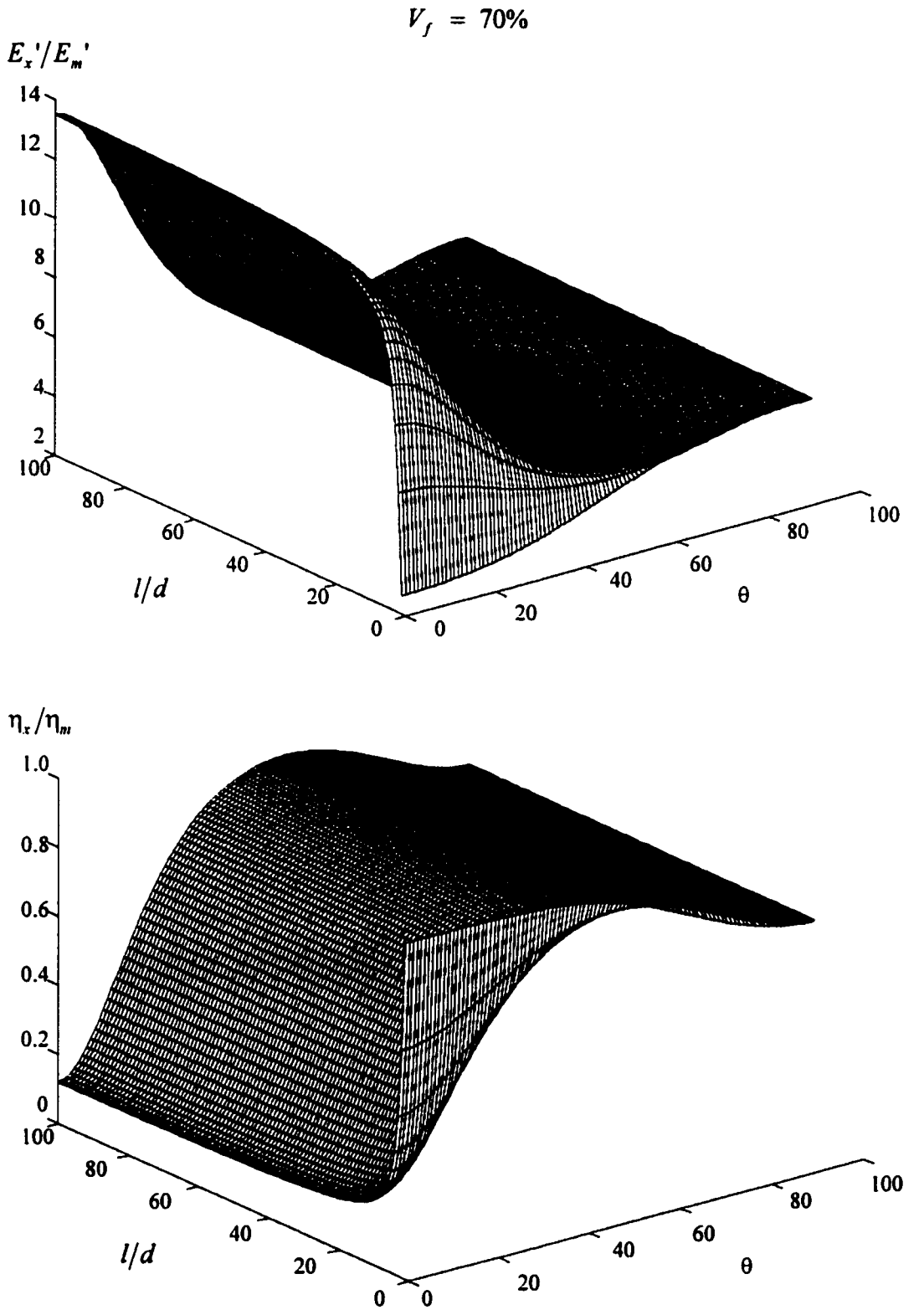

Figure 3.16 Non-dimensional Ratios η_x/η_m and E_x'/E_m' *vs* Fibre Aspect Ratio l/d and Off-Axis Angle θ. Fibre Volume Fraction V_f of the dealt with composite materials, with material properties of each component as shown in Table 3.1, is set to be 70%.

CHPATER 4

WAVE PROPAGATION - A BRIEF REVIEW

4.1 Introduction

When a localized disturbance is applied suddenly into a medium, it will soon propagate to other parts of this medium (see, e.g., Haddad[1]). This constitutes the well-recognized concept of "Wave Propagation". The transmission of sound in air and the transmission of radio waves are examples of this concept. When the mentioned localized disturbance is mechanical, e.g. a suddenly applied force, the resulting waves in the medium are referred to as "stress waves".

In recent years, there has been considerable interest from both research scientists and design engineers in the subject of wave propagation both theoretically and experimentally. Such interest is motivated primarily by the continuous emerging and extensive applications of newly developed industrial materials, such as plastics and polymeric composite material systems in aerospace, automotive and other industries. The approach of wave propagation analysis has been widely used to identify microstructural problems, such as impact damage in laminated composite systems, and to assist in the development of homogeneous and inhomogeneous material systems. Another equally important cause for the strong interest in the subject of wave propagation is the

advancement in testing and measurement techniques. Further, any new development within the realm of smart materials and structures, Haddad[1], is expected to depend on the ability to employ wave propagation as a successful detecting mechanism for a feedback concerning the status of such materials.

This chapter is focused on the area of wave propagation analysis in both homogeneous and heterogeneous materials, and laminated composites in particular. Both elastic and viscoelastic properties are taken into account. For a comprehensive review of the area of wave propagation, the reader is referred to Hillier[44], Kolsky[45], Worely[46], Moon[13], and others.

4.2 Wave Propagation in Homogeneous Materials

4.2.1 Wave Propagation in Isotropic, Elastic Solids

The governing equation for the motion of an isotropic, elastic solid, in term of the displacement, in the absence of body forces may be expressed conveniently in a vector form as

$$\rho \frac{\partial^2 u}{\partial t^2} = (\lambda + \mu)\nabla\nabla \cdot u + \mu \nabla^2 u \tag{4.2.1}$$

where λ and μ are the elastic constants, and ρ is the density of the considered material. Equation (4.2.1) corresponds to the propagation of two types of waves through an unbounded isotropic, elastic solid; namely 'dilatational' and 'rotational' waves.

A 'dilatational' wave is referred to as 'irrotational' since the propagation of such a wave involves no rotation of an elemental volume of the solid. The particle motion in a dilatational wave is longitudinal, i. e., along the direction of wave propagation. The dilatational wave velocity is dependent only on the elastic constants as well as the density of the elastic material, i.e.,

$$c_1 = \left[\frac{(\lambda + 2\mu)}{\rho} \right]^{1/2} \tag{4.2.2}$$

A 'rotational' wave is also called an 'equivoluminal' wave since there is no volume change during the propagation of the wave. In the case of a rotational wave, the particle motion is transverse, that is perpendicular to the direction of propagation of the wave. The rotational wave velocity is also dependent only on the elastic constants as well as the density of the elastic material. It is expressed as

$$c_2 = (\mu/\rho)^{1/2} \tag{4.2.3}$$

Plane waves propagate in two or three dimensions where the motion of every particle in planes perpendicular to the direction of propagation is the same. Plane waves may propagate at one or the other velocity of wave propagation (i.e., c_1 or c_2) in the isotropic, elastic medium, Equations (4.2.2) and (4.2.3) above.

'Rayleigh' surface waves were first introduced by Rayleigh[47] who identified that their effect decays rapidly with depth and that their velocity is less than that of the body wave velocity c_1 or c_2 in a semi-infinite elastic solid. Kolsky[48] later proved that Rayleigh waves do travel within a fraction ξ of the velocity c_2, Equation (4.2.3) of distortional waves where ξ is defined by the following equation.

$$\xi^6 - 8\xi^4 + \left(24 - 16b^2\right)\xi^2 + 16b^2 - 16 = 0 \qquad (4.2.4)$$

in which b is an elastic constant of the material expressed by

$$b = \left[(1-2\nu)/(2-2\nu)\right] \qquad (4.2.5)$$

where ν is Poisson's ratio.

In the case of a Rayleigh wave, the particle motion is parallel to the direction of wave propagation and it is in a plane perpendicular to the surface containing the waves during travel.

Wave propagation in bounded elastic solids, such as thin rods and bars, is conventionally classified in three categories, namely longitudinal, torsional and lateral (see, Haddad[1]).

A large number of experimental studies on the propagation of longitudinal waves in rods are used directly to determine the elastic material properties of the rod, e.g. Barton, Volterra and Citron[49], Ripperger[50], and Goldsmith Polivka and Yang[51].

The early developments in the subject of wave propagation in elastic plates are referred to Rayleigh[47] and Lamb[52]. When the wavelength is longer compared with the thickness of the plate, the velocity of propagation of a plane longitudinal wave is constant. It is expressed as

$$c_L = \left[\frac{4\mu(\lambda+\mu)}{(\lambda+2\mu)\rho} \right]^{1/2} \tag{4.2.6}$$

On the other hand, if the wavelength is shorter than the thickness of the plate, plane longitudinal waves will travel with the velocity of Rayleigh surface waves.

4.2.2 Wave Propagation in Isotropic , Viscoelastic Solids

Real materials are never perfectly elastic. As defined earlier in the thesis, the term 'internal friction' conventionally refers to the various microstructural mechanisms by

which part of the mechanical energy in the material is converted into heat, when the material is subjected to dynamic loading.

From a macroscopic point of view, the following effects of internal friction are particularly important:

{a} Static hysteresis.

{b} Viscous loss, Kolsky[48].

{c} Stress wave motion effect.

In the case of viscoelastic materials, particularly those of high polymeric origin, mechanical dissipation is particularly pronounced. The mechanical dissipation can effectively change the nature of wave motion. In addition to the significant mechanical dissipation, these materials are also 'dispersive'. In the case of dispersion, phase velocity of a wave propagating in a viscoelastic material will depend on wave frequency.

Compared with linear elasticity, the added complexity of viscoelastic nature, even in the linear case, has limited quite significantly the progress in dynamic viscoelasticity in general.

The majority of linear viscoelastic wave propagation problems that have been successfully treated have been limited to simple material representations. Hillier[53], for instance, analyzed the motion of longitudinal sinusoidal waves along a viscoelastic

filament assuming a Maxwell solid, a Voigt solid and a three element model representations. Lee and Kanter[54] studied the stress distribution in a rod of Maxwell material under impact loading. Glanz and Lee[55] used the method of characteristics to determine the stress in a viscoelastic material made of a four-parameter model. Morrison[56] examined analytically the wave propagation in a viscoelastic rod of the Voigt model type. Morrison studied also viscoelastic materials using three-element representations.

For solving wave propagation problems in a linear viscoelastic solid, Mamardi and Turchetti[57], and Mainard and Nervosi[58] attempted situations by utilizing Boltzmann's superposition method. On the other hand, Chao and Achenbach[59] employed the well-known correspondence principle[32] to solve wave propagation problems in linear viscoelasticity. These authors proved that under the restricted condition of constant Poisson's ratio, a class of viscoelastic problems might be solved provided that the solution of the corresponding elastic problem is known.

4.3 Wave Propagation in Heterogeneous Materials

Because of their relatively high strength and light weight, the applications of composite materials have grown very rapidly in the last two decades. Composite materials have been widely used in aerospace industry to replace metals in aircraft structures for weight

saving. The increasing importance of composite materials in engineering applications has generated a wide interest in the mechanical properties of such media. The methods to determine the response behavior of composite laminates under various loading conditions have appeared to be of most significant concern in this field. The capability of composite materials to withstand impact loads is often considered to be the critical feature in the design process. Thus, a comprehensive understanding of both static and dynamic behavior of composite systems under various loading conditions is needed. For static analysis, this has already received widespread attention in the last two decades. However, the study of transient response of composite materials when subjected to dynamic loading has been intensively investigated in recent years. Hence the methodology for the characterization of wave propagation in composite materials should be studied extensively because of its wide technological applications.

Because of the inhomogeneity of materials and the complexity of structural geometry, exact theoretical predictions of deformation states of composite laminae are seldom possible. There are, however, several approximate theories, which were developed and used by various researchers, and can predict wave propagation in composite system quite satisfactorily[18,19].

In the latter context, the simplest approach, known as the "Effective Modulus Theory", is to replace the composite system by a homogeneous material of an effective modulus with a minimal consideration of the internal structure, as suggested, for instance, by White and Angond[60]. An alternative model, proposed by Sun, Acherbach and Herrmann[61] and

later utilized and extended by Ma and Huang[62], Hegemier and Nayfeh[63], Hegemier and Bache[64], Nemat-Nasser and Yamada[65], Mnkunoki and Ting[66], Tang and Ting[67] and others, consists of two alternating homogeneous layers of different elastic properties known as the "Effective Stiffness Theory". For a certain class of problems, the "Effective Modulus Theory" works reasonably well. But for a high-frequency dynamic problem, the so-called "Effective Stiffness Theory" is known to be more accurate, particularly when the wavelength is comparable with some internal characteristic length, such as fiber diameter or layer thickness[61].

The next level of approximation is the so-called "Plate Theory"; namely, when the displacement field is approximated by few leading terms of a series expansion in terms of the thickness variables. A power series expansion by Mindlin[68], a Legendre polynomial expansion by Mindlin and Medick[69], and a trigonometric expansion by Lee and Nikodem[70] have been successfully applied. For homogeneous, elastic plates, Moon[14-16] utilized and developed Mindlin's approximate theory of plates to simulate wave propagation in anisotropic plates. Kim and Moon's work[71] applied Mindlin's approximate theory of plates to each identical anisotropic layer to obtain a set of difference-differential equations of motion with the use of the interlaminar stresses and displacements as explicit variables. In the above referred-to work, the Fast Fourier transformation (FFT) algorithm was utilized to obtain transient wave solutions.

On the other hand, since the ratio of Young's modulus to shear modulus can be very large for anisotropic composite laminates, a theory analogous to those presented by

Mindlin[72] for isotropic plates assumes a significant importance. The introduction of shear deflection into laminated plate theory was first accomplished by Stavsky[73] for the case of isotropic layers having identical Poisson ratio. Later, Yang, Norris and Stavsky[74] extended Mindlin's theory for homogeneous plates to laminates consisting of an arbitrary number of bonded anisotropic layers, to develop a linear laminate theory. Whitney and Pagano[75], based on Yang, Norris and Stavsky's approach, added slight modifications of the theory, and developed the well-known "First Order Shear Deformation" theory, with equations of motion in terms of the displacement variables. This theory was utilized by Sun and Lai[17], Prasad, Ambur and Starnes[76], and others to obtain wave propagation solutions for elastic composite laminates.

Barker[77] presented a model for stress wave propagation perpendicular to the plates of a bi-laminate composite material. The model consists of a stress relaxation equation of a material of the Maxwell type.

Lundergan and Drumneller[78], Kam and Chang[79], and others used finite element approach to solve the wave propagation problem in elasticity.

It is only natural then to expect that inhomogeneities such as fibres, laminates, or particles in a material matrix will result in a great dispersion of wave as the wavelength approaches the size or spacing of the composite constituents. When a composite is used in a structural application, there will be two sources of dispersion, that associated with the dimension of material elements, e.g., fibre diameter or ply thickness, and that associated

with the composite specimen macroscopic dimensions. It should also be expected that the latter would become important for wavelengths much larger than those of the order of the material elements.

On the other hand, attenuation of wave propagation represents loss of energy. In contrast to dispersion in which the wave energy is conserved but redistributed in a deformed stress pulse. Loss of energy during dynamic motion in composites can be attributed to at least four phenomena:

(i) Viscoelastic or anelastic effects of the constituents.

(ii) Wave scattering.

(iii) Microfracture.

(iv) Friction between poorly bonded constituents.

Both inhomogeneous and viscoelastic properties of a composite laminate make the wave propagation problem more complex than its isotropic and elastic counterparts. So far, to the best of knowledge of the author, there are few activities directed into the viscoelastic nature of wave propagation analysis of composite laminates. Burtin and Hamelin[80], for instance, used the "Lagrange Method" to analyze the viscoelastic behavior of composite laminate under dynamic and impact loading. Cederbaum and Aboudi[81] utilized Whitney and Pagano's "First Order Shear Deformation Theory"[75], "Higher Order Shear Deformation Theory"[82] and the "Eigenvalue Method" to predict the wave propagation properties for viscoelastic composite laminate.

CHAPTER 5

WAVE PROPAGATION IN VISCOELASTIC COMPOSITE LAMINATE PLATE UNDER AN IMPACT LOAD

5.1 Introduction

Laminated composite materials are used extensively in aerospace, automotive and other industries, due to this high specific modulus, high specific strength and superior design flexibility for specific applications compared to traditional materials. However, the interior impact properties of these materials represent an obstacle to the further use of such materials in wider areas and applications. Other than indentation, spalling, and penetration of projectiles through the structure, the impact failure of the composite laminate would include additional modes of failure such as fibre crushing, fibre pull-out, matrix cracking and delamination. Impacts do occur during manufacturing, normal operations, or maintenance. The situation is even critical for impacts which induce significant internal damage, undetectable by visual inspection, that cause large deterioration in the strength and fatigue life, increase in local stress and change of natural frequencies. Therefore, the impact analysis of laminated composite materials has become a subject of active research in the material science. A recent comprehensive review of the work performed in this area has been carried out by Abrate[18, 19]. In order to fully understand the effect of foreign object impact damage of fibre-composite

systems, one should get a deeper insight into impact dynamics of these materials.

For high velocity impacts, one could assume that the overall motion of the structure takes place over a time period much larger than the impact contact time. By further assuming that the size of the impactor is much smaller than the structure dimensions, the impact problem may be divided into two distinct parts:

(1) The local mechanics of impact with a deformable half space, and

(2) The response of the structure to a prescribed local impact force as determined in part (1) above.

For the second part of the above impact problem, by prescribing the local contact force and impact duration time, the wave propagation analysis method appears to be more practical to predict the post impact response of the targeted structure. A review in the area of impact wave propagation was presented by Moon[13].

Within the past 40 years, there have been significant efforts directed to this area both analytically[14-17, 62, 71, 76, 79, 83] and experimentally[84, 85], in which the elastic composite model was being used. Due to the significant influence of the viscoelastic nature of polymeric matrices of composite lamina, it is necessary to treat polymer composite laminates as viscoelastic materials, whose material properties are functions of time, frequency and/or temperature. So far,

there have been only a few activities directed into the viscoelastic nature of wave propagation analysis of composite laminates[80, 81].

Both the anisotropic and viscoelastic characters of composite laminates make the pertaining wave propagation problem to be more complex than its isotropic and elastic counterparts. The approximate plate theory which was suggested by Cauchy and later extended by Mindlin[68, 69] works well for anisotropic plates. There is an evidence[86] that the shear deformation must be taken into account in the analysis of the anisotropic plate when the longitudinal properties are much higher than its shear properties. The "First Shear-Deformation Theory" (FSDT) which was developed by Whitney and Pagano[75] appears to be more suitable for the analysis of composite laminates due to its high orthotropy.

The subject of this chapter concerns itself with the analytical modelling of wave propagation of a viscoelastic composite plate under impact loading. The characterization of the relationship between the wave propagation model and the material properties of the constituents of the composite is also be attempted in the presentation.

In the case of the work in this chapter, the Whitney and Pagano's plate theory is used to analyze the equations of motion of the desired composite laminate plate. In order to include the viscoelastic behaviour of the problem, the "Correspondence Principle[32]" is used. At the closure of the chapter, the closed form displacement solution in the frequency-domain is

presented.

It is generally agreed that the cause of the sudden failure must be examined from the point of view of transient wave propagation phenomena. In this context, the "Fast Fourier Transformation" (FFT) is proposed and used to invert the displacement solution from frequency-domain to time-domain.

The internal friction[1, 48] or viscoelastic damping is believed to be responsible for the wave attenuation phenomena in polymer composites. It is further recognized that discontinuous fibre reinforced composites have higher damping capacity than continuous ones[6-9], (see chapter 3). Therefore, the dynamic behaviour under impact loading is investigated in this chapter for both continuous and discontinuous fibre reinforced composite laminates. In this context, the effects of fibre volume fraction and fibre aspect ratio on the dynamic behaviour of composite laminates are examined in the present chapter.

5.2 Equations of Motion

Consider a plate of constant thickness h composed of thin layers of anisotropic materials bonded together as shown in Figure 5.1. The origin of a Cartesian coordinate system is located within

the central plane $(x - y)$ with the z-axis being normal to this plane. The material of each layer is assumed to possess a plane of elastic symmetry parallel to xy. We assume that the plate surfaces $z = \pm h/2$ are subjected to surface tractions defined as

$$\tau_{xz}(x, y, \pm h/2, t)=0, \qquad \tau_{yz}(x, y, \pm h/2, t)=0 \tag{5.2.1a}$$

$$\sigma_z(x, y, h/2, t) = q_1, \qquad \sigma_z(x, y, -h/2, t) = q_2 \tag{5.2.1b}$$

where q_1 and q_2 can be arbitrary functions of x, y, and t.

The stress and moment resultants can be defined, respectively, as

$$(N_x, N_y, N_{xy}, Q_x, Q_y) = \int_{-h/2}^{h/2} (\sigma_x, \sigma_y, \tau_x, \tau_{xz}, \tau_{yz}) dz \tag{5.2.2a}$$

$$(M_x, M_y, M_{xy}) = \int_{-h/2}^{h/2} (\sigma_x, \sigma_y, \tau_{xy}) z dz \tag{5.2.2b}$$

The stress resultants N_x, N_y and N_{xy} must be included in this analysis due to the presence of bending-extensional coupling.

Because of the existence of a plane of elastic symmetry, the constitutive relations for any given layer could be expressed as

$$\begin{bmatrix} \sigma_x \\ \sigma_y \\ \sigma_z \\ \tau_{xy} \end{bmatrix} = \begin{bmatrix} c_{11} & c_{12} & c_{13} & c_{16} \\ c_{21} & c_{22} & c_{23} & c_{26} \\ c_{31} & c_{32} & c_{33} & c_{36} \\ c_{61} & c_{62} & c_{63} & c_{66} \end{bmatrix} \begin{bmatrix} \varepsilon_x \\ \varepsilon_y \\ \varepsilon_z \\ \gamma_{xy} \end{bmatrix} \tag{5.2.3a}$$

$$\begin{bmatrix} \tau_{yz} \\ \tau_{xz} \end{bmatrix} = \begin{bmatrix} c_{44} & c_{45} \\ c_{54} & c_{55} \end{bmatrix} \begin{bmatrix} \gamma_{yz} \\ \gamma_{xz} \end{bmatrix} \tag{5.2.3b}$$

where c_{ij} are the components of the stiffness matrix and $\sigma_{()}$, $\tau_{()}$, $\varepsilon_{()}$, and $\gamma_{()}$ represent the engineering stress, shear stress, strain, and shear strain components respectively.

For future convenience, we employ a notation to express the constitutive Equations (5.2.3) into the form

$$\sigma_i = c_{ij}\varepsilon_j \qquad (i, j = 1, 2, 3, 6) \tag{5.2.4}$$

where $\sigma_1 = \sigma_x$, $\sigma_2 = \sigma_y$, $\sigma_3 = \sigma_z$, $\sigma_6 = \tau_{xy}$ and the engineering strains ε_j are annotated in an analogous manner. By obtaining the solution in term of ε_3 and re-substituting the result into Equation (5.2.4), one can arrive at

$$\sigma_i = Q_{i\alpha}\varepsilon_\alpha + \frac{c_{i3}}{c_{33}}\sigma_3 \qquad (i = 1, 2, 3, 6; \quad \alpha = 1, 2, 6) \tag{5.2.5}$$

in which $Q_{i\alpha}$ is defined as plane stress reduced stiffness and will be useful in subsequent work. Furthermore, we assume the following displacement field

$$U = U^0(x, y, t) + z\psi_x(x, y, t) \tag{5.2.6a}$$

$$V = V^0(x, y, t) + z\psi_y(x, y, t) \tag{5.2.6b}$$

$$W = W^0(x, y, t) \tag{5.2.6c}$$

where U, V and W represent the displacement components in the x, y and z directions, respectively, while ψ_x and ψ_y are the rotations of the normals to the mid-plane about the y and x axes, respectively. From Equations (5.2.2), (5.2.5) and (5.2.6), and the assumption that integrals associated with σ_z are negligible and may be dropped, we obtain

$$\begin{bmatrix} N_x \\ N_y \\ N_{xy} \\ M_x \\ M_y \\ M_{xy} \end{bmatrix} = \begin{bmatrix} A_{11} & A_{12} & A_{16} & B_{11} & B_{12} & B_{16} \\ A_{21} & A_{22} & A_{26} & B_{21} & B_{22} & B_{26} \\ A_{61} & A_{62} & A_{66} & B_{61} & B_{62} & B_{66} \\ B_{11} & B_{12} & B_{16} & D_{11} & D_{12} & D_{16} \\ B_{21} & B_{22} & B_{26} & D_{12} & D_{22} & D_{26} \\ B_{61} & B_{62} & B_{66} & D_{61} & D_{62} & D_{66} \end{bmatrix} \begin{bmatrix} U^0_{,x} \\ V^0_{,y} \\ U^0_{,y} + V^0_{,x} \\ \psi_{x,x} \\ \psi_{y,y} \\ \psi_{x,y} + \psi_{y,x} \end{bmatrix} \tag{5.2.7a}$$

and

$$\begin{bmatrix} Q_x \\ Q_y \end{bmatrix} = k \begin{bmatrix} A_{44} & A_{45} \\ A_{54} & A_{55} \end{bmatrix} \begin{bmatrix} W_{,y} + \psi_y \\ W_{,x} + \psi_x \end{bmatrix} \tag{5.2.7b}$$

where the differentiation is denoted by a comma, $(\ )_{ij} = (\ )_{ji}$, and k is introduced in the expressions for the transverse shear resultants. The coefficient k is a shear correction factor which depends upon the analytical solution of the problem and experimental evidence[75]. The value of k was set as $5/6$, $\pi^2/12$ and 2/3, respectively, by various researchers. It is found by Ten and Sun[86] that the value $\pi^2/12$ works reasonably well with the experimental results.

$$(A_{ij}, B_{ij}, D_{ij}) = \int_{-h/2}^{h/2} Q_{ij}(1, z, z^2)\, dz \qquad (i, j = 1, 2, 6) \tag{5.2.8a}$$

$$A_{ij} = \int_{-h/2}^{h/2} c_{ij}\, dz \qquad (i, j = 4, 5) \tag{5.2.8b}$$

The equations of motion in terms of stress and moment resultants are expressed as

$$N_{x,x} + N_{xy,y} = P\ddot{U}^0 + R\ddot{\psi}_x \tag{5.2.9a}$$

$$N_{xy,x} + N_{y,y} = P\ddot{V}^0 + R\ddot{\psi}_y \tag{5.2.9b}$$

$$Q_{x,x} + Q_{y,y} + q = P\ddot{W} \tag{5.2.9c}$$

$$M_{x,x} + M_{xy,y} - Q_x = R\ddot{U}^0 + I\ddot{\psi}_x \tag{5.2.9d}$$

$$M_{xy,x} + M_{y,y} - Q_y = R\ddot{V}^0 + I\ddot{\psi}_y \tag{5.2.9e}$$

while

$$(P, R, I) = \int_{-h/2}^{h/2} \rho\,(1, z, z^2)\, dz \tag{5.2.10a}$$

and also,

$$q = q_1 - q_2 \tag{5.2.10b}$$

Finally, by substituting Equations (5.2.7) into (5.2.9), one obtains the equations of motion in terms of the five unknown displacement components as(see, also, Whitney & Pagano[75])

$$\begin{aligned} &A_{11}U^0_{,xx} + 2A_{16}U^0_{,xy} + A_{66}U^0_{,yy} + A_{16}V^0_{,xx} + (A_{12} + A_{66})V^0_{,xy} + A_{26}V^0_{,yy} + B_{11}\psi_{x,xx} \\ &+ 2B_{16}\psi_{x,xy} + B_{66}\psi_{x,yy} + B_{16}\psi_{y,xx} + (B_{12} + B_{66})\psi_{y,xy} + B_{26}\psi_{y,yy} = P\ddot{U}^0 + R\ddot{\psi}_x \end{aligned} \tag{5.2.11a}$$

$$\begin{aligned} &A_{16}U^0_{,xx} + (A_{12} + A_{66})U^0_{,xy} + A_{26}U^0_{,yy} + A_{66}V^0_{,xx} + 2A_{26}V^0_{,xy} + A_{22}V^0_{,yy} + B_{16}\psi_{x,xx} \\ &+ (B_{12} + B_{66})\psi_{x,xy} + B_{26}\psi_{x,yy} + B_{66}\psi_{y,xx} + 2B_{26}\psi_{y,xy} + B_{22}\psi_{y,yy} = P\ddot{V}^0 + R\ddot{\psi}_y \end{aligned} \tag{5.2.11b}$$

$$k[A_{55}(\psi_{x,x} + \psi_{y,y}) + A_{45}(\psi_{x,y} + \psi_{y,x} + 2W_{,xy}) + A_{44}(\psi_{y,y} + W_{,yy})] + q = P\ddot{W} \tag{5.2.11c}$$

$$\begin{aligned} &B_{11}U^0_{,xx} + 2B_{16}U^0_{,xy} + B_{66}U^0_{,yy} + B_{16}V^0_{,xx} + (B_{12} + B_{66})V^0_{,xy} + B_{26}V^0_{,yy} + D_{11}\psi_{x,xx} \\ &+ 2D_{16}\psi_{x,xy} + D_{66}\psi_{x,yy} + D_{16}\psi_{y,xx} + (D_{12} + D_{66})\psi_{y,xy} + D_{26}\psi_{y,yy} - k[A_{55}(\psi_x + W_{,x}) \\ &+ A_{45}(\psi_y + W_{,y})] = R\ddot{U}^0 + I\ddot{\psi}_x \end{aligned} \tag{5.2.11d}$$

$$\begin{aligned} &B_{16}U^0_{,xx} + (B_{12} + B_{66})U^0_{,xy} + B_{26}U^0_{,yy} + B_{66}V^0_{,xx} + 2B_{26}V^0_{,xy} + B_{22}V^0_{,yy} + D_{16}\psi_{x,xx} \\ &+ (D_{12} + D_{66})\psi_{x,xy} + D_{26}\psi_{x,yy} + D_{66}\psi_{y,xx} + 2D_{26}\psi_{y,xy} + D_{22}\psi_{y,yy} - k[A_{45}(\psi_x + W_{,x}) \\ &+ A_{44}(\psi_y + W_{,y})] = R\ddot{V}^0 + I\ddot{\psi}_y \end{aligned} \tag{5.2.11e}$$

5.3 Stress Wave Propagation under Dynamic Loading

In order to present and examine the approach presented above in an illustrative fashion, one

assumes a rectangular composite laminate plate of constant thickness h composed of thin layers of anisotropic fibre (graphite/glass) reinforced laminae bonded perfectly together with the length and width as a and b, respectively. The origin of a Cartesian coordinate system is located at the corner of the central plane $(x-y)$ with the z-axis being normal to this plane as shown in Figure 5.1. Further, we assume that this plate is a symmetric cross-ply laminate and is simply supported all around on each edge, thus, we must have the following boundary conditions which are similar in the case of hinged edges free in the normal direction,

at $x = 0$ and $x = a$,

$$W = \psi_y = M_x = 0 \tag{5.3.1a}$$

$$V = N_x = 0 \tag{5.3.1b}$$

at $y = 0$ and $y = b$,

$$W = \psi_x = M_y = 0 \tag{5.3.1c}$$

$$U = N_y = 0 \tag{5.3.1d}$$

From the above definition, we also have the following condition as (for symmetric cross-ply laminate which could be treated as a homogeneous continuum of transversely isotropic material) $B_{ij} = 0$, $R = 0$, $A_{16} = A_{26} = D_{16} = D_{26} = A_{45} = 0$ and $U, V = 0$. Accordingly, the five Equations of Motion, Equation (5.2.11), can be reduced to three equations with ψ_x, ψ_y, W are the only unknowns, i.e.,

$$k[A_{55}(\psi_{x,x}+W_{,xx})+A_{44}(\psi_{y,y}+W_{,yy})]+q=PW_{,tt} \tag{5.3.2a}$$

$$D_{11}\psi_{x,xx}+D_{66}\psi_{x,yy}+(D_{12}+D_{66})\psi_{y,xy}-kA_{55}(\psi_{x}+W_{,x})=I\psi_{x,tt} \tag{5.3.2b}$$

$$(D_{12}+D_{66})\psi_{x,xy}+D_{66}\psi_{y,xx}+D_{22}\psi_{y,yy}-kA_{44}(\psi_{y}+W_{,y})=I\psi_{y,tt} \tag{5.3.2c}$$

Following the Navier solution for forced vibration of plates, the load distribution function q could be approximated by double Fourier series. Therefore, we can obtain the general expression for the desired load distribution function as

$$q=\sum_{m,n=1}^{\infty} q_{mn}(t)\sin\frac{m\pi x}{a}\sin\frac{n\pi y}{b} \tag{5.3.3}$$

where the coefficient $q_{mn}(t)$ can be found by integrating the equation below

$$q_{mn}(t)=\frac{4}{ab}\int_0^a\int_0^b q(x,y,t)\sin\frac{m\pi x}{a}\sin\frac{n\pi y}{b}\,dy\,dx \tag{5.3.4}$$

The general solutions for the above impact problem which satisfy the boundary conditions can also be expressed in the double Fourier series form as

$$W(x,y,t) = \sum_{m,n=1}^{\infty} W_{mn}(t) \sin\frac{m\pi x}{a} \sin\frac{n\pi y}{b} \tag{5.3.5a}$$

$$\psi_x(x,y,t) = \sum_{m,n=1}^{\infty} X_{mn}(t) \cos\frac{m\pi x}{a} \sin\frac{n\pi y}{b} \tag{5.3.5b}$$

$$\psi_y(x,y,t) = \sum_{m,n=1}^{\infty} Y_{mn}(t) \sin\frac{m\pi x}{a} \cos\frac{n\pi y}{b} \tag{5.3.5c}$$

In order to apply the Correspondence Principle to solve this impact problem in viscoelasticity, it is necessary to use the Fourier transformation as

$$f^F(x,y,\omega) = \int_{-\omega}^{\omega} f(x,y,t)\, e^{-i\omega t}\, dt \tag{5.3.6}$$

where the superscript $(\ )^F$ indicates the Fourier transform of the variable ( ) and ω is the Fourier parameter. By applying the Fourier transformation to Equations (5.3.2a) to (5.3.2c), (5.3.3), and (5.3.5a) to (5.3.5c), we obtain the equations of motion in the frequency-domain as

$$k[A_{55}(\psi^F_{x,x} + W^F_{,xx}) + A_{44}(\psi^F_{y,y} + W^F_{,yy})] + q^F = -\omega^2 P W^F \tag{5.3.7a}$$

$$D_{11}\psi^F_{x,xx} + D_{66}\psi^F_{x,yy} + (D_{12} + D_{66})\psi^F_{y,xy} - k A_{55}(\psi_x^{\ F} + W^F_{,x}) = -\omega^2 I \psi_x^{\ F} \tag{5.3.7b}$$

$$(D_{11} + D_{66})\psi^F_{x,xy} + D_{66}\psi^F_{y,xx} + D_{22}\psi^F_{y,yy} - k A_{44}(\psi_y^{\ F} + W^F_{,y}) = -\omega^2 I \psi_y^{\ F} \tag{5.3.7c}$$

thus, the double Fourier series of general solutions can be written as

$$W^F(x,y,\omega) = \sum_{m,n=1}^{\infty} W_{mn}^F(\omega)\sin\frac{m\pi x}{a}\sin\frac{n\pi y}{b} \tag{5.3.8a}$$

$$\psi_x^F(x,y,\omega) = \sum_{m,n=1}^{\infty} X_{mn}^F(\omega)\cos\frac{m\pi x}{a}\sin\frac{n\pi y}{b} \tag{5.3.8b}$$

$$\psi_y^F(x,y,\omega) = \sum_{m,n=1}^{\infty} Y_{mn}^F(\omega)\sin\frac{m\pi x}{a}\cos\frac{n\pi y}{b} \tag{5.3.8c}$$

and the impact loading distribution is expressed as

$$q^F(x,y,\omega) = \sum_{m,n=1}^{\infty} q_{mn}^F(\omega)\sin\frac{m\pi x}{a}\sin\frac{n\pi y}{b} \tag{5.3.9}$$

The Correspondence Principle is then adopted to transfer the above solutions from elastic plate theory to viscoelastic plate theory by simply replacing the elastic constants with their viscoelastic counterparts[87] as

$$A_{ij} = A_{ij}^{\bullet}(\omega) = A_{ij}^{\bullet},\ D_{ij} = D_{ij}^{\bullet}(\omega) = D_{ij}^{\bullet} \tag{5.3.10}$$

where $A_{ij}^{\bullet}$, $D_{ij}^{\bullet}$ are complex components.

Substituting Equations (5.3.8a) to (5.3.8c) and (5.3.9) into Equations (5.3.7a) to (5.3.7c), by

differentiating and simplification, one obtains the solutions as

$$W_{mn}^{F}(\omega) = \frac{a_4 a_5 a_- - a_5^2 a_6}{a_1 a_4 a_5 a_- - a_1 a_5^2 a_6 - a_2^2 a_5 a_- + a_2 a_3 a_5^2 - a_3^2 a_4 a_5 + a_2 a_3 a_5 a_6} q_{mn}^{F}(\omega) \tag{5.3.11a}$$

$$X_{mn}^{F}(\omega) = \frac{a_2 a_5 a_- - a_3 a_5^2}{a_2^2 a_5 a_- - a_2 a_3 a_5^2 + a_3^2 a_4 a_5 - a_1 a_4 a_5 a_- + a_1 a_5^2 a_6 - a_2 a_3 a_5 a_6} q_{mn}^{F}(\omega) \tag{5.3.11b}$$

$$Y_{mn}^{F}(\omega) = \frac{a_2 a_3 a_4 - a_2^2 a_6}{a_2 a_3^2 a_4 - a_2^2 a_3 a_6 + a_1 a_2 a_5 a_6 - a_2^2 a_3 a_5 + a_2^3 a_- - a_1 a_2 a_4 a_-} q_{mn}^{F}(\omega) \tag{5.3.11c}$$

where

$$a_1 = kA_{55}^{*}\left(\frac{m^2\pi^2}{a^2}\right) + kA_{44}^{*}\left(\frac{n^2\pi^2}{b^2}\right) - \omega^2 P \tag{5.3.12a}$$

$$a_2 = kA_{55}^{*}\left(\frac{m\pi}{a}\right); \qquad a_3 = kA_{44}^{*}\left(\frac{m\pi}{b}\right) \tag{5.3.12b}$$

$$a_4 = D_{11}^{*}\left(\frac{m^2\pi^2}{a^2}\right) + D_{66}^{*}\left(\frac{n^2\pi^2}{b^2}\right) + kA_{55}^{*} - \omega^2 I \tag{5.3.12c}$$

$$a_5 = (D_{12}^{*} + D_{66}^{*})\left(\frac{mn\pi^2}{a^2}\right); \qquad a_6 = (D_{11}^{*} + D_{66}^{*})\left(\frac{mn\pi^2}{b^2}\right) \tag{5.3.12d}$$

$$a_7 = D_{66}^{*}\left(\frac{m^2\pi^2}{a^2}\right) + D_{22}^{*}\left(\frac{m^2\pi^2}{b^2}\right) + kA_{44}^{*} - \omega^2 I \tag{5.3.12e}$$

Finally, the dynamic solutions are obtained in their frequency transform. In the following sections, the dynamic impact load will be analyzed and applied to derive the final mathematical model which will solve this transient wave propagation problem.

5.4 Transient Wave Propagation under Impact Loading

For a viscoelastic system, as illustrated in previous sections, direct solutions of the equations of motion are not obtainable. Therefore, in order to analyze transient wave propagation in an illustrative manner, Fourier Transform approach must be adopted and a dynamic viscoelastic system must be defined. First, the same viscoelastic rectangular composite laminate plate, which is composted of thin layers of anisotropic fibre reinforced laminae bonded perfectly together, and the same Cartesian coordinate system, with the origin located at the corner of central plane, Figure 5.1, are considered with the length and width of this plate being defined as a and b, respectively. Then, further, one assumes that this plate to be symmetric cross-ply laminate with three layers of stacking sequence as $[\,0,\ 90^{\circ}\,]_{2S}$, Figure 5.1. The plate is simply supported all around on all edges.

A local rectangular impulsive pressure distribution is imposed on this plate. This load is modelled as a cosine-cosine distribution with respect to the space variables and sine distribution with respect to time. Its centre is located at coordinate (x_1 , y_1) on the plate as shown in Figure 5.2. The function of this distribution can be expressed as[76]

$$q = P_0 \cos\frac{\pi}{u}(x - x_1)\cos\frac{\pi}{v}(y - y_1)\sin\frac{\pi t}{\tau_0} \tag{5.4.1a}$$

$$for \quad 0 \le t \le \tau_0, x_1 - \frac{u}{2} \le x \le x_1 + \frac{u}{2}, y_1 - \frac{v}{2} \le y \le y_1 + \frac{v}{2}$$

$$q = 0 \tag{5.4.1b}$$

$$for \quad t > \tau_0; x < x_1 - \frac{u}{2}, x > x_1 + \frac{u}{2}; y < y_1 - \frac{v}{2}, y > y_1 + \frac{v}{2}$$

Following the "Navier Approach", by substituting Equations (5.4.1a) and (5.4.1b) into Equation (5.3.4) and integrating, one obtains,

$$q_{mn}(t) = \frac{16abuvP_0 \cos(\frac{m\pi u}{2a})\cos(\frac{n\pi v}{2b})\sin(\frac{m\pi x}{a})\sin(\frac{n\pi y}{b})}{\pi^2(mu+a)(mu-a)(nv+b)(nv-b)}\sin(\frac{\pi t}{\tau_0}) \tag{5.4.2a}$$

$$for \qquad mu \neq a;\ nv \neq b$$

$$q_{mn}(t) = 0 \tag{5.4.2b}$$

$$for \qquad mu = a;\ nv = b$$

The load distribution function could then be approximated by double Fourier series as

$$q(x,y,t) = \frac{16abuvP_0}{\pi^2}\sin(\frac{\pi t}{\tau_0})\sum_{m,n=1}^{\infty}\frac{\cos(\frac{m\pi u)}{2a})\cos(\frac{n\pi v}{2b})\sin(\frac{m\pi x_1}{a})\sin(\frac{n\pi y_1}{b})\sin(\frac{m\pi x}{a})\sin(\frac{n\pi y}{b})}{(mu+a)(mu-a)(nv+b)(nv-b)} \tag{5.4.3a}$$

$$for \qquad mu \neq a;\ nv \neq b;\ 0 \leq t \leq \tau_0$$

$$q(x,y,t) = 0 \tag{5.4.3b}$$

$$for \qquad mu = a;\ nv = b;\ t > \tau_0$$

In order to find solutions for this viscoelastic dynamic system, Fourier Transform is once again applied here to transform the above load distribution function from time-domain to frequency-domain. Substituting Equations (5.4.3a) and (5.4.3b) into Equation (5.3.6), it follows that

$$q^F(x,y,\omega) = \frac{8abuvP_0\tau_0}{\pi^2}\left[\frac{1-\cos(\pi+\tau_0\omega)}{\pi+\tau_0\omega} + \frac{1-\cos(\pi-\tau_0\omega)}{\pi-\tau_0\omega} + i\left(\frac{\sin(\pi+\tau_0\omega)}{\pi+\tau_0\omega} - \frac{\sin(\pi-\tau_0\omega)}{\pi-\tau_0\omega}\right)\right]$$

$$\sum_{m,n=1}^{\infty} \frac{\cos(\frac{m\pi u}{2a})\cos(\frac{n\pi v}{2b})\sin(\frac{m\pi x_1}{a})\sin(\frac{n\pi y_1}{b})\sin(\frac{m\pi x}{a})\sin(\frac{n\pi y}{b})}{(mu+a)(mu-a)(nv+a)(nv-a)} \tag{5.4.4a}$$

$$\textit{for} \qquad mu \neq a; nv \neq b; \omega\tau_0 \neq \pi$$

$$q^F(x,y,\omega) = 0 \tag{5.4.4b}$$

$$\textit{for} \qquad mu = a; nv = b; \omega\tau_0 = \pi$$

From Equation (5.3.9), one could obtain complex coefficient $q^F_{mn}(\omega)$

$$q^F_{mn}(\omega) = \frac{8abuvP_0\tau_0 \cos(\frac{m\pi u}{2a})\cos(\frac{n\pi v}{2b})\sin(\frac{m\pi x_1}{a})\sin(\frac{n\pi y_1}{b})}{(mu+a)(mu-a)(nv+b)(nv+b)} \tag{5.4.5a}$$

$$\left[\frac{1-\cos(\pi+\tau_0\omega)}{\pi+\tau_0\omega} + \frac{1-\cos(\pi-\tau_0\omega)}{\pi-\tau_0\omega} + i\left(\frac{\sin(\pi+\tau_0\omega)}{\pi+\tau_0\omega} - \frac{\sin(\pi-\tau_0\omega)}{\pi-\tau_0\omega}\right)\right]$$

$$\textit{for} \qquad mu \neq a; nv \neq b; \omega\tau_0 \neq \pi$$

$$q^F_{mn}(\omega) = 0 \tag{5.4.5b}$$

$$\textit{for} \qquad mu = a; nv = b; \omega\tau_0 = \pi$$

Obviously, in order to obtain the desired transient wave solutions, one could combine Equations (5.4.5a) and (5.4.5b) with Equations (5.3.11a) to (5.3.11c) and (5.3.8a) to (5.3.8c), to achieve the solutions in their frequency transform.

Then, by applying the viscoelastic "constants" A^*_{44}, A^*_{55}, D^*_{11}, D^*_{12}, D^*_{22} and D^*_{66} as defined in

Appendix B, the Fast Fourier Transformation could be applied here to numerically transform these solutions from frequency-domain to time-domain. The resulted transient wave propagation problem will be further explored within the micromechanics scope

5.5 Fast Fourier Transform (FFT) and Programming

It is in general agreed upon that the cause of the sudden failure must be examined from the point of transient wave propagation phenomena. Therefore the dynamic solutions which are obtained in the frequency-domain must be inverted into time-domain and only the Fourier Transform approach appears to be feasible. It is also obvious that due to their complexity, it is impossible to invert the above frequency-domain solutions analytically. In this case, the discrete Fourier Transform appears to be effective. The discrete Fourier transform is an approximation to the continuous Fourier transform. Normally, the discrete Fourier transform pair could be expressed as[88],

$$G\left(\frac{n}{NT}\right)=\sum_{k=0}^{N-1} g(kT)e^{-i2\pi nk/N} \qquad n=0,1,\ldots,N-1 \tag{5.5.1}$$

$$g(kT)=\frac{1}{N}\sum_{n=0}^{N-1} G\left(\frac{n}{NT}\right)e^{i2\pi nk/N} \qquad k=0,1,\ldots,N-1 \tag{5.5.1}$$

where N is the total sampling number, T is sampling interval and G() and g() represent the desired function in their frequency and time domains, respectively.

In engineering computations, the reason for the wide use of Fourier transform is due to its capability to allow one to examine a function from the perspective of both time and frequency domains. The time and effort are further eased due to the development of the discrete Fourier transform which permits one to analyze behaviour of the function in the numeric fashion. However, in this case, it is still time consuming because large sampling number is required for the dynamic analysis. Therefore a faster algorithm is required, and the Fast Fourier Transform (FFT) appears to be the candidate for this application which could reduce the computation time from N^2 to $N \log N$.

The main task of FFT operation is the determination of the total sampling number N and the sampling interval T which directly affect the results of FFT computation. In the present application, it is believed that the interval time is closely related to the waveform of the desired impact loading function. The sampling number N is determined from the analysis of the different FFT results. The analysis and determination of both sampling number and interval time will be illustrated in detail later in this chapter.

The FFT algorithm which was proposed by Brigham[88] will be utilized in this application. Please refer to the APPENDIX E for the FFT computer program flowchart.

5.6 Numerical Results and Discussions

In this research, an impact system with the same geometry and loading distribution as shown in Figures 5.1 and 5.2 is explored. The dimension of the dealt with composite laminate is set as a =20.0 cm, b = 10.0 cm and h = 1.0 cm with each laminate being composed of viscoelastic matrix and glass fibres. The impact is assumed to be the unit load p = 1.0, with a contact duration $\tau_0 = 1 \times 10^{-6}$ sec, located at the centre of this plate as x_1 = 10.0 cm and y_1 = 5.0 cm, and has a square loaded area, i.e., u = v = 0.1 cm. It is further assumed that the matrix is a viscoelastic material and the real part of its complex modulus has the form[87]

$$E_{mr} = 1158(1 + 100f)^{0.1} \tag{5.6.1}$$

where f is the frequency.

The damping factors of the matrix material are assumed to be constant and set as 0.05 and 0.15 for the further comparison. Both elastic and viscoelastic (damping factor: 0.0014) glass fibres are considered in this research. The above assumed fibre damping factor (0.0014) is seen to be the combined viscoelastic effect of both fibre and fibre-matrix interface[6-9]. The elastic modulus of this glass fibre is set as 72.4GPa. The effects of both fibre volume fractions (50%, 60% and 70%) and fibre aspect ratios (5, 30, 100 and continuous) on the impact behaviour of the composite laminate are also examined. Other properties such as shear modulus, shear damping

factor, Poisson's ratio and specific gravity are assumed to be of the same values as shown in Table 3.1, Chapter 3, for both the fibre and matrix. These properties are further assumed as constants for the ease of calculations. Based on the convergence study conducted by Prasad et.al.[76], both coefficients m and n for Navier Solution are set as 150 for accuracy. The shear correction factor k is set as $\pi^2/12$ as we mentioned in the Section 5.2 of this chapter[86]. By careful comparison, the total sample number N and the sample interval T for FFT operation are set as 8192 and 2×10^{-6} sec. For the ease of illustration and comparison, only displacement along z-axis at centre point will be calculated and presented in dimensionless fashion.

Figure 5.3 shows both real and imaginary parts of the displacement in the frequency-domain as well as their inverted Fourier Transform result in the time-domain. The significant attenuation is observed due to the viscoelastic nature of this kind of materials.

The impact response of laminates with matrices with different damping factors is presented in the Figure 5.4. In this figure, one finds that under the same loading condition the laminate with the matrix having the higher damping factor produces much a smaller amplitude of the displacement waveform than the one having lower damping factor. It is obvious that the waveform of the laminate with matrix having lower damping factor is not as smooth as the one having higher damping factor and is more complex to analyze. Figure 5.4 also shows that the laminate with matrix having lower damping factor exhibits a higher attenuation rate in the first 3 - 4 ms. The

attenuation seems to slow down after 4 ms and the amplitude of the response waveform almost keeps constant after 12 ms. For the laminate with matrix having higher damping factor, slow attenuation is observed through the whole computation time scale.

The effect of viscoelasticity of the fibre material is illustrated in Figure 5.5. Both elastic and linear viscoelastic fibre materials are considered under the same loading condition. It shows that there is not much difference between the elastic and viscoelastic fibres except in the first 1 - 1.5 *ms*. This phenomenon demonstrates that for ease of computation, one could consider glass fibre as perfect elastic material. It is further confirmed that the matrix material makes major contribution to the viscoelastic nature of the laminated composites.

Figures 5.6 and 5.7 present the effect of fibre volume fraction on the impact response of the considered laminates. The same pattern could be found in the laminate systems with different values of damping factor of matrices, i.e., as 0.05 and 0.15, respectively. Apparently, the initial amplitude of response waveform with higher fibre volume fraction is much lower than the one with lower fibre volume fraction due to the decrease of stiffness with the decrease of fibre volume fraction. But the attenuation of a laminate with lower fibre volume fraction is much more significant than the one with higher fibre volume fraction. This observation further proves the conclusion of the previous chapter that the viscoelasticity of laminates increases when fibre volume fraction decreases. The delayed phase response of laminate with lower fibre volume fraction is also observed compared with the higher fibre volume fraction laminate, which is

believed to be due to the changing of their transverse properties.

Due to the high volume of discontinuous fibre reinforced composite applications in automotive and aerospace industries and their superior damping capabilities compared to continuous fibre reinforced composites, it is necessary to examine the effect of discontinuous fibre reinforcement on the dynamic response under impact loading. The effect of discontinuous fibre reinforcement on the mechanical properties under the static loading was analyzed in Chapter 3 of this thesis.

The observation made by Cox[38] shows that for fibre reinforced composite materials, the reduction of the effective longitudinal modulus due to the load transfer from fibre to fibre is important only if the fibre aspect ratio is less than 100. Figures 5.8 and 5.9 compare the dynamic responses between the continuous fibre and fibre with its aspect ratio set as 100 for the laminates with both low and high damping matrices, i.e. damping factor of matrices as 0.05 and 0.15. For the laminate with low damping matrix, the response waveform fits well with observation made by Cox that the discontinuous fibre reinforced laminate with fibre aspect ratio larger than 100 can be treated as continuous fibre reinforced material[38]. For the laminate with high damping matrix there is slight difference between the two results.

Figures 5.10 and 5.11 compare the effect of different fibre aspect ratio on the dynamic response under the impact loading for laminates with both low and high damping matrices (damping factor is 0.05 and 0.15, respectively). The same trend could be found from both figures that the

amplitude of response waveform decreases with decrease of the fibre aspect ratio, which agrees with the observations made in Chapter 3 of this thesis. It is general agreed upon that changing of fibre volume fraction will change overall properties of a considered composite, i.e., longitudinal as well as transverse properties. On the contrary, changing of fibre aspect ratio will only change material properties at its longitudinal (fibre) direction. So, compared with Figures 5.6 and 5.7, It is interesting to note that, due to their different relationship with material damping properties and stiffness, fibre aspect ratio has a different effect on impact response compared with fibre volume fraction. It is also interesting to observe that the phase of response waveform does not change with respect to the change of fibre aspect ratio. The only change of mechanical properties in the longitudinal (fibre) direction due to the change of fibre aspect ratio might be responsible for this phenomenon.

5.7 Conclusions

(1) For a given E-glass/Epoxy laminated composite, numerical results show that the matrix material makes major contribution to the attenuation of composite laminates under impact loading and that transient wave propagation must be examined within the scope of viscoelasticity. Development of the laminated composite system, using the matrix material with high damping properties, appears to be an effective approach to optimize

the control mechanism for the structural vibration under impact loading.

(2) The resulting transient wave propagation has been further explored in relation to the properties of the microstructural constituents. The attenuation of the laminate with lower fibre volume fraction is much more significant than the one with higher fibre volume fraction. The same phenomenon is also identified for the laminate with lower fibre aspect ratio compared with the one with higher fibre aspect ratio. These results have very good agreement with the observations made in Chapter 3 of this thesis that discontinuous fibre reinforced composites have a high damping property than the continuous ones and that composites with lower fibre volume fraction have superior energy absorbing capability compared with the one with higher fibre volume fraction. These results further demonstrate, as concluded in Chapter 3 of this thesis, that in order to increase the damping, it is necessary to sacrifice the stiffness, and vice versa. These trade-offs require careful examination, but, in the meantime, also provide flexibility during the course of designing a new laminated short fibre composite system.

(3) The anisotropy and the viscoelastic nature of composite laminates make wave propagation analysis much more complex as compared to their isotropic and elastic counterparts. The "First Shear Deformation Theory" (FSDT), developed by Whitney and Pagano[75], is adopted and appears to work well in this research. The Navier Solution for forced vibration plates and "Fourier Transformation" are utilised to transfer the

Equation of Motion from time-domain to frequency-domain. Then, the "Correspondence Principle" is applied to solve this impact problem in viscoelasticity. Finally, the Fast Fourier Transformation (FFT) is employed to inverse these solutions from frequency-domain into time-domain.

(4) Wave propagation analysis method could give us in-depth understanding about the possible failure mechanism of composite laminates under impact loading. The design criteria should be developed and much more attention should be paid for the future applications of composite laminates, since impact damage would cause significant decrease in the strength and fatigue life, and hence, an increase in local stress and change of natural frequencies.

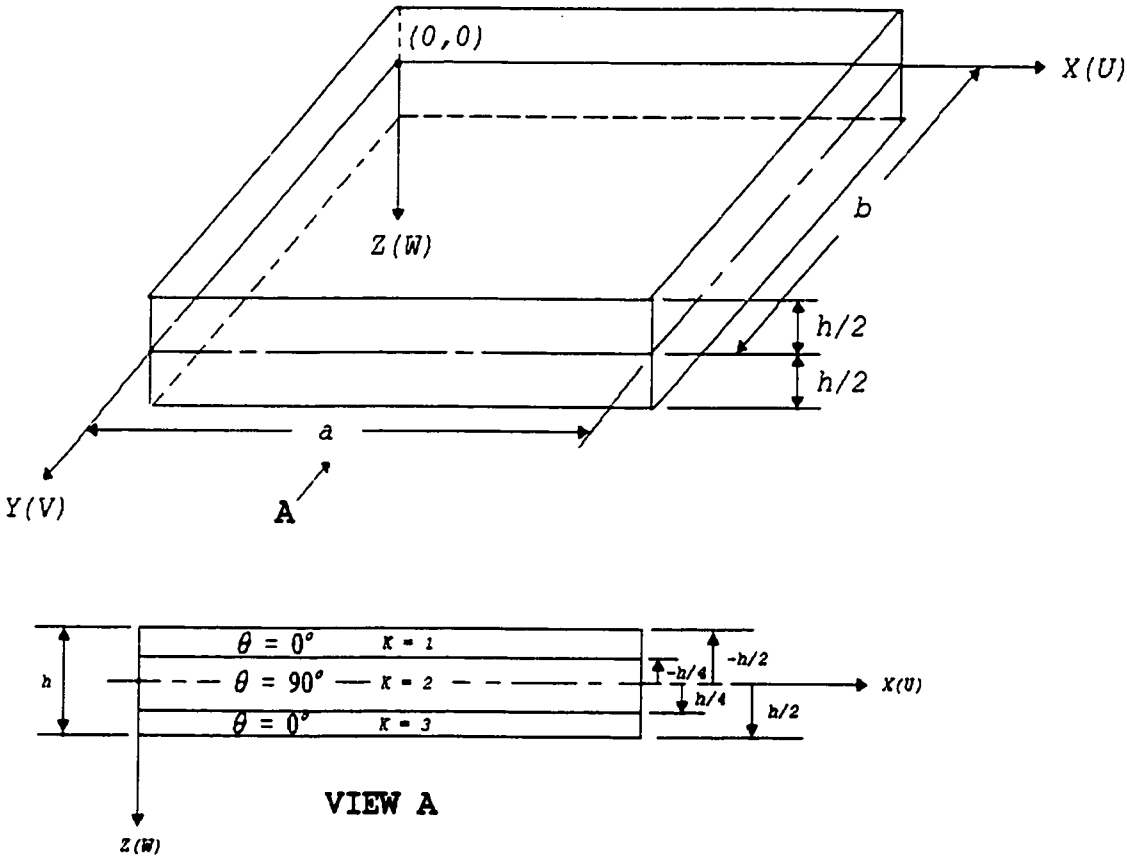

Figure 5.1 A symmetric composite laminated plate

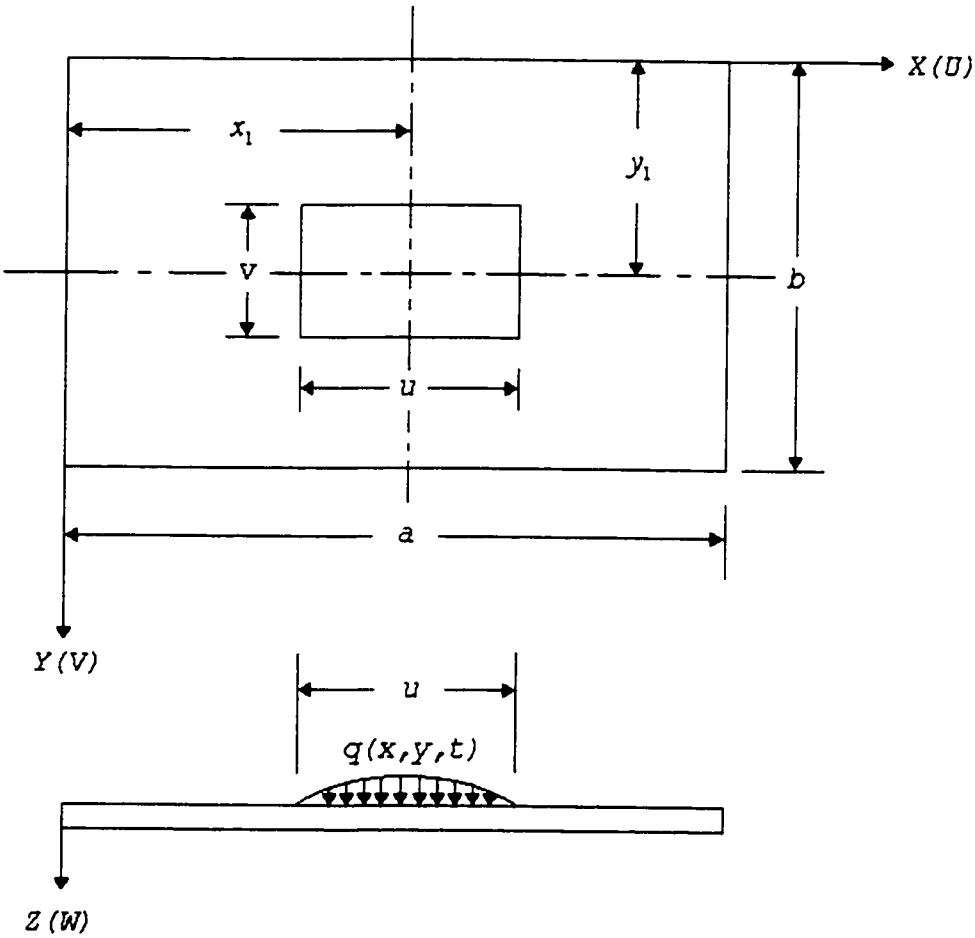

Figure 5.2 Impact pressure distribution

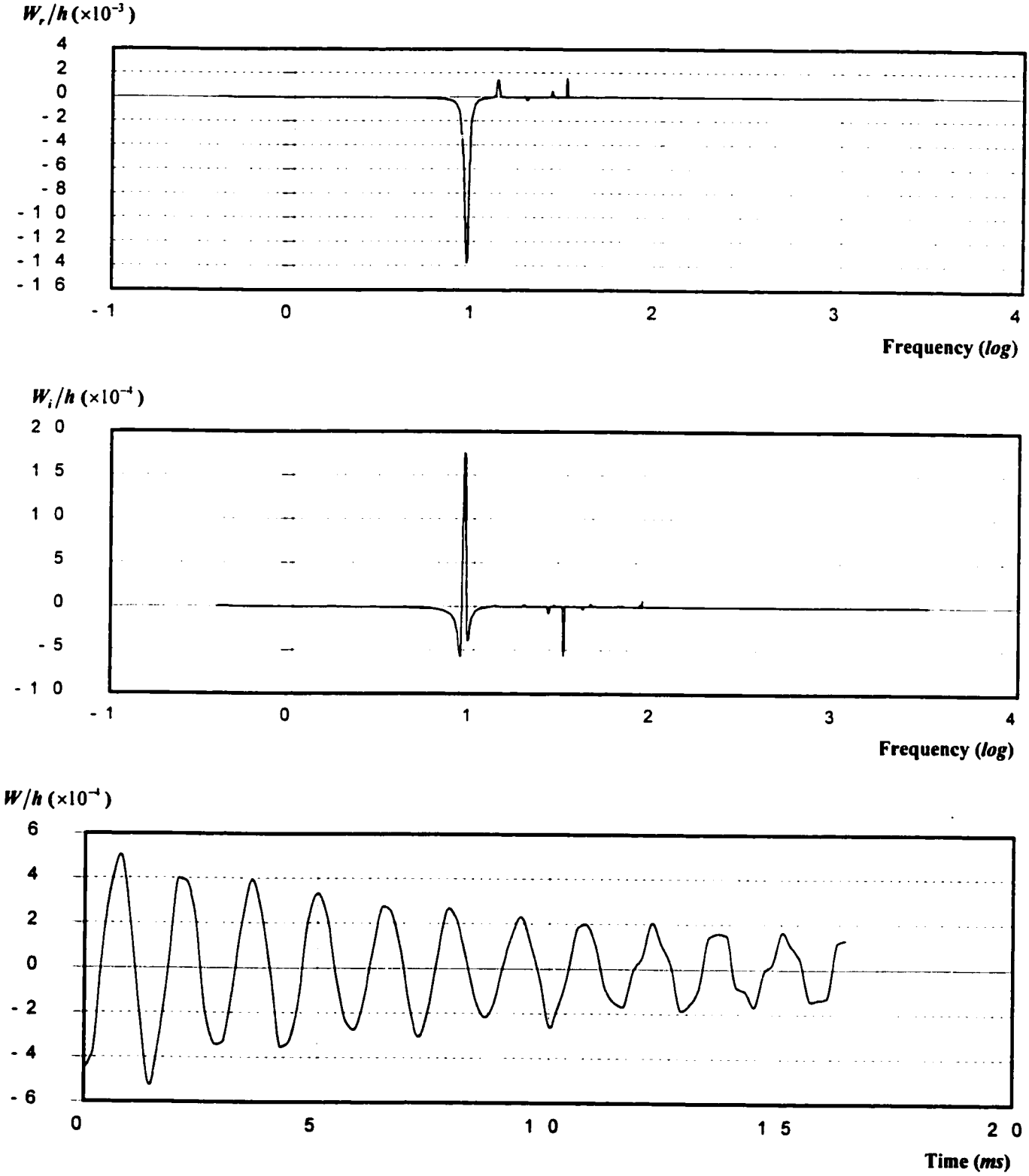

Figure 5.3 Illustration of Fourier Transformation.
The top two figures show the wave propagation solutions in their frequency-domain which can be transformed by using FFT algorithm (Fast Fourier Transformation) into time-domain as shown in bottom figure.

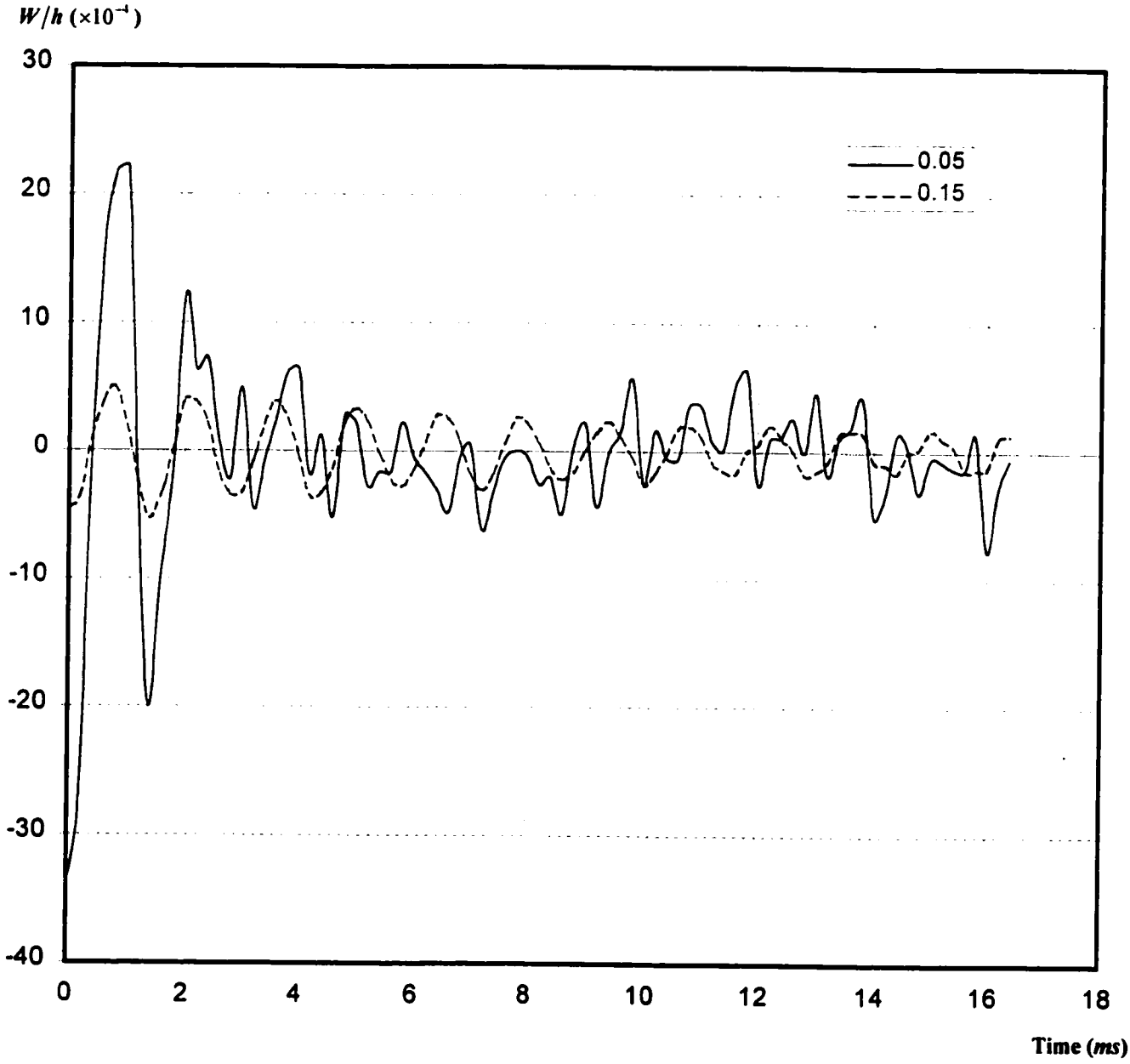

Figure 5.4 Impact response of composite laminates with matrices have different damping factors, i.e. 0.05 (solid line) and 0.15 (dashed line). Other material properties are set as: the real modulus of matrix is $E_{mr} = 1158(1 + 100f)^{0.1}$, with f as frequency, the real modulus of glass fibre (continuous) is 72.4Gpa, fibre volume fraction is 60%, and damping factor of fibre is 0.0014.

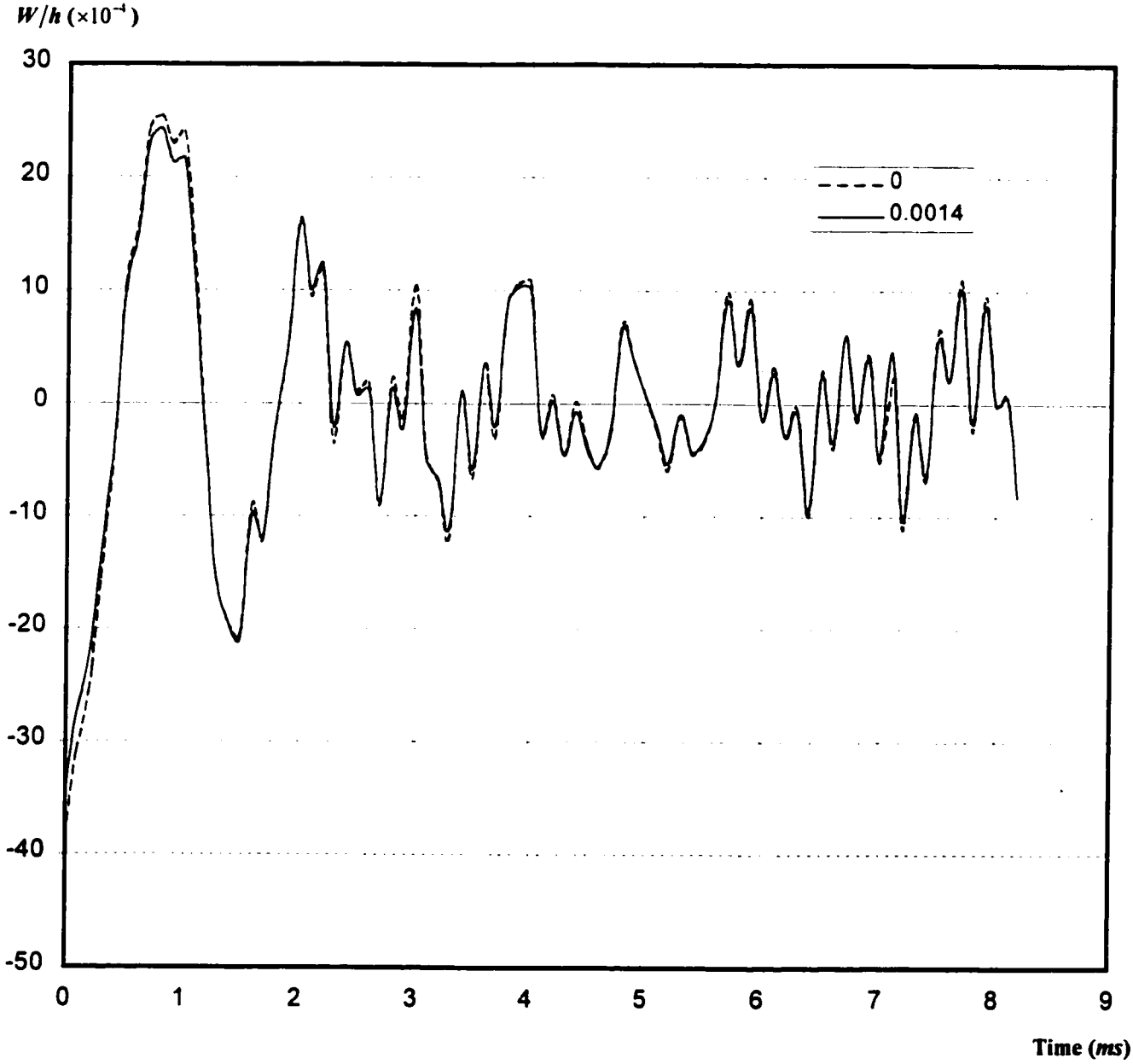

Figure 5.5 Impact response of composite laminates with elastic and viscoelastic fibres, i.e. fibre damping factors as 0.0014 (solid line) and 0.00 (dashed line). Other material properties are set as: the real modulus of glass fibre (continuous) is 72.4Gpa, fibre volume fraction is 60%, the real modulus of matrix is $E_{mr} = 1158(1 + 100f)^{0.1}$, with f as frequency, and damping factor of matrix is 0.05.

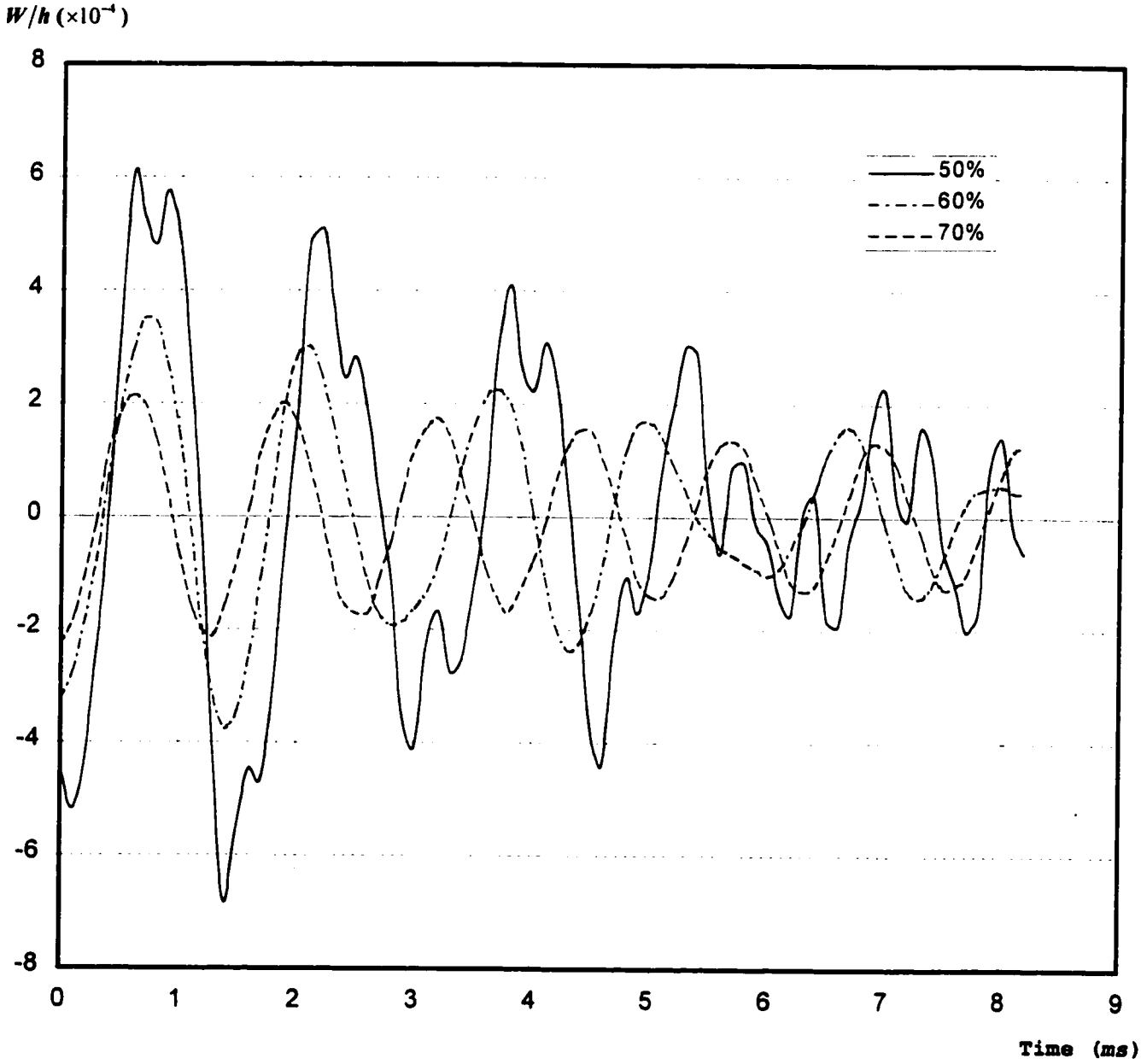

Figure 5.6 Impact response of composite laminates with various fibre volume fractions, i.e. 50% (solid line), 60% (dashdot line) and 70% (dashed line). Other material properties are set as: the real modulus of glass fibre (continuous) is 72.4Gpa, fibre damping factor is 0.0014, the real modulus of matrix is $E_{mr} = 1158(1+100f)^{0.1}$, with f as frequency, and damping factor of matrix is 0.15.

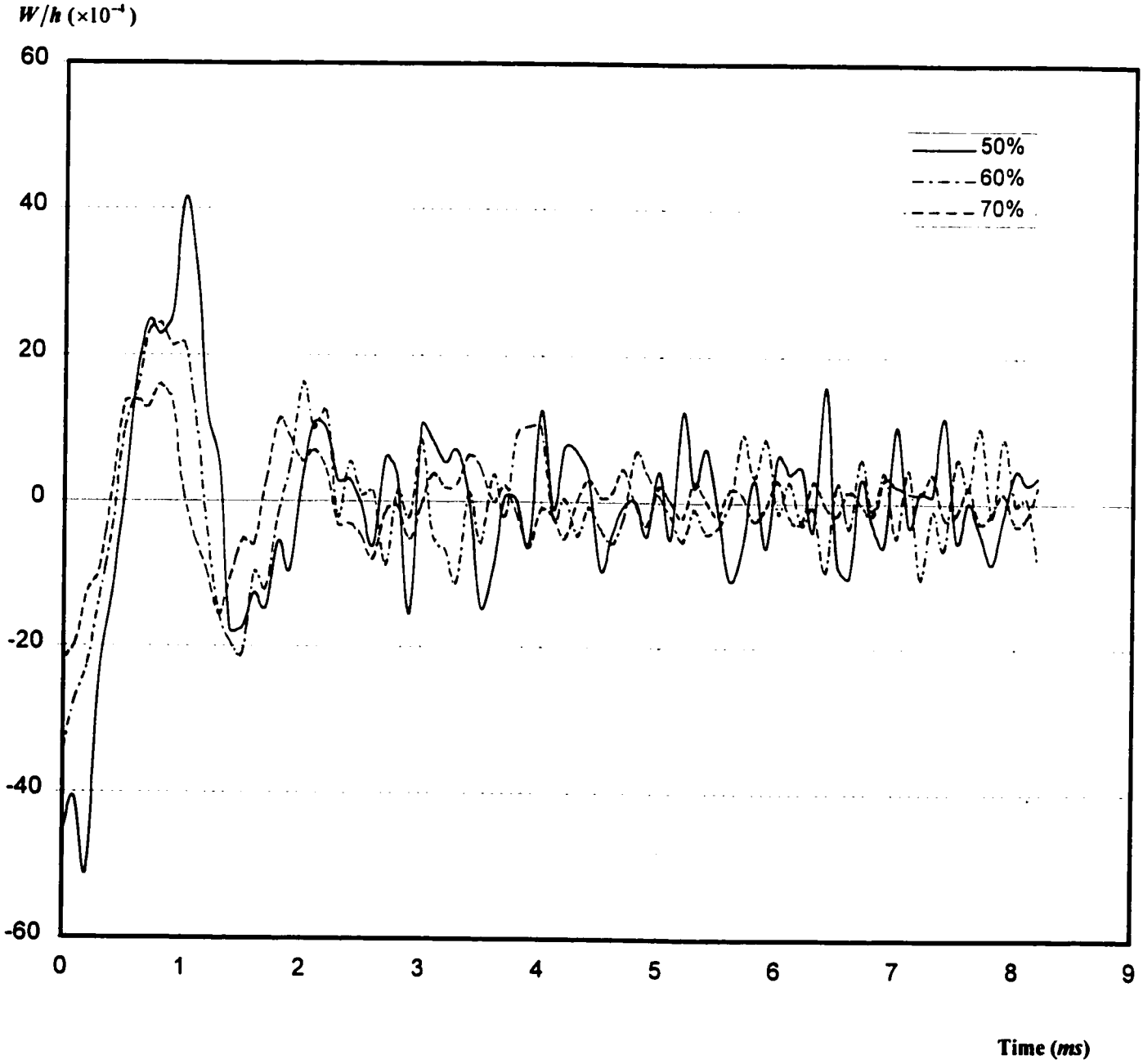

Figure 5.7 Impact response of composite laminates with various fibre volume fractions, i.e. 50% (solid line), 60% (dashdot line) and 70% (dashed line). Other material properties are set as: the real modulus of glass fibre (continuous) is 72.4Gpa, fibre damping factor is 0.0014, the real modulus of matrix is $E_{mr} = 1158(1+100f)^{0.1}$, with f as frequency, and damping factor of matrix is 0.05.

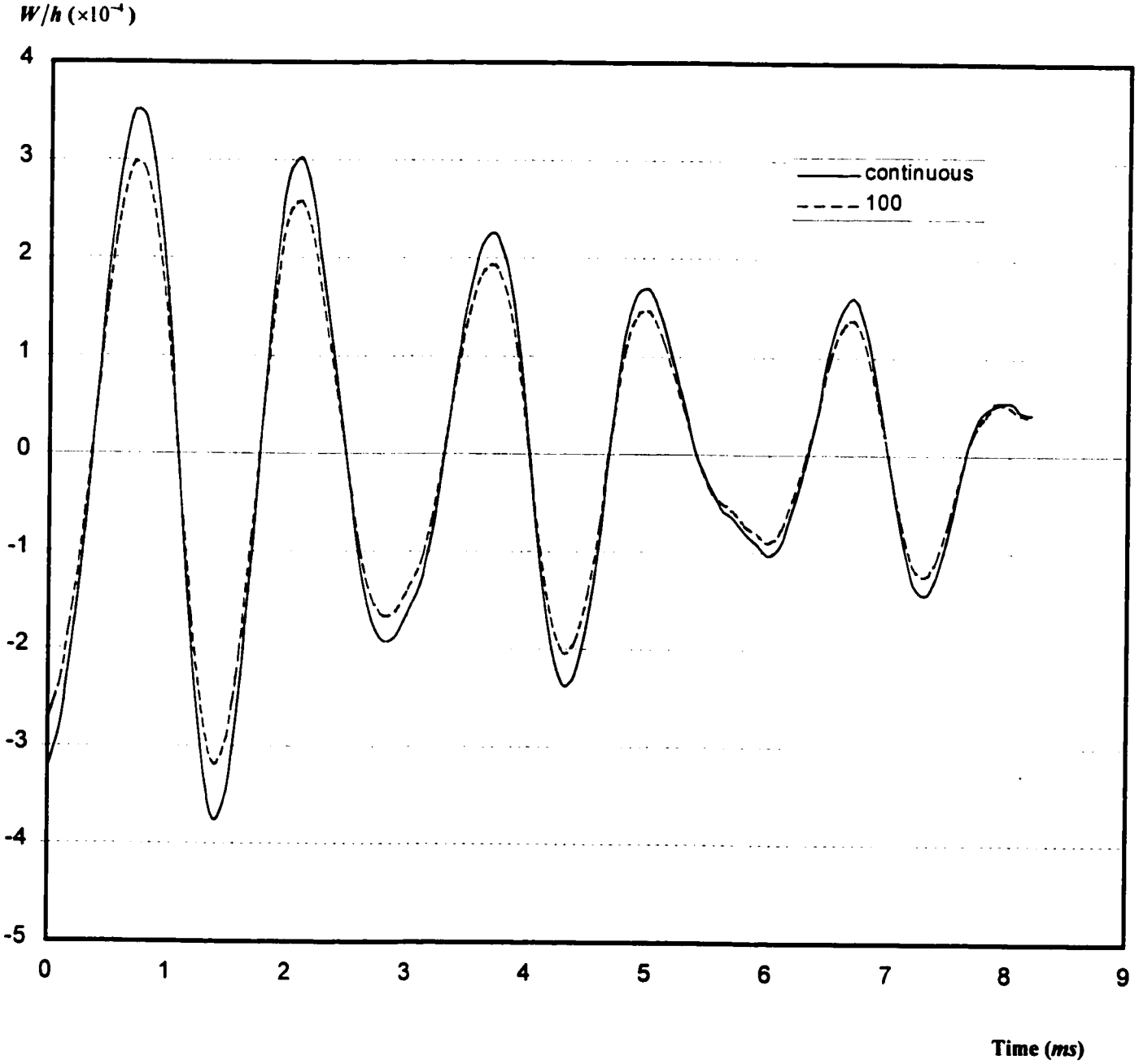

Figure 5.8 Impact response of composite laminates with various fibre aspect ratios, i.e. continuous (solid line) and 100 (dashdot line). Other material properties are set as: the real modulus of glass fibre is 72.4Gpa, fibre damping factor is 0.0014, fibre volume fraction is 60%, the real modulus of matrix is $E_{mr} = 1158(1 + 100f)^{0.1}$, with f as frequency, and damping factor of matrix is 0.15.

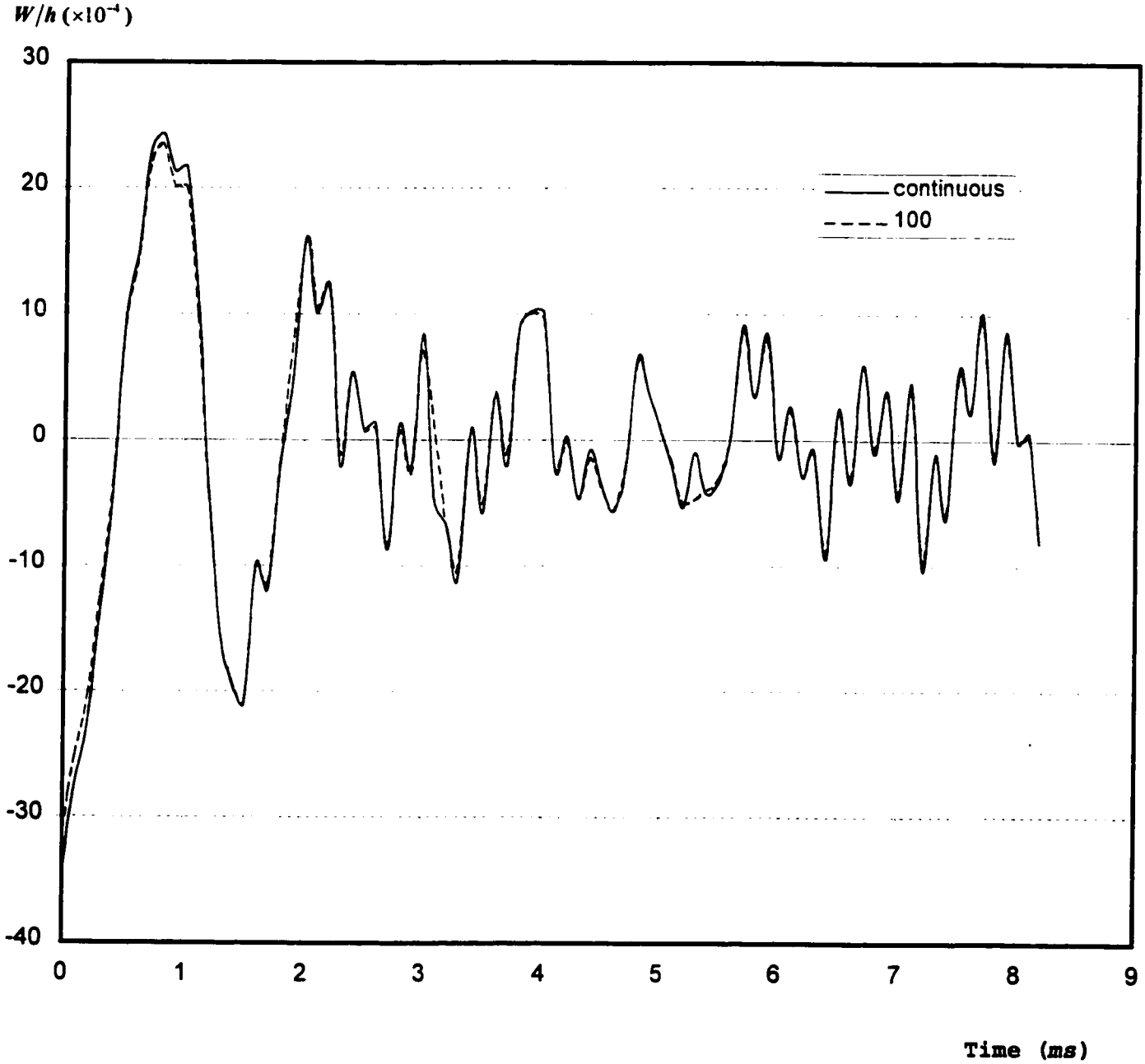

Figure 5.9 Impact response of composite laminates with various fibre aspect ratios, i.e. continuous (solid line) and 100 (dashdot line). Other material properties are set as: the real modulus of glass fibre is 72.4Gpa, fibre damping factor is 0.0014, fibre volume fraction is 60%, the real modulus of matrix is $E_{mr} = 1158(1 + 100f)^{0.1}$, with f as frequency, and damping factor of matrix is 0.05.

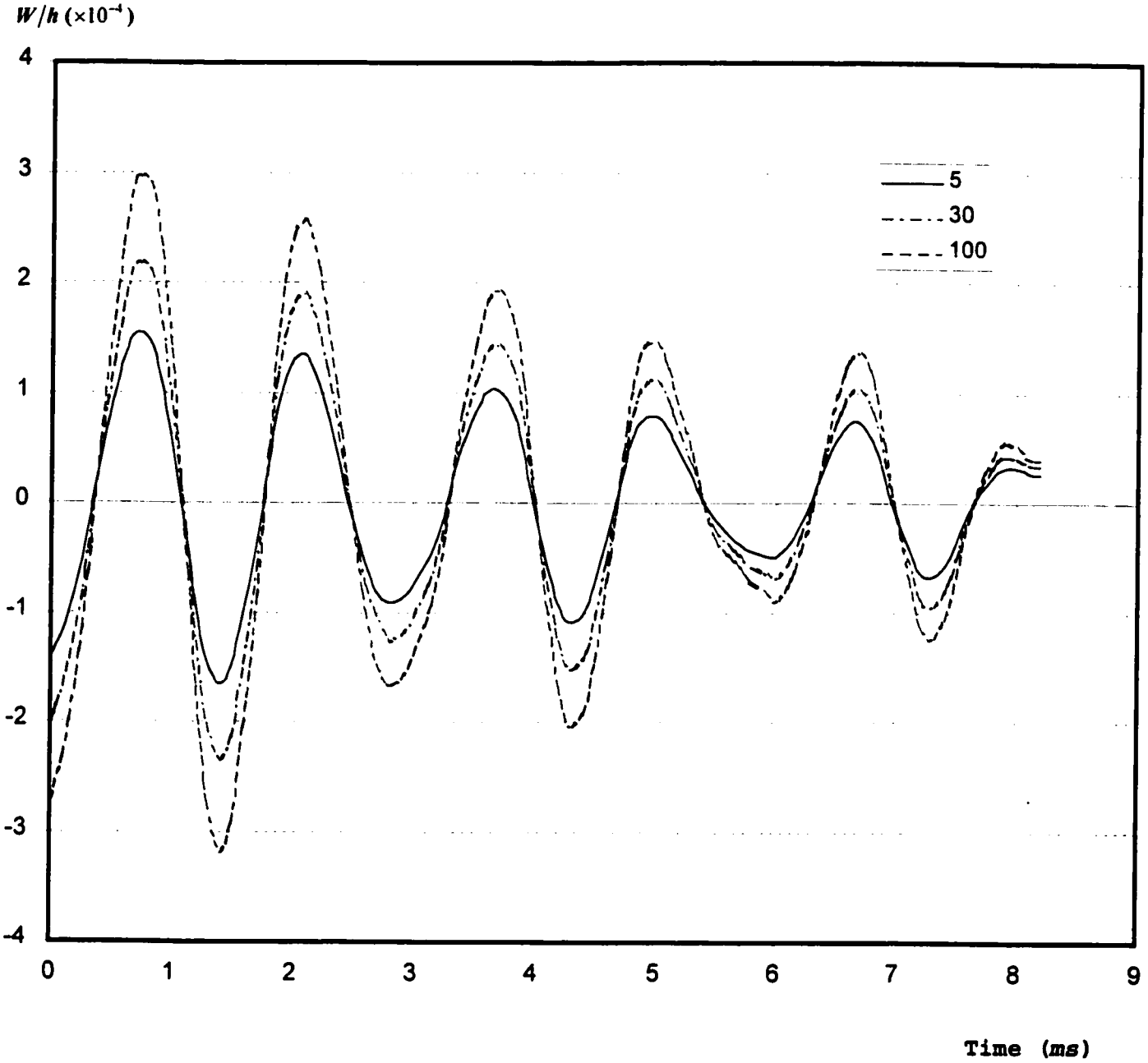

Figure 5.10 Impact response of composite laminates with various fibre aspect ratio, i.e. 5 (solid line), 30 (dashdot line), and 100 (dashed line). Other material properties are set as: the real modulus of glass fibre is 72.4Gpa, fibre damping factor is 0.0014, fibre volume fraction is 60%, the real modulus of matrix is $E_{mr} = 1158(1+100f)^{0.1}$, with f as frequency, and damping factor of matrix is 0.15.

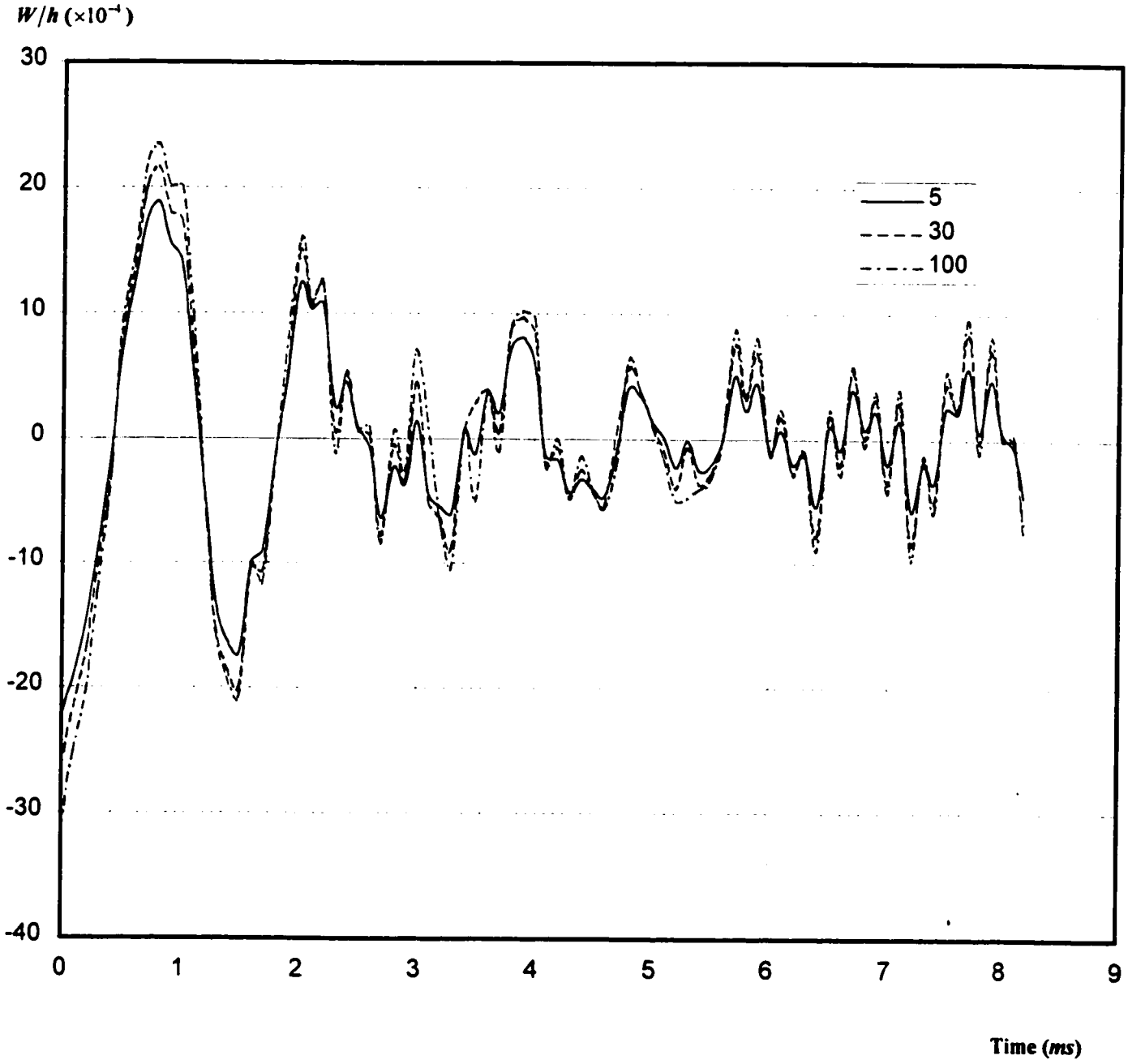

Figure 5.11 Impact response of composite laminates with various fibre aspect ratio, i.e. 5 (solid line), 30 (dashed line), and 100 (dashdot line). Other material properties are set as: the real modulus of glass fibre is 72.4Gpa, fibre damping factor is 0.0014, fibre volume fraction is 60%, the real modulus of matrix is $E_{mr} = 1158(1+100f)^{0.1}$, with f as frequency, and damping factor of matrix is 0.05.

REFERENCES

1. Haddad, Y.M. (1995) '*Viscoelasticity of Engineering Materials*', Kluwer, Dordrecht.

2. Jang, B.Z. (1990) 'Vibration Testing and Analysis of Composites', *International Encyclopedia of Composites*, Vol.6, (Edited by Lee, S.M.), VCH Publish.

3. Adams, R.D. and Bacon, D.G.C. (1973) 'Effect of Fibre Orientation and Laminate Geometry on the Dynamic Properties of CFRP', *Journal of Composite Materials* **7**, 402-428.

4. Cawley, P. and R.D. Adams (1986) 'The Predicted and Experimental Natural Modes of Free-Free CFRP Plates', *Journal of Composite Materials* **20**, 2-18.

5. Cawley, P. and Adams, R.D. (1987) 'Vibration Technique', in *Non-destructive Testing of Fibre Reinforced Plastics Composites*, Vol.1, (Edited by Summerscales, J.), Elsevier Applied Science, pp.151-200.

6. Gibson, R.F. and Yau, A. (1980) 'Complex Moduli of Chopped Fibre and Continuous Fibre Composites: Comparison of Measurements with Estimated Bounds', *Journal of Composite Materials* **14**, 155-167.

7. Gibson, R.F., Chaturvedi, S.K. and Sun, C.T. (1982) 'Complex Moduli of Aligned Discontinuous Fibre-reinforced Polymer Composites', *Journal of Materials Science* **17**, 1982, 3499-3509.

8. Sun, C.T., Gibson, R.F. and Chaturvedi, S.K. (1985) 'Internal Materials Damping of Polymer Matrix Composites Under Off-axis Loading', *Journal of Materials Science* **20**, 2575-2585.

9. Suarez, S.A., Gibson, R.F., Sun, C.T. and Chaturvedi, S.K. (1986) 'The Influence of Fibre Length and Fibre Orientation on Damping and Stiffness of Polymer Composite Materials', *Experimental Mechanics* **6**, 175-184.

10. Caprino, G., Crivelli-Viscoati, I. and Di Ilis, A. (1984) 'Elastic Behaviour of Composite Structures under Low Velocity Impact', *Composites* **15**(3), 231-234.

11. Sjoblom, P., Hartness, J. and Cordell, T. (1988) 'On Low Velocity Impact Testing of Composite Materials', *Journal of Composite Materials* **22**(1), 30-52.

12. Shivakecmar, K.N., Elber, W. and Illg, W. (1985) 'Prediction of Impact Force and Duration due to Low Velocity Impact on Circular Composite Laminates', *Journal of Applied Mechanics* **52,** 674-680.

13. Moon, F.C. (1975) 'Wave Propagation and Impact in Composite Materials', *Composite Materials,* Vol. 7, Structural Design and Analysis, Part I, (Edited by Chamis, C.C.), pp.259-332.

14. Moon, F.C. (1972) 'Wave Surfaces Due to Impact on Anisotropic Plates', *Journal of Composite Materials* **6**, 62-79.

15. Moon, F.C. (1973) 'One-Dimensional Transient Waves in Anisotropic Plates', *Journal of Applied Mechanics* **6**, 485-490.

16. Moon, F.C. (1973) 'Stress Wave Calculations in Composite Plates Using the Fast Fourier Transform', *Computers and Structures* **3**, 1195-1204.

17. Sun, C.T. and Lai, R.Y.S. (1974) 'Exact and Approximate Analyses of Transient Wave Propagation in an Anisotropic Plate', *AIAA Journal* **10**, 1415-1417.

18. Abrate, S. (1991) 'Impact on Laminated Composite Materials', *Applied Mechanics Review* **44**(4), 155-190.

19. Abrate, S., (1994) 'Impact on Laminated Composites: Recent Advances', *Applied Mechanics Review* **47**(11), 517-544.

20. Greszczuk, L.B. (1975) 'Response of Isotropic and Composite Materials to Particle Impact', *Foreign Object Impact Damage to Composites,* STP 568, ASTM, pp.183-211.

21. Haddad, Y.M. (1999) *'Mechanical Behaviour of Engineering Materials'*, Kluwer, Dordrecht, to be published.

22. Yim, J.H. (1993) 'Damping in Laminated, Partially Delaminated and Textile Structural Composites', Ph.D. Dissertation, Auburn University, AL.

23. Suarez, S.A. (1984) 'Optimization of Internal Damping in Fibre Reinforced Composite Materials', Ph.D. Dissertation, University of Idaho.

24. White, R.G. and Palmer, T.A. (1984) 'Control of the Properties of Carbon Fibre Reinforced Plastics', *AIAA Journal* **22**(11), 1662-1669.

25. Gibson, R.F. and Plunkett, R. (1976) 'Dynamic Mechanical Behaviour of Fibre Reinforced Composites: Measurement and Analysis', *Journal of Composite Materials* **10**, 325-341.

26. Chang, S. and Bert, C.W. (1973) 'Analysis of Damping for Filamentary Composite Materials', *Composite Materials in Engineering Design*, ASM, Metals Park, OH, pp.51-62.

27. Sun, C.T., Wu, J.K. and Gibson, R.F. (1985) 'Prediction of Material Damping in Randomly Oriented Short Fibre Polymer Matrix Composites', *Journal Reinforced Plastics Composites* **4**, 262-271.

28. Hwang, S.J. and Gibson, R.F. (1987) 'Micromechanical Modeling of Damping in Discontinuous Fibre Composites Using a Strain Energy/Finite Element Approach', *Journal of Engineering Materials and Technology* **109**(1), 47-52.

29. Hwang, S.J. (1985) 'Finite Element Modeling of Damping in Discontinuous Fibre Reinforced Composites', M.S. Thesis, University of Idaho.

30. Lee, E.H. (1955) 'Stress Analysis in Viscoelastic Bodies', *Quarterly Applied Mathematics* **13**, 183-190.

31. Schapery, R.A. (1967) 'Stress Analysis of Viscoelastic Composite Materials', *Journal of Composite Materials* **1**, 228-266.

32. Hashin, Z. (1970) 'Complex Moduli of Viscoelastic Composites. I. General Theory and Application to Particulate Composites', *International Journal Solids and Structure* **6**, 539-552.

33. Nashif, A.D., Jones, D.I.G. and Henderson, J.P. (1965) '*Vibration Damping*', Wiley, New York.

34. Bert, C.M. and Clary, R.R. (1974) 'Composite Materials: Testing and Design (3rd Conference)', ASTM STP 546 (The American Society for Testing and Materials, Philadelphia), pp.250-265.

35. Bert, C.M. (1980) 'Damping Applications for Vibrations Controls', ASME AMD-38 (The American Society of Mechanical Engineers, New York), pp.53-63.

36. McLean, D. and Read, B.E. (1975) 'Storage and Loss Moduli in Discontinuous Composites', *Journal of Materials Science* **10**, 481-492.

37. Sun, C.T., Wu, J.K. and Gibson, R.F. (1986) 'Prediction of Material Damping of Laminated Polymer Matrix Composites', *Damping 1986 Proceedings*, AT-WAL-TR-86-3059, Vol.2, Paper FE-1.

38. Cox, H.L. (1952) 'The Elasticity and Strength of Paper and Other Fibrous Materials', *British Journal of Applied Physics* **3**, 72-84.

39. Chamis, C.C. (1974) 'Mechanics of Load Transfer at the Interface', *Composite Materials* **6**, Academic Press, New York.

40. Agarwal, B.D. and Broutman, L.J. (1980) *'Analysis and Performance of Fibre Composites'*, Wiley Interscience, New York.

41. Rao, S.S. (1984) '*Optimization: Theory and Applications*', Wiley Eastern Limited, Second Edition, pp.649-651.

42. Spendley, W., Hext, G.R., and Himsworth, F.R. (1962) 'Sequential Application of Simplex Designs of Optimization and Evolutionary Operations', *Technometrics* **4**, 441-461.

43. Nelder, J.A. and Mead, R., (1964) 'A Simplex Method for Function Minimization', *Computer Journal* **7**, 308-313.

44. Hillier, K.W. (1960) 'A Review of the Progress in the Measurement of Dynamic Elastic Properties', *Int. Symp. On Stress Wave Propagation in Materials*, (Editor Davids, N.), Interscience, Lodon, pp.183-198.

45. Kolsky, H. (1960) 'Viscoelastic Waves', *Int. Symp. On Stress Wave Propagation in Materials* (Editor N. Davids) Interscience, Lodon, pp.59-90.

46. Worely, W.J. (1962) 'Experimental Techniques in Shock and Vibration', ASME, New York.

47. Rayleigh, J.W.S. (1887) 'On Waves Propagated Along the Plane Surface of an Elastic Solid', *Proc. London Math. Soc.* **17**, pp.4-11.

48. Kolsky, H. (1963) *'Stress Waves in Solids'*, Dover Publications, Inc., USA.

49. Barton, C.S., Volterra, E.G. and Citron, S.J. (1958) 'On Elastic Impacts of Spheres on Long Rods', *Proc 3rd US Natl. Cong. on Applied Mechanics*, pp.89-94.

50. Ripperger, E.A. (1953) 'The Propagation of Pulses in Cylindrical Bars. An Experimental Study', Proc. 1st Midwest Conf. On Solid Mechanics, pp.29-39.

51. Goldsmith, W., Polivka, M. and Yang, T. (1966) 'Dynamic Behaviour of Concrete', *Experimental Mechanics* **23**, 65-79.

52. Lamb, H. (1917) 'On Waves in an Elastic Plate', *Proc. R. Soc. London, Series A* **93**, pp.114-128.

53. Hillier, K. W. (1949) 'A Method of Measuring Some Dynamic Elastic Constants and its Application to the Study of High Polymers', *Proc. Phys. Soc.*, **52**(2), 701-713.

54. Lee, E. H. and Kanter, I. (1953) 'Wave Propagation in Finite Rods of Viscoelastic Materials', *Journal of Applied Physics*, **24**(9), 1115-1122.

55. Glanz, R.D. and Lee, E.H. (1954) 'Transient Wave Analysis in a Linear Time-Dependent Material', *Journal of Applied Physics* **25**, 947-953.

56. Morrison, J.A. (1956) 'Wave Propagation in Rods of Voigt Material and Viscoelastic Materials with Three-Parameter Models', *Quarterly Applied Mathematics* **14**, 153-169.

57. Mainardi, F. and Turchetti, G. (1979) 'Positive Constraints and Approximation Methods in Linear Viscoelasticity', *Lett. Nuovo. Cim.* **26**, 38-40.

58. Mainardi, F. and Nervosi, R.(1980) 'Transient Waves in Finite Viscoelastic Rods', *Lett. Nuovo. Cim.* **29**, 443-447.

59. Chao, C. and Achenbach, J.D. (1964) 'A Simple Viscoelastic Analogy for stress Wave', *Stress Waves in Anelastic Solids*, (Editors Kolsky, H. and Prager, W.), IUTAM Symp., Brown University, Providence, RJ, April 3-5, 1963, Springer, Berlin, pp.222-238.

60. White, J.E. and Angona, F.A. (1955) 'Elastic Wave Velocities in Laminated Media', *Journal of the Acoustical Society of America* **27**, 310-317.

61. Sun, C.T., Achenbach, J.D. and Herrmann, G. (1968) 'Continuum Theory for the Laminated Media', *Journal of Applied Mechanics* **35**, 467-475.

62. Ma, C.C. and Huang, K.H. (1995) 'Wave propagation in Layered Elastic Media for Antiplane Deformation', *Journal of Solids Structures* **32**(5), 665-678.

63. Hegemier, G.A. and Nayfeh, A.H.(1973) 'A Continuum Theory for Wave Propagation in Laminated Composites. Case 1: Propagation Normal to the Laminates', *ASME Journal of Applied Mechanics* **40**, 503-510.

64. Hegemier, G.A. and Bache, T.C. (1973) 'A Continuum Theory for Wave Propagation in Laminated Composites. Case 2: Propagation Parallel to Laminates', *Journal of Elasticity* **3**, 125-140.

65. Nemat-Nasser, S. and Yamada, M. (1981) 'Harmonic Waves in Layered Transversely Isotropic Composites', *Journal of Sound Vibration* **79**, 161-170.

66. Mukunoki, I. and Ting, T.C.T. (1980) 'Transient Wave Propagation Normal to the Layering of a Finite Layered Medium', *Int. Journal of Solids and Structures* **16**, 239-251.

67. Tang, Z. and Ting, T.C.T (1985) 'Transient Waves in a Layered Anisotropic Elastic Medium', *Proc. R. Soc. London, A397*, pp.67-85.

68. Mindlin, R.D. (1961) 'High Frequency Vibrations of Crystal Plates', *Quarterly of Applied Mathematics* **19**(1), 51-61.

69. Mindlin, R.D. and Medick, M.A. (1959) 'Extensional Vibrations of Elastic Plates', *Journal of Applied Mechanics* **26**, 561-569.

70. Lee, P.C.Y. and Nikodem, Z. (1972) 'An Approximate Theory for High-Frequency Vibrations of Elastic Plates', *Int. Journal of Solids and Structures* **8**, 581-612.

71. Kim, B.S. and Moon, F.C. (1977) 'Impact Induced Stress Waves in an Anisotropic Plate', *AIAA Journal* **17**(10), 1126-1133.

72. Mindlin, R.D. (1951) 'Influence of Rotatory Inertia and Shear on Flexural Motions of Isotropic, Elastic Plates', *Journal of Applied Mechanics* **18**(1), Trans. ASME **73**, 31-38.

73. Stavsky, Y. (1959) 'On the Theory of Heterogeneous Anisotropic Plates', Doctor's Thesis, M.I.T., Cambridge, Mass., also Air Force Technical Documentary Report No. WADD-TR-60-746.

74. Yang, P.C., Norris, C.H. and Stavsky, Y. (1966) 'Elastic Wave Propagation in Heterogeneous Plates', *Int. Journal of Solids and Structures* **2**, 665-684.

75. Whitney, J.M. and Pagano, N.J. (1970) 'Shear Deformation in Heterogeneous Anisotropic Plates', *Journal of Applied Mechanics* **12**, 1031-1036.

76. Prasad, C.B., Ambur, D.R. and Stames, J.H. Jr.(1993) 'Response of Laminated Composite Plates to Low-Speed Impact by Air-Gun-Propelled and Dropped-Weight Impactors', AIAA-93-1402-CP, *Collection of Papers of AIAA*, Part.2, pp.887-900.

77. Barker, L.M. (1971) 'A Model for Stress Wave Propagation in Composite Materials', *Journal of Composite Materials* **5**, 140-162.

78. Lundergan, C.D. and Drumneller, D.S. (1971) 'Propagation of Stress Waves in a Laminates Plate Composite', *Journal of Applied Physics* **42**(2), 669-675.

79. Kam, T.Y. and Chang, W.J. (1995) 'Impact Analysis of Shear Deformable Laminated Composite Plates', *Journal of Energy Resources Technology* **117**, 219-227.

80. Burtin, C. and Hamelin, P. (1986) 'Effect of Viscoelastic Characteristics of Polymers for a Composite Behaviour under Dynamic and Impact Loading', *Mechanical Behaviour of Composites and Laminates,* (Edited by Green, W.A and Micunonic, M.), European Mechanics Colloquium 214, Kupari, Croatia, pp.32-44.

81. Cederbaum, G. and Aboudi, J. (1989) 'Dynamic Response of Viscoelastic Laminated Plates', *Journal of Sound and Vibration* **133**(2), 225-238.

82. Reddy, J.N. (1984) 'A Simple Higher-Order Theory for Laminated Composite Plates', *Journal of Applied Mechanics* **51**, 745-752.

83. Green, W.A. and Baylis, E.R. (1988) 'The Propagation of Impact Stress Waves in Anisotropic Fibre Reinforced Laminates', *Wave Propagation in Structural Composites* (ASME, Applied Mechanics Division), Vol. 90, Publ by ASME, New York, USA, pp.53-68.

84. Sun, C.T. and Wang, T. (1986) 'Impact Wave Response and Failure in Composite Laminates', *Mechanical Behaviour of Composites and Laminates,* (Edited by Green, W.A and Micunovic, M.), European Mechanics Colloquium 214, Kupari, Croatia, pp.19-31.

85. Daniel, I.M., Liber, T. And LaBedz, R.H. (1979) 'Wave Propagation in Transversely Impacted Composite Laminates', *Experimental Mechanics* **1**, 9-16.

86. Ten, T.M. and Sun, C.T. (1983) 'Impact wave Propagation of Fibre Reinforced Composite Laminates', PhD dissertation, Department of Mechanical Engineering, Purdue University, USA.

87. Christensen, R.M. (1979) *'Mechanics of Composite materials'*, Wiley, New York, USA.

88. Brigham, E. Oran, (1988) *'The Fast Fourier Transformation & its Applications'*, Prentice Hall, Englewood Cliffs, New Jersey, USA.

APPENDIX A

Derivation of Equation (3.2.20)

One could start with Equation (3.2.19). By proper manipulating and separating, the real and imaginary parts can be expressed as follow,

$$\eta_2' = \frac{A_1 C_1 + B_1 D_1}{C_1^2 + D_1^2} \qquad (A.1)$$

$$\eta_2'' = \frac{B_1 C_1 - A_1 D_1}{C_1^2 + D_1^2} \qquad (A.2)$$

$$A_1 = G_f' - G_m' \qquad (A.3)$$

$$B_1 = G_f' \eta_{Gf} - G_m' \eta_{Gm} \qquad (A.4)$$

$$C_1 = G_f' + G_m' \qquad (A.5)$$

$$D_1 = G_f' \eta_f + G_m' \eta_m \qquad (A.6)$$

Substitute Equations (A.1) and (A.2) into Equation (3.2.16), by using the same methods as previous operation, it gives,

$$G_{LT}' = \frac{A_2 C_2 + B_2 D_2}{C_2^3 + D_2^2} \qquad (A.7)$$

$$G_{LT}'' = \frac{B_2 C_2 - A_2 D_2}{C_2^2 + D_2^2} \qquad (A.8)$$

$$\eta_{GLT} = \frac{G_{LT}''}{G_{LT}'} = \frac{B_2 C_2 - A_2 D_2}{A_2 C_2 + B_2 D_2} \qquad (A.9)$$

$$A_2 = G_m' + G_m' \eta_2' V_f - G_m' \eta_{Gm} \eta_2'' V_f \qquad (A.10)$$

$$B_2 = G_m' \eta_2'' V_f + G_m' \eta_{Gm} + G_m' \eta_{Gm} \eta_2' V_f \qquad (A.11)$$

$$C_2 = 1 - \eta_2' V_f \qquad (A.12)$$

$$D_2 = -\eta_2'' V_f \qquad (A.13)$$

From Equation (3.2.18), with careful manipulating and separating real & imaginary parts, it follows,

$$\eta_1' = \frac{A_3 C_3 + B_3 D_3}{C_3^2 + D_3^2} \qquad (A.14)$$

$$\eta_1'' = \frac{B_3 C_3 - A_3 D_3}{C_3^2 + D_3^2} \qquad (A.15)$$

$$A_3 = E_f' - E_m' \qquad (A.16)$$

$$B_3 = E_f' \eta_f - E_m' \eta_m \qquad (A.17)$$

$$C_3 = E_f' + 2 E_m' \qquad (A.18)$$

$$D_3 = E_f' \eta_f + 2 E_m' \eta_m \qquad (A.19)$$

In order to separate real and imaginary parts for Equation (3.2.15), one must substitute Equations (A.14) and (A.15) into it, which follows,

$$E_T' = \frac{A_4 C_4 + B_4 D_4}{C_4^2 + D_4^2} \qquad (A.20)$$

$$E_T'' = \frac{B_4 C_4 - A_4 D_4}{C_4^2 + D_4^2} \qquad (A.21)$$

$$\eta_T = \frac{E_T''}{E_T'} = \frac{B_4 C_4 - A_4 D_4}{A_4 C_4 + B_4 D_4} \qquad (A.22)$$

$$A_4 = E_m' + 2 E_m' \eta_1 V_f - 2 E_m' \eta_m \eta_1'' V_f \qquad (A.23)$$

$$B_4 = 2 E_m' \eta_1'' V_f + E_m' \eta_m + 2 E_m' \eta_m \eta_1' V_f \qquad (A.24)$$

$$C_4 = 1 - \eta_1' V_f \qquad (A.25)$$

$$D_4 = -\eta_1'' V_f \qquad (A.26)$$

Substitute Equations (3.2.21) and (3.2.22) into Equation (3.2.14). By proper manipulating and separating real and imaginary parts, it shows,

$$E_L' = E_f' V_f \left[1 - \frac{\tanh(\beta l / 2)}{(\beta l / 2)}\right] - \frac{E_f' \eta_f V_f}{2} (\eta_{Gm} - \eta_f) \left[\frac{\tanh(\beta l / 2)}{(\beta l / 2)} - \frac{1}{\cosh^2(\beta l / 2)}\right] + E_m'(1 - V_f) \qquad (A.27)$$

$$E_L'' = E_f' \eta_f V_f \left[1 - \frac{\tanh(\beta l / 2)}{(\beta l / 2)}\right] + \frac{E_f' V_f}{2} (\eta_{Gm} - \eta_f) \left[\frac{\tanh(\beta l / 2)}{(\beta l / 2)} - \frac{1}{\cosh^2(\beta l / 2)}\right] + E_m' \eta_m (1 - V_f) \qquad (A.28)$$

$$\eta_L = \frac{E_L''}{E_L'} \qquad (A.29)$$

Finally, one could derive the solutions for Equation (3.2.20). By using Equations (A.7), (A.8), (A.9), (A.20), (A.21), (A.22), (A.27), (A.28) and (A.29), and proper manipulating and separating real and imaginary parts, it arrives,

$$E_x' = \frac{A_5 C_5 + B_5 D_5}{C_5^2 + D_5^2} \qquad (A.30)$$

$$E_x'' = \frac{B_5 C_5 - A_5 D_5}{C_5^2 + D_5^2} \qquad (A.31)$$

$$\eta_x = \frac{E_x''}{E_x'} = \frac{B_5 C_5 - A_5 D_5}{A_5 C_5 + B_5 D_5} \qquad (A.32)$$

$$A_5 = E_L' E_T' G_{LT}' (1 - \eta_L \eta_T - \eta_T \eta_{GLT} - \eta_L \eta_{GLT}) \qquad (A.33)$$

$$B_5 = E_L' E_T' G_{LT}' (\eta_L + \eta_T + \eta_{GLT} - \eta_L \eta_T \eta_{GLT}) \qquad (A.34)$$

$$C_5 = E_T' G_{LT}' \cos^4\theta (1 - \eta_T \eta_{GLT}) + E_L' G_{LT}' \sin^4\theta (1 - \eta_L \eta_{GLT}) + E_L' E_T' \sin^2\theta \cos^2\theta (1 - \eta_L \eta_T) - 2\nu_{LT} E_T' G_{LT}' \sin^2\theta \cos^2\theta (1 - \eta_T \eta_{GLT}) \qquad (A.35)$$

$$D_5 = E_T' G_{LT}' \cos^4\theta (\eta_T + \eta_{GLT}) + E_L' G_{LT}' \sin^4\theta (\eta_L + \eta_{GLT}) + E_L' E_T' \sin^2\theta \cos^2\theta (\eta_T + \eta_L) - 2\nu_{LT} E_T' G_{LT}' \sin^2\theta \cos^2\theta (\eta_T + \eta_{GLT}) \qquad (A.36)$$

APPENDIX B

Derivation of Viscoelastic "Constants"

In this research, we define that matrix is viscoelastic material and that fibre is elastic material. Poisson's ratio is constant for both matrix and fibre. Because the material properties in the transverse direction of each lamina are dominated by matrix, we could assume the follow,

$$\upsilon_{23} = \upsilon_m \; ; \; G^*_{23} = G^*_m$$

By further assume the lamina is transversely isotropic, we could get

$$G^*_{12} = G^*_{13} \; ; \; E^*_{22} = E^*_{33}$$

$$\upsilon_{12} = \upsilon_{13} = \upsilon_m (1 - V_f) + \upsilon_f V_f$$

$$\upsilon_{21} = \frac{\upsilon_{12} |E_{22}|}{|E_{11}|}$$

$$|E_{11}| = \sqrt{E^2_{11R} + E^2_{11I}} \; ; \; |E_{22}| = \sqrt{E^2_{22R} + E^2_{22I}}$$

From the above assumptions, we could get the following properties,

$$A^*_{44} = A_{44R} + i A_{44I} \qquad (B.1)$$

$$A_{44R} = \frac{5h}{96} (5 Q_{44R} + 11 Q_{55R}) \qquad (B.2)$$

$$A_{44I} = \frac{5h}{96} (5 Q_{44I} + 11 Q_{55I}) \qquad (B.3)$$

$$A^*_{55} = A_{55R} + i A_{55I} \qquad (B.4)$$

$$A_{55R} = \frac{5h}{96} (5 Q_{55R} + 11 Q_{44R}) \qquad (B.5)$$

$$A_{55I} = \frac{5h}{96} (5 Q_{55I} + 11 Q_{44I}) \qquad (B.6)$$

$$D^*_{11} = D_{11R} + i D_{11I} \qquad (B.7)$$

$$D_{11R} = \frac{h^3}{96} (7 Q_{11R} + Q_{22R}) \qquad (B.8)$$

$$D_{11I} = \frac{h^3}{96} (7 Q_{11I} + Q_{22I}) \qquad (B.9)$$

$$D_{12}^{*} = D_{12R} + i\, D_{12I} \qquad (B.10)$$

$$D_{12R} = \frac{h^3}{12} Q_{12R} \qquad (B.11)$$

$$D_{12I} = \frac{h^3}{12} Q_{12I} \qquad (B.12)$$

$$D_{22}^{*} = D_{22R} + i\, D_{22I} \qquad (B.13)$$

$$D_{22R} = \frac{h^3}{96} (7\, Q_{22R} + Q_{11R}) \qquad (B.14)$$

$$D_{22I} = \frac{h^3}{96} (7\, Q_{22I} + Q_{11I}) \qquad (B.15)$$

$$D_{66}^{*} = D_{66R} + i\, D_{66I} \qquad (B.16)$$

$$D_{66R} = \frac{h^3}{12} Q_{66R} \qquad (B.17)$$

$$D_{66I} = \frac{h^3}{12} Q_{66I} \qquad (B.18)$$

$$Q_{44R} = G_{23R} \qquad (B.19)$$

$$Q_{44I} = G_{23I} \qquad (B.20)$$

$$Q_{55R} = G_{13R} = G_{12R} \qquad (B.21)$$

$$Q_{55I} = G_{13I} = G_{12I} \qquad (B.22)$$

$$Q_{11R} = \frac{E_{11R}}{1 - \upsilon_{12}\, \upsilon_{21}} \qquad (B.23)$$

$$Q_{11I} = \frac{E_{11I}}{1 - \upsilon_{12}\, \upsilon_{21}} \qquad (B.24)$$

$$Q_{12R} = \frac{\upsilon_{12}\, E_{22R}}{1 - \upsilon_{12}\, \upsilon_{21}} \qquad (B.25)$$

$$Q_{12I} = \frac{\upsilon_{12}\, E_{22I}}{1 - \upsilon_{12}\, \upsilon_{21}} \qquad (B.26)$$

$$Q_{22R} = \frac{E_{22R}}{1 - \upsilon_{12}\, \upsilon_{21}} \qquad (B.27)$$

$$Q_{22I} = \frac{E_{22I}}{1 - \upsilon_{12}\, \upsilon_{21}} \qquad (B.28)$$

$$Q_{66R} = G_{12R} \tag{B.29}$$
$$Q_{66I} = G_{12I} \tag{B.30}$$

$$E_{11R} = E_f V_f + E_{mR} (1 - V_f) \tag{B.31}$$
$$E_{11I} = E_{mI} (1 - V_f) \tag{B.32}$$

$$E_{22R} = \frac{A_1 C_1 + B_1 D_1}{C_1^2 + D_1^2} \tag{B.33}$$
$$E_{22I} = \frac{B_1 C_1 - A_1 D_1}{C_1^2 + D_1^2} \tag{B.34}$$

$$A_1 = E_{mR} (1 + 2 \eta_{1R} V_f) - 2 E_{mI} \eta_{1I} V_f \tag{B.35}$$
$$B_1 = 2 E_{mR} \eta_{1I} V_f + E_{mI} (1 + 2 \eta_{1R} V_f) \tag{B.36}$$
$$C_1 = 1 - \eta_{1R} V_f \tag{B.37}$$
$$D_1 = - \eta_{1I} V_f \tag{B.38}$$

$$\eta_{1R} = \frac{A_2 C_2 + B_2 D_2}{C_2^2 + D_2^2} \tag{B.39}$$
$$\eta_{1I} = \frac{B_2 C_2 - A_2 D_2}{C_2^2 + D_2^2} \tag{B.40}$$

$$A_2 = E_f - E_{mR} \tag{B.41}$$
$$B_2 = - E_{mI} \tag{B.42}$$
$$C_2 = E_f + 2 E_{mR} \tag{B.43}$$
$$D_2 = 2 E_{mI} \tag{B.44}$$

$$G_{12R} = \frac{A_3 C_3 + B_3 D_3}{C_3^2 + D_3^2} \tag{B.45}$$
$$G_{12I} = \frac{B_3 C_3 - A_3 D_3}{C_3^2 + D_3^2} \tag{B.46}$$

$$A_3 = G_{mR} (1 + \eta_{2R} V_f) - G_{mI} \eta_{2I} V_f \tag{B.47}$$
$$B_3 = G_{mR} \eta_{2I} V_f + G_{mI} (1 + \eta_{2R} V_f) \tag{B.48}$$
$$C_3 = 1 - \eta_{2R} V_f \tag{B.49}$$
$$D_3 = - \eta_{2I} V_f \tag{B.50}$$

$$\eta_{2R} = \frac{A_4 C_4 + B_4 D_4}{C_4^2 + D_4^2} \qquad (B.51)$$

$$\eta_{2I} = \frac{B_4 C_4 - A_4 D_4}{C_4^2 + D_4^2} \qquad (B.52)$$

$$A_4 = G_f - G_{mR} \qquad (B.53)$$

$$B_4 = -G_{mI} \qquad (B.54)$$

$$C_4 = G_f + G_{mR} \qquad (B.55)$$

$$D_4 = G_{mI} \qquad (B.56)$$

$$G_f = \frac{E_f}{2(1+\upsilon_f)} \qquad (B.57)$$

$$G_{mR} = \frac{E_{mR}}{2(1+\upsilon_m)} \qquad (B.58)$$

$$G_{mI} = \frac{E_{mI}}{2(1+\upsilon_m)} \qquad (B.59)$$

APPENDIX C

Flowchart of Simplex Optimization Method

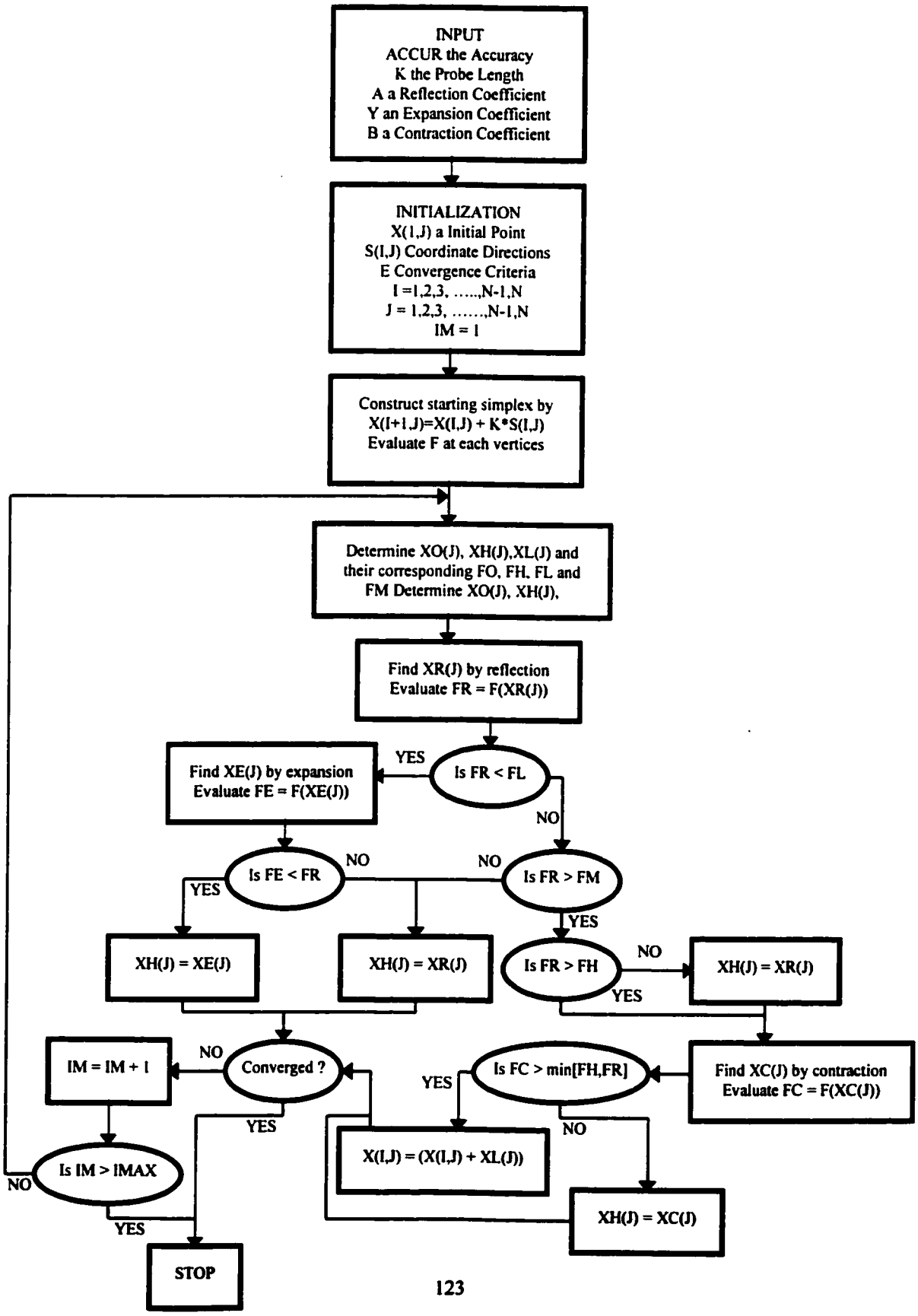

APPENDIX D

NON-SYMMETRIC SIMPLEX (NELDER & MEAD[43]) NONLINEAR OPTIMIZATION

Fortune Program Code

```
*************************************************************
* X(I,J) -- VERTICES OF A SIMPLEX                           *
* F(I) -- VALUE OF OBJECTIVE FUNCTION CORRESPONDING TO EACH*
* VERTEX                                                    *
* S(I,J) -- DIRECTIONS USED TO CONSTRUCT THE INITIAL        *
*           SIMPLEX                                         *
* K -- PROBE LENGTH USED TO CONSTRUCT THE INITIAL SIMPLEX   *
*      ENTERED BY USER                                      *
* A -- REFLECTION COEFFICIENT ENTERED BY USER               *
* Y -- EXPANSION COEFFICIENT ENTERED BY USER                *
* B -- CONTRACTION COEFFICIENT ENTERED BY USER              *
* XH(I) -- THE VERTEX CORRESPONDING TO THE HIGHEST VALUE OF*
* THE OBJECTIVE FUNCTION AMONG THE VERTICES OF A SIMPLEX    *
* FH -- THE HIGHEST VALUE OF THE OBJECTIVE FUNCTION AMONG   *
* THE VERTICES OF A SIMPLEX                                 *
* XL(I) -- THE VERTEX CORRESPONDING TO THE LOWEST VALUE OF  *
*          THE OBJECTIVE FUNCTION AMONG THE VERTICES OF A   *
*          SIMPLEX                                          *
* FL -- THE LOWEST VALUE OF OBJECTIVE FUNCTION AMONG THE    *
*       VERTICES OF A SIMPLEX                               *
* FM -- THE SECOND HIGHEST VALUE OF THE OBJECTIVE FUNCTION  *
*       AMONG THE VERTICES OF A SIMPLEX                     *
* XO(I) -- THE CENTROID OF ALL THE VERTICES 'X' EXCEPT 'XH'*
* FO -- THE VALUE OF OBJECTIVE FUNCTION CORRESPONDING TO    *
*       THE VERTEX 'XO'                                     *
* XR(I) -- THE REFLECTED POINT BY REFLECTION TECHNIQUE      *
* XE(I) -- THE EXPANDED POINT BY EXPANSION TECHNIQUE        *
* XC(I) -- THE CONTRACTED POINT BY CONTRACTION TECHNIQUE    *
* ACCUR -- REQUIRED ACCURACY CRITERIA ENTERED BY USER       *
* E -- THE SMALLER VALUE USED IN CONVERGENCY TEST WHICH     *
*      COULD BE DEFINED BY USER                             *
* Q -- THE VALUE OF CONVERGENCY TEST FUNCTION               *
* VF -- FIBRE VOLUME FRACTION                               *
* LD -- FIBRE ASPECT RATIO                                  *
* O -- OFF-AXIS ANGLE                                       *
* UMIN -- INVERTED UTILITY FUNCTION                         *
* U(I) -- INVERTED UTILITY FUNCTIONS FOR EACH OBJECTIVE     *
*         FUNCTION                                          *
* ER -- REAL PART OF COMPLEX MODULUS AT LOAD AXIS           *
* EI -- IMAGINARY PART OF COMPLEX AT LOAD AXIS              *
* N -- DAMPING FACTOR AT LOAD AXIS                          *
```

```
* ELR -- REAL PART OF LONGITUDINAL MODULUS                          *
* ELI -- IMAGINARY PART OF LONGITUDINAL MODULUS                      *
* NL -- LONGITUDINAL DAMPING FACTOR                                  *
* ETR -- REAL PART OF TRANSVERSE MODULUS                             *
* ETI -- IMAGINARY PART OF TRANSVERSE MODULUS                        *
* NT -- TRANSVERSE DAMPING FACTOR                                    *
* GLTR -- REAL PART OF IN-PLANE SHEAR MODULUS                        *
* GLTI -- IMAGINARY PART OF IN-PLANE SHEAR MODULUS                   *
* NGLT -- IN-PLANE SHEAR DAMPING FACTOR                              *
*********************************************************************

*********************************************************************
* OBFUNC -- THE SUBROUTINE TO DETERMINE THE VALUE OF                 *
*           INVERTED UTILITY FUNCTION                                *
* OBFUN1 -- THE SUBROUTINE TO DETERMINE THE VALUE OF                 *
*           LONGITUDINAL COMPLEX MODULUS AND DAMPING FACTOR*
* OBFUN2 -- THE SUBROUTINE TO DETERMINE THE VALUE OF                 *
*           TRANSVERSE COMPLEX MODULUS AND DAMPING FACTOR            *
* OBFUN3 -- THE SUBROUTINE TO DETERMINE THE VALUE OF IN-             *
*           PLANE SHEAR MODULUS AND DAMPING FACTOR                   *
*********************************************************************

      PROGRAM SIMPLX
*
* THIS IS A PROGRAM USING NON-SYMMETRIC SIMPLEX (NELDER & MEAD)
* NONLINEAR OPTIMIZATION METHODS FOR NON-CONSTRAINED
* MULTIVARIABLE PROBLEM --- NON-GRADIENT TECHNIQUE
*
      INTEGER I, N, M, IH, IL, IM, IMAX
      REAL X(4,3), F(4), XO(3), XH(3), XR(3), XE(3), XC(3)
      REAL XL(3), S(3,3), ACCUR, K, A, B, Y, E
      REAL FH, FL, NX, FM, FO, Q, CVE, V(3)
      REAL TR(3), TRFUN1, T, TRFUN2, VF, LD, O
      N=3
      NX=3.0
      IM=0
      IMAX=1000
      T=0.1
      PRINT*,'PLEASE ENTER REQUIRED ACCURACY CRITERIA!'
      READ*, ACCUR
      PRINT*,'PLEASE ENTER INITIAL PROBE LENGTH!'
      READ*, K
      PRINT*,'PLEASE ENTER THE REFLECTION COEFFICIENT (A>0)!'
 10   READ*, A
      IF(A.LE.0) THEN
      PRINT*,'THE VALUE OF REFLECTION COEFFICIENT YOU ENTER IS'
        PRINT*,'LESS THAN 0!!!'
        PRINT*,'PLEASE RE-ENTER THE REFLECTION
        COEFFICIENT!'
```

```
          GO TO 10
        ENDIF
        PRINT*,'PLEASE ENTER THE EXPANSION COEFFICIENT (Y>1)!'
   20   READ*, Y
        IF(Y.LE.1) THEN
        PRINT*,'THE VALUE OF EXPANSION COEFFICIENT YOU ENTER IS'
        PRINT*,'LESS THAN 1!!!'
        PRINT*,'PLEASE RE-ENTER THE EXPANSION COEFFICIENT!'
        GO TO 20
        ENDIF
        PRINT*,'PLEASE ENTER THE CONTRACTION COEFFICIENT
        (0<B<1)!'
   30   READ*, B
        IF(B.LE.0.OR.B.GE.1) THEN
        PRINT*,'THE VALUE OF CONTRACTION COEFFICIENT YOU
        ENTER IS'
        PRINT*,'EITHER LESS THAN 0 OR GREAT THAN 1!!!'
        PRINT*,'PLEASE RE-ENTER THE CONTRACTION EFFICIENT!'
        GO TO 30
        ENDIF
*
* SET INITIAL POINTS TO CONSTRUCT STARTING SIMPLEX
*
        DO 50 M=1, N, 1
        DO 40 I=1, N, 1
           S(M,I)=0
   40   CONTINUE
   50   CONTINUE
        DO 60 M=1, N, 1
           TR(M)=0.0
           S(M,M)=1
   60   CONTINUE
        E=ACCUR/100.0
        CALL OBFUNC(TR,TRFUN1)
   62   TR(2)=TR(2)+T
        CALL OBFUNC(TR,TRFUN2)
        IF(TRFUN2.GT.TRFUN1) THEN
          TRFUN1=TRFUN2
          GO TO 62
        ENDIF
        DO 65 I=1, N, 1
           X(1,I)=TR(I)
   65   CONTINUE
        DO 80 I=1, N, 1
        DO 70 M=1, N, 1
           X(I+1,M)=X(1,M)+K*S(I,M)
   70   CONTINUE
   80   CONTINUE
*
```

```
* EVALUATE THE FUNCTION VALUE
*
   90    IM=IM+1
         IF(IM.GE.IMAX) THEN
           PRINT*,'THE NUMBER OF ITERATION IS OUT OF
           MAXIMUM!!'
           PRINT*,'PLEASE RE-CHOOSE THE ACCURACY OR EACH
           COEFFICIENT!!!'
           STOP
         ENDIF
         DO 100 I=1, N+1, 1
         DO 95 M=1, N, 1
            V(M)=X(I,M)
   95    CONTINUE
            CALL OBFUNC(V,F(I))
  100    CONTINUE

*
* DETERMINE THE VERTICES CORRESPONDING TO THE MINIMUM FUNCTION
* VALUE (XL) AND THE MAXIMUM FUNCTION VALUE (XH) AND THE CENTROID
* (XO) OF ALL POINTS EXCEPT 'XH'
*
         FH=F(1)
         FL=F(1)
         IL=1
         IH=1
         DO 110 I=2, N+1, 1
            IF(F(I).GE.FH) THEN
              IH=I
              FH=F(I)
            ELSEIF(F(I).LE.FL) THEN
              IL=I
              FL=F(I)
            ENDIF
  110    CONTINUE
         DO 120 I=1, N, 1
            XL(I)=X(IL,I)
            XH(I)=X(IH,I)
            XO(I)=0.0
  120    CONTINUE
         FM=FL
         DO 130 I=1, N+1, 1
            IF(I.NE.IH) THEN
              IF(F(I).GE.FM) THEN
                FM=F(I)
              ENDIF
            ENDIF
  130    CONTINUE
         DO 150 I=1, N+1, 1
```

```
      DO 140 M=1, N, 1
         XO(M)=XO(M)+X(I,M)
140   CONTINUE
150   CONTINUE
      DO 160 I=1, N, 1
         XO(I)=(XO(I)-XH(I))/NX
160   CONTINUE
      CALL OBFUNC(XO,FO)
*
* DETERMINE THE REFLECTED POINT 'XR' BY REFLECTION TECHNIQUE
*
      DO 170 I=1, N, 1
         XR(I)=(1.0+A)*XO(I)-A*XH(I)
170   CONTINUE
      CALL OBFUNC(XR,FR)
*
* DETERMINE THE EXPANDED POINT 'XE' BY EXPANSION TECHNIQUE
*
      IF(FR.LT.FL) THEN
        DO 180 I=1, N, 1
           XE(I)=Y*XR(I)+(1.0-Y)*XO(I)
180     CONTINUE
        CALL OBFUNC(XE,FE)
        IF(FE.LE.FL) THEN
          DO 190 I=1, N, 1
             X(IH,I)=XE(I)
190       CONTINUE
        ELSE
          DO 200 I=1, N, 1
             X(IH,I)=XR(I)
200       CONTINUE
        ENDIF
      ELSE
*
* DETERMINE THE CONTRACTED POINT 'XC' BY CONTRACTION TECHNIQUE
*
        IF(FR.GE.FM) THEN
          IF(FR.LE.FH) THEN
            DO 210 I=1, N, 1
               XH(I)=XR(I)
210         CONTINUE
            FH=FR
          ENDIF
          DO 220 I=1, N, 1
             XC(I)=B*XH(I)+(1.0-B)*XO(I)
220       CONTINUE
          CALL OBFUNC(XC,FC)
          IF(FC.GE.FH) THEN
            DO 240 I=1, N+1, 1
```

```
              DO 230 M=1, N, 1
                 X(I,M)=(X(I,M)+XL(M))/2.0
  230         CONTINUE
  240         CONTINUE
            ELSE
              DO 250 I=1, N, 1
                 X(IH,I)=XC(I)
  250         CONTINUE
            ENDIF
          ELSE
            DO 260 I=1, N, 1
               X(IH,I)=XR(I)
  260       CONTINUE
          ENDIF
        ENDIF
*
* TEST OF CONVERGENCY
*
        CVE=0
        DO 270 I=1, N+1, 1
           CVE=CVE+(((F(I)-FO)**2)/(NX+1.0))
  270   CONTINUE
        Q=CVE**0.5
        IF(Q.GT.E) THEN
          GO TO 90
        ENDIF
        O=90.0*((SIN(XL(1)))**2)
        LD=1.0+99.0*((SIN(XL(2)))**2)
        VF=0.5+0.2*((SIN(XL(3)))**2)
        PRINT*,'THE MINIMUM POINT OF THIS OBJECTIVE FUNCTION
        IS'
        PRINT*,'OFF-AXIS ANGLE:',O,'  DEGREE'
        PRINT*,'FIBRE ASPECT RATIO:',LD
        PRINT*,'FIBRE VOLUME FRACTION:',VF
        PRINT*,'UMIN:',FL
        END
*
*
* THIS IS A SUBROUTINE TO DETERMINE THE VALUE OF OBJECTIVE
* FUNCTION
*
*
        SUBROUTINE OBFUNC(X,UMIN)
*
* THIS IS THE OBJECTIVE FUNCTION FOR THE PROJECT TO OPTIMIZE
* THE PERFORMANCE OF SHORT FIBRE REINFORCED COMPOSITES
*
        REAL ELR, NL, ETR, NT, GLTR, NGLT, VF, LD, VLT
        REAL EXR, NX, EXI, W, ANG, PI, O, A, B, C, D
```

```
REAL XC, YC, ZC, VC, XD, YD, ZD, VD, EM, NM, PM, WD
REAL ER, EI, N, WN, EF, GM, GF, NF, NGM, ELI, WC
REAL ETI, GLTI, U(3), X(3), UMIN
PI=3.1415927
VF=0.5+0.2*((SIN(X(3)))**2)
LD=1.0+99.0*((SIN(X(2)))**2)
O=90.0*((SIN(X(1)))**2)
EF=72.4
EM=3.79
GM=1.38
GF=30.3
NF=0.0014
NM=0.015
NGM=0.018
PM=1.23
CALL OBFUN1(VF,LD,GM,EF,EM,NF,NGM,NM,ELR,ELI,NL)
CALL OBFUN2(VF,EF,EM,NF,NM,ETR,ETI,NT)
CALL OBFUN3(VF,GF,GM,NF,NGM,GLTR,GLTI,NGLT)
VLT=0.36-0.16*VF
ANG=(O/360.0)*2.0*PI
A=ELR*ETR*GLTR*(1.0-NL*NT-NT*NGLT-NL*NGLT)
B=ELR*ETR*GLTR*(NL+NT+NGLT-NL*NT*NGLT)
XC=ETR*GLTR*((COS(ANG))**4)*(1.0-NT*NGLT)
YC=ELR*GLTR*((SIN(ANG))**4)*(1.0-NL*NGLT)
ZC=ELR*ETR*((SIN(ANG))**2)*((COS(ANG))**2)*(1.0-
NT*NL)
VC=-2.0*VLT*ETR*GLTR*((SIN(ANG))**2)
WC=((COS(ANG))**2)*(1.0-NT*NGLT)
C=XC+YC+ZC+VC*WC
XD=ETR*GLTR*((COS(ANG))**4)*(NT+NGLT)
YD=ELR*GLTR*((SIN(ANG))**4)*(NL+NGLT)
ZD=ELR*ETR*((SIN(ANG))**2)*((COS(ANG))**2)*(NT+NL)
VD=-2.0*VLT*ETR*GLTR*((SIN(ANG))**2)
WD=((COS(ANG))**2)*(NT+NGLT)
D=XD+YD+ZD+VD*WD
EXR=(A*C+B*D)/(C**2+D**2)
EXI=(B*C-A*D)/(C**2+D**2)
NX=(B*C-A*D)/(A*C+B*D)
W=1.23+1.43*VF
ER=EXR/EM
EI=EXI/EM
N=NX/NM
WN=W/PM
U(1)=1.0/N
U(2)=1.0/ER
U(3)=1.0/WN
UMIN=0.5130*U(1)+0.3870*U(2)-0.10*U(3)
RETURN
END
```

```
*
*
      SUBROUTINE OBFUN1(VF,LD,GM,EF,EM,NF,NGM,NM,ELR,ELI,NL)
*
* THIS IS A SUNROUTIME TO DETERMINE THE REAL MODULUS AND DAMPING
* FACTOR AT LONGITUDINAL DIRECTION
*
      REAL VF, PI, BL, ELR, NL, LD, ELI, NM, GM, ZEL
      REAL XELI, YELI, XELR, YELR, EF, EM, NF, NGM, BLS
      PI=3.1415927
      BLS=45.05456
      BL=LD*(((2.0*GM)/(EF*(ALOG((PI/(4.0*VF))**0.5))))**0.5)
      XELI=EF*NF*VF*(1.0-((TANH(BL))/BL))+EM*NM*(1.0-VF)
      YELI=((EF*VF)/2.0)*(NGM-NF)
      XELR=EF*VF*(1.0-((TANH(BL))/BL))+EM*(1.0-VF)
      YELR=-((EF*NF*VF)/2.0)*(NGM-NF)
      IF (BL.LE.BLS) THEN
      ZEL=((TANH(BL))/BL)-(1.0/((COSH(BL))**2))
      ELSE
      ZEL=((TANH(BL))/BL)
      ENDIF
      ELI=XELI+YELI*ZEL
      ELR=XELR+YELR*ZEL
      NL=ELI/ELR
      RETURN
      END
*
*

      SUBROUTINE OBFUN2(VF,EF,EM,NF,NM,ETR,ETI,NT)
*
* THIS IS A SUBROUTINE TO DETERMINE THE MODULUS (REAL & IMAGE)
* AND DAMPING FACTOR AT TRANSVERSE DIRECTION
*
      REAL ETR, ETI, N1R, N1I, VF, NT
      REAL EF, EM, NF, NM
      REAL A1, B1, C1, D1, A2, B2, C2, D2
      A1=EF-EM
      B1=EF*NF-EM*NM
      C1=EF+2.0*EM
      D1=EF*NF+2.0*EM*NM
      N1R=(A1*C1+B1*D1)/(C1**2+D1**2)
      N1I=(B1*C1-A1*D1)/(C1**2+D1**2)
      C2=1.0-N1R*VF
      D2=-N1I*VF
      A2=EM+2.0*EM*N1R*VF-2.0*EM*NM*N1I*VF
      B2=2.0*EM*N1I*VF+EM*NM+2.0*EM*NM*N1R*VF
      ETR=(A2*C2+B2*D2)/(C2**2+D2**2)
      ETI=(B2*C2-A2*D2)/(C2**2+D2**2)
```

```
      NT=ETI/ETR
      RETURN
      END
*
*

      SUBROUTINE OBFUN3(VF,GF,GM,NF,NGM,GLTR,GLTI,NGLT)
*
* THIS A SUBROUTINE TO DETERMINE THE IN-PLANE SHEAR MODULUS (REAL
& IMAGE) AND DAMPING FACTOR vs. FIBRE VOLUME FRACTION
*
      REAL GLTR, GLTI, NGLT, VF
      REAL GF, GM, NF, NGM, A3, B3, C3, D3
      REAL A4, B4, C4, D4, N2R, N2I
      A3=GF-GM
      B3=GF*NF-GM*NGM
      C3=GF+GM
      D3=GF*NF+GM*NGM
      N2R=(A3*C3+B3*D3)/(C3**2+D3**2)
      N2I=(B3*C3-A3*D3)/(C3**2+D3**2)
      C4=1.0-N2R*VF
      D4=-N2I*VF
      A4=GM+GM*N2R*VF-GM*NGM*N2I*VF
      B4=GM*N2I*VF+GM*NGM+GM*NGM*N2R*VF
      GLTR=(A4*C4+B4*D4)/(C4**2+D4**2)
      GLTI=(B4*C4-A4*D4)/(C4**2+D4**2)
      NGLT=GLTI/GLTR
      RETURN
      END
```

APPENDIX E

FFT Computer Program Flowchart

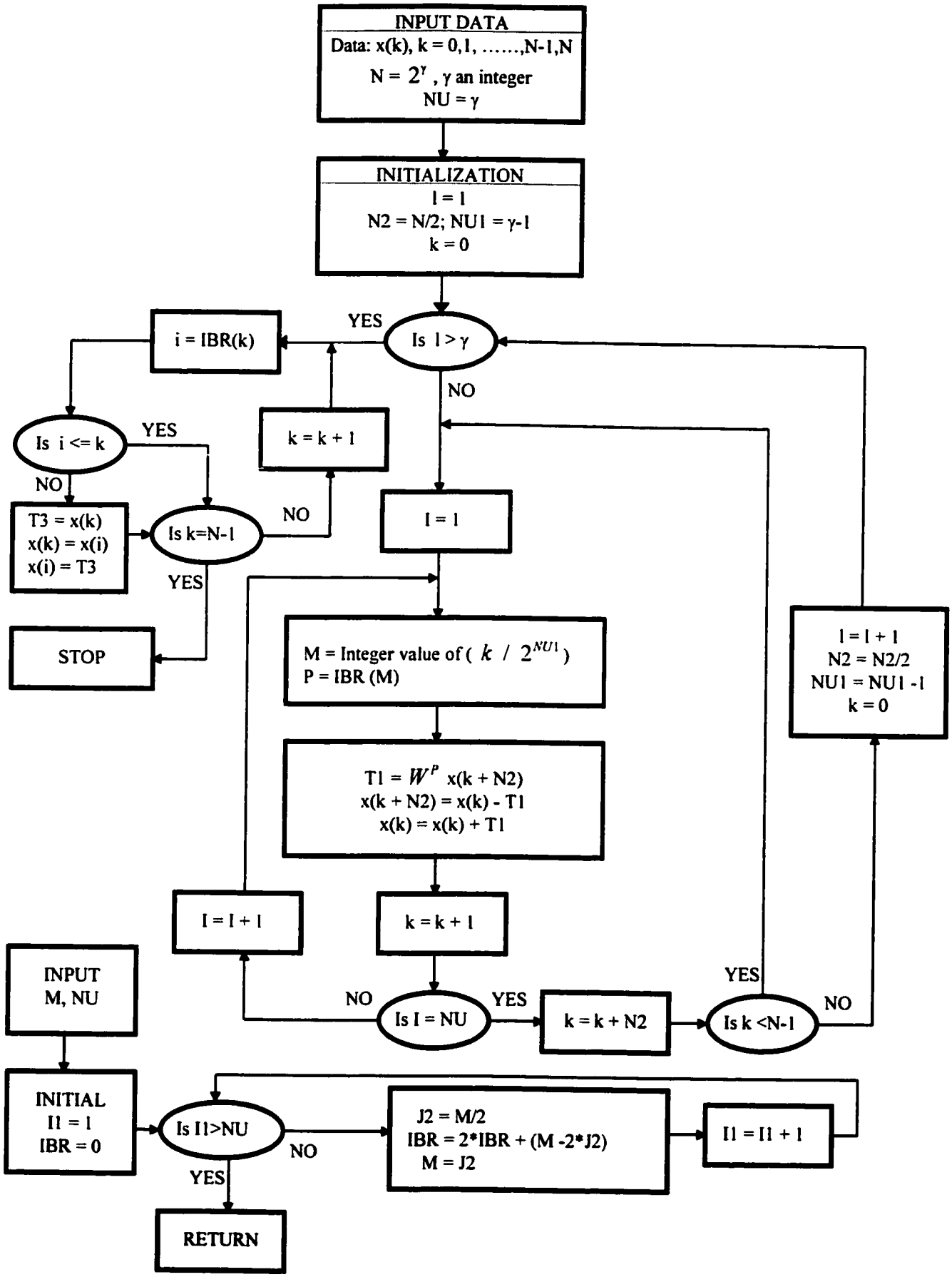

APPENDIX F

Transient Wave Propagation under Impact Loading

C Program Code (UNIX)

```
#
# This makefile makes the Frequency.c Displace.c Property.c
# Loading.c fftrans.c to the executable file Frequency-Time.
#                              --- Jie Feng, 1996.
#                                  Dept. of Mechanical Eng.
#                                  University of Ottawa
#

SOURCES=Frequency-Time.c Displace.c Loading.c Property.c
fftrans.c evenodd.c

OBJECTS=Frequency-Time.o Displace.o Loading.o Property.o
fftrans.o evenodd.c

CC = cc

Frequency-Time: $(OBJECTS)
          $(CC) -g $(OBJECTS) -lm -o Frequency-Time

$(OBJECTS):


lint:
          lint $(SOURCES)

clean:
          rm $(OBJECTS)
```

```
*************************************************************
#include <stdio.h>
#include <math.h>
#include <malloc.h>
#include <stdlib.h>

#define PI 3.141592654
```

```
/* Frequency-Time.c
** This program calculates the imapct response of composite
** materials in the frequency-domain.  It will generate the
** data file with the file name which could be selected by
** user.  There are three sub-programs with this program,
** namely 'Displace.c', 'Loading.c' and 'Property.c'.  The
** reason that I separate this program into four files is
** that I can easily manipulate in this way by modifying the
** each file with the condition changing, such as impact
** loading, boundary condition or material properties.
**
** In order to easily handle the above problem, it is
** desired to have the 'makefile' file which make this
** project more easy to handle.  The necessary information
** of how to compile this program is in the file of
** 'makefile'.  user is recommended that use the 'make'
** command in the present directory to perform the above
** task.
**
** Later, the generated data file could be proper
** manipulated ('evenodd.c') and the Fast Fourier
** Transformation (FFT) program 'fftrans.c' could be also
** applied to transfer the data form frequency-domain to
** time-domain to get the desired transient response of the
** composite laminate **under impact loading.
**
**
**                        ------- Jie Feng 1996
**                                Dept. Of Mechanical Eng.
**                                University of Ottawa
*/

double Wmnr, Wmni, *data_real, *data_imag;
double *num3;
main()
{
double x, y, a, b, h, Wbr, Wbi, *omega, *ome_log;
double p, u, v, x1, y1, angx, angy, dt, t0, ome;
unsigned long m, n, i, j, k, nmax, num_samp, numb, num1;
int isign;
char filename1[20];
char filename2[20];
FILE *fprt1, *freadme;
FILE *fprt2;
```

```
void Displace();
void evenodd();
void fftrans();

/*Input the necessary information about the desired plate */

printf("This is a program calculate the imapct response
of\n");
printf("composite materials in the frequency-domain!\n");
printf("\nPlease input the desired output filename of
frequency:\n");
gets(filename1);
printf("\nPlease input the desired output filename of time-
domain:\n");
gets(filename2);
printf("\nPlease input the desired length of composite plate
a=");
scanf("%lf", &a);
printf("\nPlease input the desired width of this plate b=");
scanf("%lf", &b);
printf("\nPlease input the desired thichness of the plate
h=");
scanf("%lf", &h);
printf("\nPlease input the desired load of the impact
loading p=");
scanf("%lf", &p);
printf("\nPlease input the desire length of squre loading
u=");
scanf("%lf", &u);
printf("\nPlease input the desired width of squre loading
v=");
scanf("%lf", &v);
printf("\nPlease input the desired centeral point of
loading\n");
printf("\nx1=");
scanf("%lf", &x1);
printf("y1=");
scanf("%lf", &y1);
printf("\nPlease input the desired impact loading durations
t=");
scanf("%lf", &t0);
printf("\nPlease input the desired valure m=");
scanf("%ld", &i);
printf("\nPlease input the desired valure n=");
scanf("%ld", &j);
```

```
printf("\nPlease input the desired response point as");
printf("\nx=");
scanf("%lf", &x);
printf("y=");
scanf("%lf", &y);
printf("\nPlease input the total sampling point number:");
scanf("%ld", &nmax);
printf("\nPlease input the sampling time interval dt=");
scanf("%lf", &dt);

isign=1;

num_samp=nmax*2;
omega=malloc((num_samp+1)*sizeof(double));
data_real=malloc((num_samp+1)*sizeof(double));
data_imag=malloc((num_samp+1)*sizeof(double));
num3=malloc((num_samp+1)*sizeof(double));
ome_log=malloc((num_samp+1)*sizeof(double));

freadme=fopen("readme", "a");
fprintf(freadme, "Filename:\t");
fputs(filename1, freadme);
fprintf(freadme, "\t");
fputs(filename2, freadme);

fprintf(freadme, "\n\n");
fprintf(freadme, "x=%lf  \t y=%lf\n", x, y);
fprintf(freadme, "a=%lf   b=%lf   h=%lf\n", a, b, h);
fprintf(freadme, "p=%lf   u=%lf   v=%lf\n", p, u, v);
fprintf(freadme, "x1=%lf  y1=%lf   t0=%lf\n", x1, y1, t0);
fprintf(freadme, "m=%ld  \t n=%ld \n", i, j);
fprintf(freadme, "dt=%lf  nmax=%ld  num_samp=%ld\n\n", dt,
nmax, num_samp);
fprintf(freadme, "This is a inverse FFT transformation\n");

for(k=1; k<=60; k++)
    fputc('*', freadme);
fprintf(freadme, "\n\n\n");
fclose(freadme);

for(k=0; k<=(nmax-1); k++)
   {
   omega[k]=2.0*PI*(double)k/((double)nmax*dt);
   ome_log[k]=log10(omega[k]);
   ome=omega[k];
```

```
    Wbr=0.0;
    Wbi=0.0;
    for(m=1; m<=i; m++)
       {
       angx=((double)m*PI*x)/a;
       for(n=1; n<=j; n++)
          {
          angy=((double)n*PI*y)/b;
/* Displace function compute the Variables Wmnr and Wmni */
          Displace(m,n,ome,a,b,p,u,v,x1,y1,h,t0);
          Wbr+=Wmnr*sin(angx)*sin(angy);
          Wbi+=Wmni*sin(angx)*sin(angy);
          }
       }
    data_real[k]=Wbr;
    data_imag[k]=Wbi;
    }

evenodd(nmax,num_samp);

for(k=nmax; k<=(num_samp-1); k++)
    {
    omega[k]=2.0*PI*(double)k/((double)nmax*dt);
    ome_log[k]=log10(omega[k]);
    }


fprt1=fopen(filename1, "w");
for(k=0; k<=(num_samp-1); k++)
   fprintf(fprt1, "%05ld   %le   %le   %le\n", k,
ome_log[k], data_real[k],
           data_imag[k]);
fclose(fprt1);

printf("\n\nWell Done, Jie!\n\n");
puts(filename1);

numb=num_samp;
for(num1=0; numb!=1; num1++)
   numb/=2;

fftrans(num_samp,dt,num1,isign);
fprt2=fopen(filename2, "w");
for(k=0; k<=(num_samp-1); k++)
```

```
fprintf(fprt2, "%05ld   %le   %le
%le\n",k,num3[k],data_real[k],
        data_imag[k]);
fclose(fprt2);

printf("\n\nWell Done, Jie!\n");
puts(filename2);
printf("\n\n\n");
}



*************************************************************
#include <stdio.h>
#include <math.h>

#define PI 3.141592654

/* Displace.c
** This sub-program compute the displacement in the
** Z-direction of the transversly isotropic composite
** laminated rectangulatar plate simply supported at four
** sides under the rectangulatar cosine-cosine impact
** loading.  The output of this program is Wmnr and Wmni.
** The sub-porgram of this program are 'Property.c' and
** 'Loading.c'.   If you change your boundary condition, it
** is necesssary to modify this program.
**                                -- Jie Feng, 1996.
**                                   Dept. of Mechanical Eng.
**                                   University of Ottawa
*/

double Wmnr, Wmni, qr, qi, desn;
double
q11r,q11i,q12r,q12i,q22r,q22i,q44r,q44i,q55r,q55i,q66r,q66i;
void
Displace(m,n,ome,a,b,p,u,v,x1,y1,h,t0)
double ome, a, b, p, u, v, x1, y1, h, t0;
unsigned long m, n;
{
double a1r, a1i, a2r, a2i, a3r, a3i, a4r, a4i, a5r, a5i,
a6r, a6i, a7r, a7i;
double aa, bb, cc, dd, cf, b1r, b1i;
```

```
double a55r, a55i, a44r, a44i, d11r, d11i, d12r, d12i, d22r,
d22i;
double d66r, d66i, pia, ip;
double pi2, m2, n2, a2, b2, h3, ome2;
void Loading(), Property();

cf=pow(PI,2.0)/12.0;
pi2=pow(PI,2.0);
m2=pow((double)m,2.0);
n2=pow((double)n,2.0);
a2=pow(a,2.0);
b2=pow(b,2.0);
h3=pow(h,3.0);
ome2=pow(ome,2.0);

/* the Loading() compute the impact loading which is imposed
** on the desired plate
*/
Loading(a,b,u,v,p,m,n,x1,y1,t0,ome);

/* The Propery() compute the material properties of each
** lamina
*/
Property(ome);

/*The the coefficients of the material properties matrics!*/
a44r=((5.0*h)/96.0)*(5.0*q44r+11.0*q55r);
a44i=((5.0*h)/96.0)*(5.0*q44i+11.0*q55i);

a55r=((5.0*h)/96.0)*(5.0*q55r+11.0*q44r);
a55i=((5.0*h)/96.0)*(5.0*q55i+11.0*q44i);

d11r=(h3/96.0)*(7.0*q11r+q22r);
d11i=(h3/96.0)*(7.0*q11i+q22i);

d66r=(h3/12.0)*q66r;
d66i=(h3/12.0)*q66i;

d12r=(h3/12.0)*q12r;
d12i=(h3/12.0)*q12i;

d22r=(h3/96.0)*(7.0*q22r+q11r);
d22i=(h3/96.0)*(7.0*q22i+q11i);

pia=desn*h;
```

```
ip=(desn*h3)/12.0;

a1r=cf*pi2*((m2/a2)*a55r+(n2/b2)*a44r)-ome2*pia;
a1i=cf*pi2*((m2/a2)*a55i+(n2/b2)*a44i);

a2r=(cf*(double)m*PI*a55r)/a;
a2i=(cf*(double)m*PI*a55i)/a;

a3r=(cf*(double)n*PI*a44r)/b;
a3i=(cf*(double)n*PI*a44i)/b;

a4r=(m2*pi2*d11r)/a2+(n2*pi2*d66r)/b2+cf*a55r-ome2*ip;
a4i=(m2*pi2*d11i)/a2+(n2*pi2*d66i)/b2+cf*a55i;

a5r=(((double)m*(double)n*pi2)/(a*b))*(d12r+d66r);
a5i=(((double)m*(double)n*pi2)/(a*b))*(d12i+d66i);

a6r=(((double)m*(double)n*pi2)/(a*b))*(d11r+d66r);
a6i=(((double)m*(double)n*pi2)/(a*b))*(d11i+d66i);

a7r=(m2*pi2*d66r)/a2+(n2*pi2*d22r)/b2+cf*a44r-ome2*ip;
a7i=(m2*pi2*d66i)/a2+(n2*pi2*d22i)/b2+cf*a44i;

b1r=a4r*a5r*a7r-a4r*a5i*a7i-a4i*a5r*a7i-a4i*a5i*a7r
    -pow(a5r,2.0)*a6r+2.0*a5r*a5i*a6i+pow(a5i,2.0)*a6r;
b1i=a4r*a5r*a7i+a4r*a5i*a7r+a4i*a5r*a7r-a4i*a5i*a7I
    -pow(a5r,2.0)*a6i-2.0*a5r*a5i*a6r+pow(a5i,2.0)*a6i;

aa=b1r*qr-b1i*qi;
bb=b1r*qi+b1i*qr;

cc=a1r*a4r*a5r*a7r-a1r*pow(a5r,2.0)*a6r-pow(a2r,2.0)*a5r*a7r
   +a2r*a3r*pow(a5r,2.0)-pow(a3r,2.0)*a4r*a5r
   +a2r*a3r*a5r*a6r-a1r*a4r*a5i*a7i*+a1r*a5r*a5i*a6I
   +pow(a2r,2.0)*a5i*a7i-a2r*a3r*pow(a5i,2.0)
   +pow(a3r,2.0)*a4i*a5I-a2r*a3r*a5i*a6i
   -a1r*a4i*a5r*a7i+a1r*a5i*a5r*a6i+a2r*a2i*a5r*a7I
   -a2r*a3i*a5r*a5i+a3r*a3i*a4r*a5i-a2r*a3i*a5r*a6i
   -a1r*a4i*a5i*a7r+a1r*pow(a5i,2.0)*a6r+a2r*a2i*a5i*a7r
   -a2r*a3i*a5i*a5r+a3r*a3i*a4i*a5r-a2r*a3i*a5i*a6r
   -a1i*a4r*a5r*a7i+a1i*pow(a5r,2.0)*a6i+a2i*a2r*a5r*a7I
   -a2i*a3r*a5r*a5i+a3i*a3r*a4r*a5i-a2i*a3r*a5r*a6i
   -a1i*a4r*a5i*a7r+a1i*a5r*a5i*a6r+a2i*a2r*a5i*a7r
   -a2i*a3r*a5i*a5r+a3i*a3r*a4i*a5r-a2i*a3r*a5i*a6r
   -a1i*a4i*a5r*a7r+a1i*a5i*a5r*a6r+pow(a2i,2.0)*a5r*a7r
```

```
    -a2i*a3i*pow(a5r,2.0)+pow(a3i,2.0)*a4r*a5r
    -a2i*a3i*a5r*a6r+a1i*a4i*a5i*a7i-a1i*pow(a5i,2.0)*a6I
    -pow(a2i,2.0)*a5i*a7i+a2i*a3i*pow(a5i,2.0)
    -pow(a3i,2.0)*a4i*a5I+a2i*a3i*a5i*a6i;

dd=a1r*a4r*a5r*a7i-a1r*pow(a5r,2.0)*a6i-pow(a2r,2.0)*a5r*a7I
    +a2r*a3r*a5r*a5i-pow(a3r,2.0)*a4r*a5i+a2r*a3r*a5r*a6i
    +a1r*a4r*a5i*a7r-a1r*a5r*a5i*a6r-pow(a2r,2.0)*a5i*a7r
    +a2r*a3r*a5i*a5r-pow(a3r,2.0)*a4i*a5r+a2r*a3r*a5i*a6r
    +a1r*a4i*a5r*a7r-a1r*a5i*a5r*a6r-a2r*a2i*a5r*a7r
    +a2r*a3i*pow(a5r,2.0)-a3r*a3i*a4r*a5r+a2r*a3i*a5r*a6r
    -a1r*a4i*a5i*a7i+a1r*pow(a5i,2.0)*a6i+a2r*a2i*a5i*a7i
    -a2r*a3i*pow(a5i,2.0)+a3r*a3i*a4i*a5i-a2r*a3i*a5i*a6i
    +a1i*a4r*a5r*a7r-a1i*pow(a5r,2.0)*a6r-a2i*a2r*a5r*a7r
    +a2i*a3r*pow(a5r,2.0)-a3i*a3r*a4r*a5r+a2i*a3r*a5r*a6r
    -a1i*a4r*a5i*a7i+a1i*a5r*a5i*a6i+a2i*a2r*a5i*a7I
    -a2i*a3r*pow(a5i,2.0)+a3i*a3r*a4i*a5i-a2i*a3r*a5i*a6i
    -a1i*a4i*a5r*a7i+a1i*a5i*a5r*a6i+pow(a2i,2.0)*a5r*a7I
    -a2i*a3i*a5r*a5i+pow(a3i,2.0)*a4r*a5i-a2i*a3i*a5r*a6i
    -a1i*a4i*a5i*a7r+a1i*pow(a5i,2.0)*a6r
    +pow(a2i,2.0)*a5i*a7r-a2i*a3i*a5i*a5r
    +pow(a3i,2.0)*a4i*a5r-a2i*a3i*a5i*a6r;

Wmnr=(aa*cc+bb*dd)/(pow(cc,2.0)+pow(dd,2.0));
Wmni=(bb*cc-aa*dd)/(pow(cc,2.0)+pow(dd,2.0));
}



**************************************************************
#include <stdio.h>
#include <math.h>

/* Loading.c
** The Loading function computes the imposed impact load on
** the desired composite laminate.  Whenever there is a
** change for the impact loading condition, please modify
** this code file.
**                              -- Jie Feng, 1996.
**                                 Dept. of Mechanical Eng.
**                                 University of Ottawa
*/

#define PI 3.141592654
```

```
double qr, qi;
void
Loading(a,b,u,v,p,m,n,x1,y1,t0,ome)
double a, b, u, v, m, n, x1, y1;
double t0, ome;
{
double ang1, ang2, ang4, ang5;
double pi2, qmn1, qmnr, qmni , vn, um;

pi2=pow(PI,2.0);
ang1=(double)m*PI*u/(2.0*a);
ang2=(double)m*PI*x1/a;
um=(double)m*u;
ang4=(double)n*PI*v/(2.0*b);
ang5=(double)n*PI*y1/b;
vn=(double)n*v;

if(um!=a && vn!=b && (t0*ome)!=PI)
     {

     qmn1=(8.0*a*b*u*v*p*cos(ang1)*sin(ang2)*cos(ang4)
          *sin(ang5)*t0)/(pi2*(um+a)*(um-a)*(vn+b)*(vn-b));
     qmnr=(1.0-cos(PI+t0*ome))/(PI+t0*ome)+(1.0-cos(PI-t0
          *ome))/(PI-t0*ome);
     qmni=sin(PI+t0*ome)/(PI+t0*ome)-sin(PI-t0*ome)/(PI
          -t0*ome);
     }
else
     {
     qmn1=0.0;
     qmnr=0.0;
     qmni=0.0;
     }
qr=qmn1*qmnr;
qi=qmn1*qmni;
}



*****************************************************************
#include <stdio.h>
#include <math.h>
```

```
#define PI 3.141592654

/* Property.c
** This program computes the material properties of desired
** composite lamina.  If later, the different material
** system would be examined, this program is the one to be
** modified.
**                                -- Jie Feng, 1996.
**                                   Dept. Of Mechanical Eng.
**                                   University of Ottawa
*/

double q11r, q11i, q12r, q12i, q22r, q22i, q44r, q44i, q55r,
q55i, q66r, q66i, desn;
double Er, Ei;
void
Property(ome)
double ome;

{
double Emr, Emi, Efr, Gmr, Gmi, Gfr, Vf, posm, posf, n1r,
n1i, n2r, n2i;
double Efi, Gfi, desnf, desnm;
double E11r, E11i, E22r, E22i, G12r, G12i, G23r, G23i,
pos12, pos21;
double a1, b1, c1, d1, a2, b2, c2, d2, a3, b3, c3, d3, a4,
b4, c4, d4;
double E11, E22;
void Separate();

/*Material properties is constant*/
Emr=1158.0*pow((1.0+100.0*ome/(2.0*PI)),0.1);
Emi=0.15*Emr;

Efr=72.4e03;
Efi=101.36;
Vf=0.60;
posm=0.38;
posf=0.2;
desnm=1.23;
desnf=2.54;

desn=desnf*Vf+desnm*(1.0-Vf);

Gmr=Emr/(2.0*(1.0+posm));
```

```
Gmi=Emi/(2.0*(1.0+posm));

Gfr=Efr/(2.0*(1.0+posf));
Gfi=Efi/(2.0*(1.0+posf));

E11r=Efr*Vf+Emr*(1.0-Vf);
E11i=Efi*Vf+Emi*(1.0-Vf);

a2=Efr-Emr;
b2=Efi-Emi;
c2=Efr+2.0*Emr;
d2=Efi+2.0*Emi;

Separate(a2,b2,c2,d2);
n1r=Er;
n1i=Ei;

a1=Emr+2.0*Emr*n1r*Vf-2.0*Emi*n1i*Vf;
b1=2.0*Emr*n1i*Vf+Emi+2.0*Emi*n1r*Vf;
c1=1.0-n1r*Vf;
d1=-n1i*Vf;

Separate(a1,b1,c1,d1);
E22r=Er;
E22i=Ei;

a3=Gfr-Gmr;
b3=Gfi-Gmi;
c3=Gfr+Gmr;
d3=Gfi+Gmi;

Separate(a3,b3,c3,d3);
n2r=Er;
n2i=Ei;

a4=Gmr+Gmr*n2r*Vf-Gmi*n2i*Vf;
b4=Gmr*n2i*Vf+Gmi+Gmi*n2r*Vf;
c4=1.0-n2r*Vf;
d4=-n2i*Vf;

Separate(a4,b4,c4,d4);
G12r=Er;
G12i=Ei;

pos12=posm*(1.0-Vf)+posf*Vf;
```

```
G23r=Gmr;
G23i=Gmi;

E11=sqrt(pow(E11r,2.0)+pow(E11i,2.0));
E22=sqrt(pow(E22r,2.0)+pow(E22i,2.0));
pos21=(E22*pos12)/E11;

q44r=G23r;
q44i=G23i;
q55r=G12r;
q55i=G12i;
q11r=E11r/(1.0-pos12*pos21);
q11i=E11i/(1.0-pos12*pos21);
q22r=E22r/(1.0-pos12*pos21);
q22i=E22i/(1.0-pos12*pos21);
q12r=(pos12*E22r)/(1.0-pos12*pos21);
q12i=(pos12*E22i)/(1.0-pos12*pos21);
q66r=G12r;
q66i=G12i;
}


void
Separate(a,b,c,d)
double a,b,c,d;
{
Er=(a*c+b*d)/(pow(c,2.0)+pow(d,2.0));
Ei=(b*c-a*d)/(pow(c,2.0)+pow(d,2.0));
}



*****************************************************************
#include <stdio.h>
#include <math.h>

#define PI 3.141592654

/* fftrans.c
** The Fast Fourier Transform (fft) subroutine below is made
** according to FFt computation flowchart presented by E.
** Oran Brigham in his book 'The Fast Fourier Transform and
** its Applications'.  Refer to Appendix D for flowchart.
**                                -- Jie Feng 1996.
```

```
**                                    Dept. of Mechanical Eng.
**                                    University of Ottawa
*/

double *data_real, *data_imag, *num3;
void
fftrans(num_samp, time_intv, num1, isign)
unsigned long num_samp, num1;
int isign;
double time_intv;

{
unsigned long num2, numu, k, l, i, m, nk;
double warg, wtemp, c, s;
double temp_real, temp_imag, temp3;
unsigned long bit_reverse(), wp;

num2=num_samp/2;
numu=num1-1;
temp_real=0.0;
temp_imag=0.0;

for(l=1; l<=num1; l++)
   {
   for(k=0; k<(num_samp-1); k+=num2)
      {
      for(i=1; i<=num2; i++)
      {
      m=k/(int)pow(2.0,(double)numu);
      wp=bit_reverse(m, num1);
      warg=2.0*PI*(double)wp/(double)num_samp;
      c=cos(warg);
      s=sin(warg);
      temp_real=(data_real[k+num2]*c)-((double)isign
                *data_imag[k+num2]*s);
      temp_imag=(data_imag[k+num2]*c)+((double)isign
                *data_real[k+num2]*s);
      data_real[k+num2]=data_real[k]-temp_real;
      data_imag[k+num2]=data_imag[k]-temp_imag;
      data_real[k]=data_real[k]+temp_real;
      data_imag[k]=data_imag[k]+temp_imag;
      k++;
      }
      }
   num2/=2;
```

```
    numu--;
    }
 for(k=0; k<=(num_samp-1); k++)
    {
    i=bit_reverse(k, num1);
    if(i>k)
       {
       temp_real=data_real[k];
       temp_imag=data_imag[k];
       data_real[k]=data_real[i];
       data_imag[k]=data_imag[i];
       data_real[i]=temp_real;
       data_imag[i]=temp_imag;
       }
     }

 if(isign == 1)
    {
    for(k=0; k<=(num_samp-1); k++)
       {
       data_real[k]*=(1.0/(2.0*PI));
       data_imag[k]*=(1.0/(2.0*PI));
       num3[k]=(double)k*time_intv;
       }
     }
 else
    {
    for(k=0; k<=(num_samp-1); k++)
       num3[k]=2.0*PI*(double)k/((double)num_samp*time_intv);
    }
 }

 unsigned long
 bit_reverse(m, num1)
 unsigned long m, num1;

 {
 unsigned long i, j1, j2, k;
 k=0;
 j1=m;

 for(i=1; i<=num1; i++)
    {
    j2=j1/2;
    k=2*k+(j1-2*j2);
```

```
    j1=j2;
    }

return(k);
}
```

```
*****************************************************************
#include <stdio.h>
#include <math.h>

/* evenodd.c
** This function manipulate the data_real and data_imag
** array to make the data_real a even function and data_imag
** a odd function within the size of total sapmling points.
**                                -- Jie Feng, 1996.
**                                   Dept. of Mechanical Eng.
**                                   University of Ottawa
*/

double *data_real, *data_imag;
void
evenodd(nmax, num_samp)
unsigned long nmax, num_samp;
{
unsigned long k, n;
n=num_samp-1;

for(k=1; k<=(nmax-1); k++)
    {
    data_real[n]=data_real[k];
    data_imag[n]=(-1.0)*data_imag[k];
    n--;
    }
data_real[nmax]=data_real[nmax+1];
data_imag[nmax]=data_imag[0];
}
```